TECHNISCHE UNIVERSITÄT
ILMENAU
Faculty for Informatics and Automation
Systems and Software Engineering Group

Energy-Efficient Resource Management for Continuous Scenario Fulfillment by UAV Fleets

by

Thomas Dietrich

Doctoral Thesis
in partial fulfillment of the requirements
for the degree of Doktoringenieur (Dr.-Ing.)

Supervisor:	Prof. Dr.-Ing. habil. Armin Zimmermann
Second Reviewer:	Prof. Dr.-Ing. habil. Andreas Mitschele-Thiel
External Reviewer:	Maître de conférences HDR Jean-Yves Choley
Author ORCID iD:	https://orcid.org/0000-0001-7292-5553
Date of Submission:	August 09, 2018
Date of Ph.D. Defense:	July 11, 2019

urn:nbn:de:gbv:ilm1-2019000375

Acknowledgments

The completion of this project would not have been possible without the continued support and encouragement from various colleagues and friends.

First, I thank Prof. Armin Zimmermann for giving me the opportunity and freedom to perform the studies leading to this thesis, as well as for his provided guidance. Furthermore, I would like to thank Prof. Mitschele-Thiel and Prof. Choley for agreeing to read and asses this work.

A special thanks goes to my Ph.D. colleagues Silvia Krug, Jana Thomann, and Christoph Bodenstein for the invaluable discussions and the joint work on projects and publications. Our coffee breaks, deep discussions, and late-night paper sprints sparked new and interesting ideas pushing the completion of this thesis forward.

I am also thankful to Prof. Hotz and his Ph.D. student Stefan Heyder of the TU Ilmenau Stochastics group for their invaluable support with encountered mathematical challenges.

Finally, I want to thank my parents, siblings, and grandparents who always supported me and my ambitions, by giving me the freedom to explore the world and to find myself.

Kurzfassung

Unbemannte Luftfahrzeuge (unmanned aerial vehicles, UAV) sind autonom fliegende und flexibel einsetzbare mobile Roboter, welche durch ihre große Flexibilität und Erweiterbarkeit viele Möglichkeiten bieten. Insbesondere im Bereich der Katastrophenbewältigung erlangen sie immer stärkere Bedeutung, da die Aufgaben zur Aufklärung im Gebiet und zur Erschaffung einer Kommunikationsinfrastruktur ungebunden undschnell durch sie bewältigt werden können. Der Forschungsschwerpunkt dieser Arbeit liegt in der Herausforderung der Ressourcenverwaltung in einem solchen Szenario. Während die Priorität des UAV Einsatzes klar darin besteht die Katastrophenbekämpfung unterbrechungsfrei zu unterstützten, muss ebenso auf die Verwaltung limitierter Ressourcen, wie elektrischer Energie, eingegangen werden. Wir präsentieren ein entsprechendes Systemdesign einer Ressourcenverwaltung und Strategien zur Verbesserung der Leistung und damit zur Erhöhung der Energieeffizienz des Gesamtsystems. Die Implementierung und gründliche Untersuchung eines solchen komplexen Systems von Teilsystemen ist verbunden mit hohen finanziellen Kosten, großem Test-Risiko und einer langen Entwicklungsdauer. Aus diesem Grund setzt diese Arbeit auf abstrakte ausführbare Modelle der Umgebung, des Verwaltungssystems und der UAVs. Die Verwendung dieser Modelle in einer Massensimulation mit beliebiger Komplexität und Konfiguration ermöglicht die schnelle und kostengünstige Verifikation der Funktionstüchtigkeit und die Bewertung verschiedener Verwaltungsstrategien. Im Vergleich zu der präsentierten trivialen Lösung ist die entwickelte verbesserte Lösung in der Lage den zeitlichen Anteil einzelner UAVs im Missionseinsatz zu erhöhen und die insgesamt nötige Menge an UAVs für die dauerhafte Abdeckung aller Aufgaben zu reduzieren. Die Schritte zur Optimierung reduzierten im analysierten Beispiel den Gesamtenergiebedarf aller UAVs um nahezu 20 Prozent.

Abstract

Unmanned aerial vehicles (UAV) are autonomous and flexible robotic systems with a remarkable degree of freedom and extendibility. They are especially valuable in the context of disaster scenarios, where arising use cases for reconnaissance and mobile communication infrastructure creation have to be addressed rapidly and unbound from restrictions in the operation field. The research focus of this thesis lies in the challenge of resource management during such an application. While the priority of the UAV utilization lies on uninterrupted task execution, concern for limited resources, like electrical energy, and resultant maintenance processes has to be dealt with on a lower management layer. We present a resource management system design and multiple competing strategies to improve its performance and overall energy efficiency. The implementation and thorough evaluation of such a complex system of systems is linked to high costs, great operational risks, and a long development time. For that reason, we developed executable models representing the environment, the resource management system, and the UAV. Through mass simulation of these models in various scenario constellations and configurations, we are able to verify the applicability of our proposed resource management system and to evaluate and optimize various aspects of its processes. In comparison to a presented trivial solution, we are able to increase the UAV flight utilization efficiency and decrease the needed amount of provided UAVs in the scenario. Our optimization efforts reduce the overall energy demand of UAVs in the analyzed example scenario by almost 20 percent.

Table of Contents

1. Introduction

Disasters are a constant threat in many parts of the world. Today, the question is not if the crisis will happen, but when. Hurricane Katrina, one of the most prominent cases in recent years, resulted in approximately 1330 deaths, $96 billion in damages, 3 million disconnected land-line phones, and rendering up to 2000 cell sites out of service [Tow06; Mil06]. Immediate response is a key requirement to mitigate the effect of the disaster, prevent loss of human life and damage to nature. Response personnel are constantly faced with recurring and unforeseen challenges that need to be overcome [LA11]. The provision of a comprehensive communication network plays an important role in reconnaissance and in the effective and unhindered coordination of response actions [Rei+15].

Unmanned aerial vehicles (UAV) can play an important role in disaster scenario response. In recent years UAVs enjoyed increased interest and significance, thanks to multifarious development and availability of reliable and affordable products in the domestic market. A typical UAV has the size and power to carry and use sensors, cameras, and actuators for a wide variety of tasks within a large operational radius. UAVs can rapidly provide a variety of services, with almost no infrastructure dependencies and through a wide hardware extendibility.

Utilization of UAVs in disaster response reduces the response time and increases the ability to navigate within the operational area. Thus it offers previously unimagined possibilities. Using a fleet of UAVs accentuates these advantages by coordinated and cooperative task execution, with the sum of UAVs and the controlling entity serving as a system of systems. Long-term UAV fleet utilization and the resulting resource management requirements represent new research challenges.

Self-organized mobile communication systems for disaster scenarios was the research focus of the Graduate School of Mobile Communications (GS MOBICOM) at Technische Universität Ilmenau, between 2009 and 2014. The research offers a wide range of

interesting new topics around various aspects of mobile, adaptive, and heterogeneous networks [Mit11]. Multicopter UAVs were chosen as the universal mobile platform for communication, and received additional attention in the research focus. The work presented here results out of the cooperation between the graduate school and the author of this thesis.

1.1. Motivation

Missions derived from a disaster scenario are potentially long-lasting and far-reaching. Multiple UAVs have to be used in such cases, leading to issues of resource coordination and optimal allocation of restricted resources. Just like most other mobile robots, UAVs are powered by an electric battery and are thus limited in their utilization lifetime. While a mission could last hours or days, the utilization time of a UAV is limited to approximately 15 to 60 minutes with state of the art technology. Restoration of battery capacity through recharging is not feasible during flight and only at certain locations.

Such primitive limitations are magnified in disaster scenarios, where human life may be at risk. Requirements and restrictions of response planning are unique to each scenario. Ideally, the planning process should be unfettered by resource limitations. A resource management system is needed to coordinate resource provision and maintenance processes alongside the planned response tasks. The achievable separation between physical UAV nodes and logical mission-operation entities should be able to support service continuity without consideration for resources. Maintenance processes under resource management should not impair continuity and overall response execution.

Unrestricted response planning accompanied by restricted resource utilization yields new interesting research questions. This thesis discusses and analyzes a resource management system based on replacement and recharging processes for service continuity during disaster response scenarios. The system is rule-based and works in live fashion to deal with any deviation and changes. Different replacement strategies are analyzed to evaluate their effectiveness and efficiency under conditions of resource limitation, especially the overall energy demand and number of available UAVs.

1.2. Problem Statement

The planning of resource management tasks is a proactive process. The forthcoming state of a UAV system has to be estimated in order to schedule the necessary processes, in particular, the replacement of one UAV with another. In order to predict the state of a complex system, the system must be well understood. Knowledge of scenario-derived missions along with UAV flight and energy consumption behavior must be available beforehand. The creation and parameterization of a precise realistic prediction model is the first challenge of this thesis. The model has to be generic, to include all UAVs, yet be precise for a calibrated UAV build. Mathematical models of the UAV physics [ARB15; MCL16; Büd14] were found to be too detailed and with the unnecessary focus on low-level system behavior. A near-blackbox model focused on resulting movement and energy consumption behavior will be presented in this thesis.

Uncertainty and the differences introduced between the real-world behavior and the model-based prediction pose additional challenges. External factors such as wind affect the system and introduce uncertainty in the representing model. Uncertain outcomes can delay maintenance processes and mission execution, causing interruption and potential termination of the disaster response, thus potentially exacerbating loss of human life and damage to nature. The inclusion of reasonable safety margins in the prediction of future development can help cope these issues. Maintenance processes inherently reduce the probability of delay or termination, when pessimistic values for future movements and energy consumption are assumed. Resource efficiency is traded for the enhanced system safety thus achieved.

A resource management system based on a sound prediction model and mission knowledge is able to reliably foresee future system behavior within probabilistic bounds, and plan and coordinate maintenance processes accordingly. Replacement of UAVs is at the core of our continuity approach. Planning the location and time of replacement, as well as maintenance flights to and from the replacement location in a timely fashion, does not allow for obvious simple solutions. Different strategies for replacement offer optimization potential for resource utilization.

The feasibility of a successful resource management system and the margin of optimization potential in the replacement coordination, form the central research question of this thesis.

Evaluation and quantitative comparison of these solutions in the system of systems context bears challenges due to different modeling domains. The system offers a variety of sub-systems with both continuous and discrete aspects. Representation in a pure numeric model for analysis and optimization is not feasible under moderate bounds of complexity and time effort.

Model-based systems engineering (MBSE) treats models as the primary artifact of system development and is widely regarded as a risk-reducing and quality-improving approach to systems engineering [GDT14, p. 120]. The approach unifies different modeling disciplines and increases the level of automation throughout the system life cycle. The refined modeling and simulation-based systems engineering (M&SBSE) approach, as discussed in various forms by Gianni, D'Ambrogio, and Tolk [GDT14], emphasizes the possibility to simulate, evaluate, and optimize a system before or during development cycles. The presented thesis follows the approach in order to represent the system and optimize system aspects, without the need for an actual real-world implementation.

1.3. State of the Art and Contribution of this Thesis

The central object of research in this thesis are individual and fleets of UAVs utilized in disaster response scenarios. Arising tasks are manifold and the subject of broad research. UAV fleets can execute multiple tasks in parallel, but can also act together to fulfill tasks of higher complexity, like cooperative surveillance [MO07; RD08], coordinated swarming [Haf+15], or aerial imagery [Seg+11]. These and other projects with the subject of UAVs as distributed communication and sensing platforms show the importance of the research field. However, literature of this category concentrates on the technical and strategical implementation and operation of the special tasks and does not address and overcome energy and flight time limitations.

Research in the area of UAV utilization in disaster response scenarios also concentrates on the special tasks surrounding the application field, e.g., the reconstruction of communication networks [BHR15; Rei+15; Wan+16] or the rapid and efficient execution of cooperative reconnaissance [Seg+11].

Long-term UAV fleet utilization and the resulting resource management requirements have not yet received equal consideration. In the application examples by Maza and

Ollero [MO07] and Ortiz-Peña et al. [Ort+13] the issue is addressed by energy-aware mission planning. The approach, in which tasks are scheduled in length, route, and frequency to be within boundaries of the utilized UAVs, represents the simplest solution but adds additional requirements to the planning process. The aim of this thesis is to overcome these implicit limitations on task generation to allow result-oriented task definition, crucial for the success of disaster response utilization.

A different approach is taken by the research groups around Dasgupta [Das08] and Leonard et al. [LST12], who utilize UAV swarms in their application examples to compensate for single UAV fluctuations. Rather than assigning a task to a single UAV, a broader task is assigned to a swarm of UAVs, whose size can vary over time. Utilization of swarms is out of the scope of this work, which focuses on tasks for single UAVs and their continuous execution.

A solution for automated maintenance as means for energy management is presented by Leonard, Savvaris, and Tsourdos [LST13]. The authors concentrate on the physical setup of a charging station, then present an auction algorithm to allocate UAVs to existing charging stations under minimization of the additional travel time. The work assumes single-port charging stations and static low battery thresholds. Furthermore does it neither consider the need for a replacement UAV to carry on the task, nor does it tackle the challenges of uncertainty in all movement and consumption processes.

Ure et al. [Ure+15] address the problem of temporary unavailability of UAVs due to the long charging time by a special battery replacement procedure. The authors introduce a Markov process to simulate the movement of UAVs between charging stations and operation areas. Probabilistic uncertainties are considered as part of the modelled Markov process and magnitudes estimated during an experiment. The aim of the research project was to reduce the low utilization of individual UAVs and thus the needed number of UAVs to service a continuous mission. The work provides an interesting aspect to the research topic of this thesis, but lacks to address seamless replacement of a UAV before returning to its charging station, the availability of multiple charging stations, and the efficient temporal and spatial planning of the replacement process.

The focus of the presented thesis lies on resource management for UAV fleets with long-lasting missions. The basic question during a running UAV fleet mission is the following: How long should an active UAV continue to serve its current mission before being sent to a charging station to avoid depletion, and which replacement UAV should be sent to

take over its task. Such decisions should be done by the envisioned management and control entity in a way that is close to optimal with regard to the use of a minimum of available UAV resources. Theoretically, this scheduling task can be characterized as an online optimization problem [Lu13], as settings and environment of the problem may change during a mission. Moreover, as measurements are noisy and not all influences can be captured and predicted, the task is also a stochastic optimization problem [BH06; Meg08].

The research topic can thus be classified as a stochastic online scheduling optimization problem for a system with mixed continuous and discrete processes. Megow [Meg08] describes stochastic online scheduling as the generalization of models for dealing with stochastic processes and with processes with unknown future development. The author addresses the mathematical problems of both models and of their combined challenges. In the literature, there are several application examples in logistics and others, for which sample problems can be transferred into approximate models such as integer linear programming problems to be solved with modern optimization methods. However, there is no generally applicable method that could solve this type of problem. In general, only very problem-specific solutions are reported in the scientific literature.

Even for comparably simple problems such as job scheduling, such optimization problems are hard to tackle [Vre11]. A simulation-based approach forms an alternative to a mathematical solution and can offer more flexibility. This thesis follows the M&SBSE methodology to enable the systematic development of an improvement for a complex system of systems. As opposed to a theoretically optimal online solution, we propose strategic rules that decide about the resource allocation problem solution in certain settings, which is the typical approach in the engineering of complex systems for which no provable perfect solution is known. To evaluate and validate the effectiveness of such rules, they have to be tested against many different settings and missions, based on a model describing the states and dynamics of the overall system. Therefore, we present a design process to build a black-box model of the movement and energy consumption behavior of a UAV based on a reproducible empirical study, which is later used in a mass-simulation evaluation of multiple strategies for UAV fleet management. The underlying model of our system includes mixed continuous and discrete processes, for which not even general numerically exact analytical solutions exist and simulation is the only available approach.

One of the three key contributions of this thesis is the definition of an introduced resource management abstraction layer in the control system of the UAV fleet. The layer relieves the disaster response planning process of resource limitation considerations and, therefore, allows result-driven planning of UAV missions.

The second key contribution is the described reproducible energy consumption measurement, analysis, and modeling process. The existence of an accurate and precise model is crucial for a simulation-based approach and its development for the UAV system is described as a step-wise process to follow along. The description of the steps taken, especially with regards to variance and thus safety margin estimation, will guide future research with similar research problems.

The definition and simulation-based comparison of heuristics for the different steps of the complex UAV replacement process is the third key contribution. The thesis discusses each aspect of the process, including real world influences and resulting uncertainties, and heuristics are used to minimize the absolute amount of UAVs and the gross energy consumption of the UAV fleet.

Another noteworthy contribution is the developed and publicly available discrete event simulation framework for strategy evaluation in UAV fleet management. The framework enables further research and development in the field and is seen as an important addition to the existing tools landscape.

1.4. Structure

The structure of this thesis resembles the typical steps of the model-based systems engineering approach, from preliminary analysis to the concluding model-based system evaluation.

Chapter 2 introduces UAVs as versatile mobile robots and highlights their structure and relevant electricity consuming components. An electric battery forms the functional counterpart to all on-board components and is the subject of the second part of the technical background. Chapter 3 then focuses on disaster scenarios and reviews the applicability of UAVs in disaster response actions. As a first step towards model-based simulation analyses, the chapter presents a conceptional UAV response model and discusses

the base requirements of an underlying resource management system. For the chapter that follow, Chapter 3 ends with an overview of our utilized measurement and testing system, consisting of two testbed UAVs and the surrounding control and maintenance components.

The model-based systems engineering method depends on accurate and precise models of the relevant parts of a real-world application. Chapter 4 accordingly discusses an analysis of a UAV in general, and of our testbed UAVs in particular. This is done to create an abstract but detailed flight behavior and energy consumption simulation and prediction model.

Chapter 5 and Chapter 6 focus on the already introduced resource management system and the associated maintenance processes. Chapter 5 begins with a structured analysis of the requirements and Chapter 6 presents our novel management system and various applicable UAV replacement and recirculation strategies.

Our model-based simulation framework, developed as part of the work on this thesis, is presented in Chapter 7. The framework combines all system-design decisions from the previous chapters, and the testbed UAV model from Chapter 4. The chapter highlights the flexibility of the framework as a general UAV fleet resource-management simulation framework.

The thesis ends with a mock disaster scenario and evaluates the applicability of our resource management approach in Chapter 8. Different resource management configurations and the proposed replacement strategies are evaluated by mass simulation and statistical measurements analysis. The chapter ends with a recommendation for replacement strategy selection and parameterization.

Finally, the work is summarized in Chapter 9, where it also invites future research by highlighting the not yet discussed aspects of resource management, and by defining the as of yet unemployed simulation framework features.

2. Technical Background

This chapter will introduce more details about mobile robotics and their electrical components. The main focus lies on UAVs and the electric battery as the commonly used energy storage in such systems, to provide a good basis for later discussion. An overview on the battery life cycle, which is important for resource management, will conclude the chapter.

2.1. Mobile Robotics and Aircrafts

Robotic systems are omnipresent in the modern world. From children's toys to complex conveyor belt production systems with robotic arms and manipulators, electromechanical robotics enable and meet a variety of demands in industry, construction, medicine, and the military. These systems are often highly specialized towards a certain application field and task, and therefore unique in their properties.

Mobile robots are robotic systems with the ability for movement and locomotion, often used to perform tasks at distinct locations. According to Siegwart et al. [SNS11, pp. 13 sqq.] these systems can be categorized as following:

- Land-based legged mobile robots
- Land-based wheeled or tracked mobile robots
- Aerial mobile robots
- Water-based floating or diving robots
- Miscellaneous and combined robots

Most mobile robots can be clearly categorized into one or more of these categories. The main distinguishing factor is the application field and task. While an underwater cable inspection submarine will naturally be classified as a submerging robot, a flying

platform for infrared camera based reconnaissance is of the airborne robots category. Both examples are also good candidates for robotic systems, that are highly specialized in their physical, functional, and computational properties. A specialization is common for task-oriented robots and has to be taken into account during a generalized discussion.

2.2. Unmanned Aerial Vehicles

According to the European Aviation Safety Agency (EASA) [UAV04] the term unmanned aerial vehicle (UAV) represents an aircraft without a human pilot aboard. UAVs, like other mobile robots, are commonly controlled by a distant ground control station and a suited communication link. The flight, navigation, and operation of a UAV can happen at different degrees of autonomy, depending on the intended task and the invested development effort.

The most conventional term used for unmanned aircrafts of all kinds is UAV and perhaps the most commonly used lay term to describe UAVs in the media is “drone”. The term drone often carries with it a stigma, inherited from the historically controversial military applications of drones in the battlefield. Micro aerial vehicle (MAV) is also a commonly used term to refer to UAVs with emphasis on their small form factor.

The term unmanned aircraft system (UAS), comprises not only the aircraft but the aircraft in combination with the ground control station and the communication link, forming a complete system for remote and autonomous applications, rather than for the transportation of humans or goods. The term is precisely defined in *Unmanned Aircraft Systems (UAS)* [ICA11] by the International Civil Aviation Organization. The often encountered term small unmanned aircraft system (sUAS) is almost synonymous to UAS but highlights the reduced form factor of addressed models.

The term UAV will be used throughout this thesis to address unmanned aircrafts in general.

2.2.1. Historical Background

The first ever UAVs were developed and used for combat purposes during World War I. Nikola Tesla had already described an armed and pilotless aircraft by 1915. In the years that followed, unmanned aircrafts were used in the form of guided missiles, as missile launching vehicles and as training targets for anti-aircraft artillery. Advances followed up to and during World War II and in the following years, throughout the Cold War. Reach, capabilities and autonomy of unmanned aircrafts were the focus of continuous improvements and developments, especially in the United States Air Force, cf. [Dem10].

The first piloted aircrafts with multiple rotors were developed in the 1920s but were technologically insufficient. The "Convertawings Model 'A'" by Kaplan [Kap61] was the first quadrotor aircraft to fly, in 1956. A few other models arrived in the years to come, but all of them suffered from mechanical difficulties and did not have any significant advantages over full-sized single rotor helicopters. The market for piloted passenger or cargo aircrafts was saturated with airplane and helicopter types, and thus the development of multirotor aircrafts stopped.

In recent years, UAVs have been deployed as part of many countries' military operations. According to Horgan [Hor13], over 50 countries were using UAVs as part of their military operations by 2013. The United States alone deployed more than 11 000 UAVs.

Interest in multicopters resurfaced around 2005, when the demand and development of electronic robotic components entered a new era. New application fields necessitated the use of autonomous flying robotic systems, and the multicopter concept satisfied the ensuing requirements as a small experimental and task execution platform, cf. [Sta07]. Palm-sized quadcopter toys can be bought off the shelf for an affordable price, the sports-camera company GoPro released an amateur video drone in 2016, and professional full-time UAV pilots offer a variety of services such as site surveys and field inspections.

2.2.2. Application Today

UAVs have their historical background in military operations, but have since found use in domestic society, for private, commercial, and public applications. Rae [Rae14,

pp. 98 sqq.] describes the potential applications as “nearly endless” in the society and names the following and more use cases:

- Surveying and photographing archeological, open-cast or real estate sites
- Gathering data on natural resources
- Delivering goods, like medicine, to remote locations
- Recording atmospheric data and forecasting weather conditions
- Monitoring pipelines and power lines for damages
- Executing search-and-rescue missions
- Mapping, assessing, and fighting wildfires
- Assessing damage after natural disasters, like hurricanes, floods, avalanches, and earthquakes
- Aiding in disaster relief efforts

The wide range of applications attracted the interest of organizations and individuals, and thus also of manufacturers. Matching UAVs for the listed use cases are commercially available. They offer a customized build with an aligned selection of hardware components, to meet the needs of the individual use case.

2.2.3. Classification

UAV designs are manifold in their main structure, their propulsion system and resulting flight principles, and their individual advantages and disadvantages in comparison to others. Quan [Qua17, p. 3] classifies the commonly known UAV robotic systems into three major types:

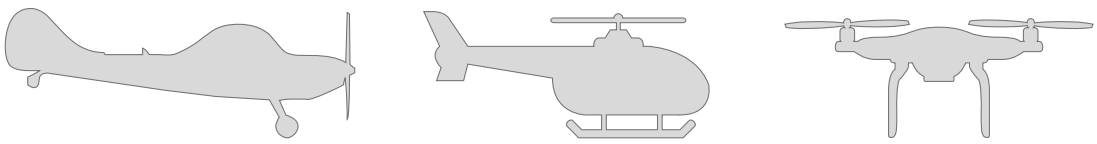

a: Airplane **b:** Helicopter **c:** Multicopter

Figure 2.1 – Major UAV types shown as schematic examples.

Airplanes A fixed set of main wings characterizes this aircraft class. A forward-facing propeller produces thrust, and the aerodynamics of the wings generate an uplift force. The advantages of this class are its simple structure, and the low energy consumption at high speeds and heavier payloads.

Due to the aircraft's aerodynamic properties, a certain forward directed airspeed is necessary to maintain altitude. A fixed-wing airplane cannot stop and stay at a certain position, nor is it able to change its course rapidly. For take-off and landing a runway is unavoidable. This need for movement poses as a disadvantage for many of the mentioned use cases of UAVs.

Helicopters The helicopter class is normally characterized by an upwards directed main rotor, and a small tail rotor. While the main rotor supplies lift and thrust, the tail rotor is needed as an anti-torque control to compensate for torque induced by the rotation of the main rotor blade. The relative position and orientation of the blades attached to the rotors can be controlled individually to enable movement in all directions.

The helicopter class is able to perform vertical take-off and landing, and can hover at fixed positions. It has advantages over the fixed-wing airplane in scenarios where a steady position and precise horizontal, vertical or lateral movement is required. The main drawback of helicopters is the complexity of the rotor control system, which forms a single point of failure and therefore a high safety risk.

Multicopters Multiple upwards directed propellers characterize the multicopter class. Instead of a complex rotor system atop a helicopter, the multicopter is equipped with three, four, six, eight or any other number of motor-propeller combinations. Other than a complex rotor control system of a helicopter, the propellers of a multicopter feature simple fixed blades. The motors are positioned around the balance point of the vehicle, and when used in combination provide the means to control rapid and precise positional adjustments of the vehicle. Each propeller's angular speed is adjusted to hold or bring the copter in a certain orientation or movement. Due to different directions of rotation, the torque induced by one single propeller is canceled out by the torque of the others. Different propeller counts and arrangements are depicted in Figure 2.2 and influence stability, bearable payload or overall size. The flight principles of a multicopter, are not altered by the propeller count or their particular layout. This knowledge is important for

later discussion of the energy consumption during movement of a generic multicopter. All multicopters are capable of vertical take-off and landing (VTOL), which is important for many use cases.

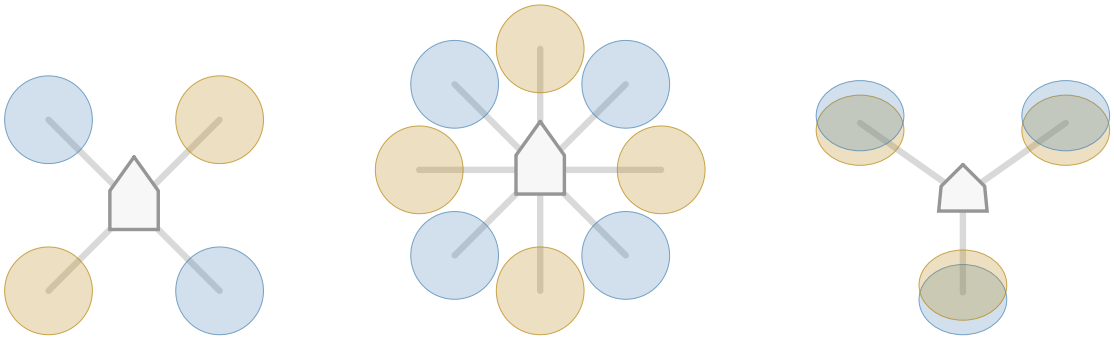

a: Quadcopter **b:** Octocopter **c:** Tricopter/Y6

Figure 2.2 – Different exemplary multicopter arrangements. The quadcopter is light and versatile, the octocopter is safer and for heavy duty, the Y6 is a compact dual-motor medium arrangement.

The utilization of multiple smaller motor-propeller combinations reduces vibrations and noise emission. Mueller and D'Andrea [MD14] highlight, that an increased propeller count also ensures flight safety in case of single propeller failure. Hardware and ground safety, as well as availability and reliability of a task-fulfilling UAV are important meta-requirements of the presented use cases.

Multicopters are usually not seen as bigger piloted aircrafts, and are thus subjected to relatively relaxed engineering certification and licensing challenges, to otherwise ensure their piloted airworthiness[1]. Because of that and the simple mechanical design compared with the helicopter class, acquisition and maintenance costs for multicopters are generally low.

Interestingly, despite its attested flexibility and rapidness, the multicopter design theoretically qualifies as a non-holonomic robot. A robot is holonomic, when the number of controllable degrees of freedom is equal to the total degrees of freedom [HH94]. The multicopter design can achieve six degrees of freedom, but only by planning positional changes that make use of its four controllable degrees of freedom. Nevertheless,

[1] Airworthiness: The ability of an aircraft to be operated without significant hazard to aircrew, ground crew, passengers or to third parties.

no hard non-holonomic constraints are imposed on the free flying body of the multicopter. Therefore, a simplified model could present the multicopter as a holonomic system.

2.2.4. Use Case Specific UAV Selection

Besides the distinguished three main aircraft classes, mixed and custom forms exist for special use cases. An example is a hybrid airplane with multicopter features as presented by Gu et al. [Gu+17]. The company Uber recently proposed a similar scaled-up aircraft design for their common reference model eCRM-001 [Moo18] aimed at the special requirements of urban air mobility services behind the Uber Elevate program. The example shows that the selection of a particular UAV design highly depends on the requirements and restrictions of the use case at hand.

The fixed-wing airplane has its clear purpose as a UAV for fast and long-distance maneuvers. The helicopter UAV is popular in scenarios where precise movement is needed in combination with high payload requirements. In most of the presented use cases for application of UAVs in today's society on page 11, the multicopter class is a recommendable choice, thanks to its simplicity and compact form-factor, free and rapid maneuverability, easy maintenance and flight failure safety. The variety of multicopter build types additionally increase their usefulness for individual use cases and Magnussen et al. give a detailed overview on the selection process in their work "Multicopter UAV Design Optimization" [MHO14]. UAVs on today's market are generally modular in their component structure and additional components to fulfill the use case requirements are easily attached.

Not long ago, the legal requirements and limitations for UAV application in the domestic society, and liability in case of human or hardware failure, were not clearly or insufficiently regulated in the western world. The situation hindered the acceptance and wide utilization in the public domain. On June 21, 2016 the United States Federal Aviation Administration (FAA) finalized the regulatory framework for drone certification process, named "Small Unmanned Aircraft Regulations" under "Part 107" [FAA16b]. The European Commission and the European Aviation Safety Agency (EASA) expects to have a regulatory framework in effect by 2019, cf. [Eur16]. On the basis of the given information, we expect an increase of UAV utilization for the presented and other use cases.

For the remainder of this thesis, we will address UAVs in general and analyze and discuss multicopters in particular. All conclusions and results will be preferential towards multicopters but can be reflected or extended to cover other UAV classes. Crucial research results will be discussed for multicopters and UAVs.

2.3. Electrical Energy Consumption of UAV Systems

UAV systems were introduced as flexible and modular platforms with numerous mandatory, optional and additional components. Most of these components use electrical energy to enable operation and active processes. After a recap of basic electronics, we will discuss individual electronic components of UAV systems, and their energy needs.

2.3.1. Overview of Basic Electronic Principles

In physical terms, the law of conversion of energy states that energy can neither be created nor destroyed, but rather transformed from one energy form to the other. Motors transform electrical energy into kinetic energy, radio transceivers emit electromagnetic radio energy, and microcontrollers produce heat while processing data. Throughout this work the terms “energy use” or “energy consumption” will be used as synonymous to a transformation of electrical energy to other forms of energy.

Electrical energy is a form of energy that originates from electric potential energy in an electrical circuit. Every electrical circuit can be understood as a combination of an electrical energy source and an arbitrarily complex consumer. The energy source possesses an electric charge that creates an electric potential difference, also called a voltage, which causes electric current flow through the consumer part of the circuit.

Electric power is the rate at which energy is transformed. It is defined as the product of an electric voltage U and the electric current flow I induced by it:

$$P = U \cdot I \tag{2.1}$$

Electric power leads to electrical energy consumption. While electric power is a momentary measure for the conversion rate of energy, energy consumption denotes an accumulated amount of electric charge. A battery as a typical confined energy source is able to store a limited amount of electric charge. Electric charge Q can be given as the integral product of current over time, electrical energy E (consumption) is denoted by the integral product of power over time:

$$Q = \int I(t)\,\mathrm{d}t \;\text{ in [mA h]} \qquad E = \int P(t)\,\mathrm{d}t \;\text{ in [W h]} \tag{2.2}$$

The key difference is the inclusion of voltage in the second formula. Voltage is typically constant for steady power sources, thus making both measures proportional. In Section 2.4.3.3 we will go into the details of battery voltage. For now, it is important to recognize that the voltage of a battery is variant and depends on its remaining electric charge and the outside load.

Throughout this thesis, we will use both measures to describe different aspects of battery powered applications. Power and electrical energy will be used in all cases, in which the application is discussed. Current and electric charge will be the subject of battery-centered analysis steps. An approximate conversion between the two can always be achieved by multiplying or dividing with the nominal power source voltage.

2.3.2. Electrical Categorization of UAV Components

The electrical energy system of a UAV can be divided into groups of different components. The combination of available components in one UAV model is highly dependent on its build specifics and its use case requirements. Components may be added or removed to add additional and special capabilities, or save weight. Some components are indispensable for flight, while others are optional. Potential component categories are depicted in Figure 2.3.

Flight Controller The central flight controller is the heart of the UAV, and is connected to all other components. It is typically a small lightweight microcontroller with

input/output capabilities and the computational power to handle higher amounts of sensor data and the partially needed complex post-processing steps. The energy consumption of this class of microcontrollers is generally low in comparison to other components of the UAV.

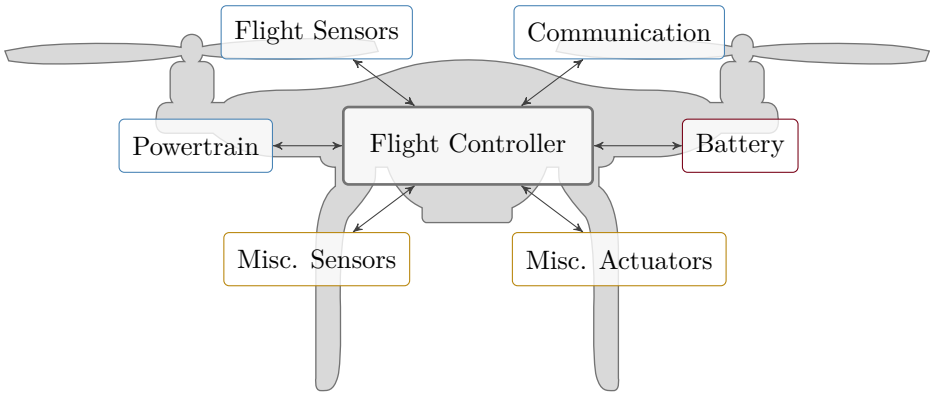

Figure 2.3 – Typical multicopter component categories. All components form an interconnected system with the flight controller at the center and the battery as the common energy source.

Flight Sensors These are hardware components that assist in the positioning, orientation, and flight stabilization of the UAV. The most commonly found sensor module on a UAV is the inertial measurement unit (IMU), which includes a three-axis gyroscope and a three-axis accelerometer to measure and control the orientation of the UAV in air. Additional sensors can include a compass, a GPS receiver or ultrasonic sensors. Many more sensors may be installed to provide or improve certain movement or interaction capabilities. In general, sensors process externally provided movement or signals, and are therefore typically available as small and energy-efficient components. The topic of localization and navigation sensors was discussed as part of this thesis project by Hakim Moussaoui [Mou14].

Communication Different communication technologies and protocols can be applied to link UAV-to-UAV, UAV-to-Controller or UAV-to-Client communication. Traditionally, a high-frequency radio communication link was used for basic remote steering control of unmanned model aircrafts. With the introduction of more sophisticated UAVs,

featuring autonomous flight and navigation capabilities, the requirements of communication links have shifted. Nowadays a combination of various communication links can be found on a typical UAV, each offering its own advantages, like high data transfer rates or long range communication. The energy consumption of communication components receiving control data is relatively low, transmitting or transceiving components have a higher consumption impact.

Powertrain Besides passive components, the powertrain mainly consists of a number of electric motors, depending on the type of UAV. Each motor is generally accompanied by one The electronic speed controller is a device connecting a flight controller and motors to provide power and control speed. (ESC), which converts the pulse-width modulated (PWM) control value of the flight controller to a corresponding level of electrical power. The control value dictates the force generated by the propellers and the energy consumed by the electric motor. By evaluating the positional data received from the IMU and from other flight control sensors against the set target, the flight controller adjusts the set points for all motors. The electrical power of individual motors is slightly decreased or increased to stabilize the UAV's position and movement. From an energy consumption perspective, the powertrain of the UAV is the most influential category.

Miscellaneous Consumers As mentioned before, every UAV type or product may house additional hardware components. Additionally, the UAV use case might require special additions. Such hardware can range from cameras over Wi-Fi access points up to mechanical grippers. The energy consumption of these components needs to be taken into account when preparing the UAV utilization and its flight details.

Battery Energy Storage In a typical UAV a component that produces or harvests electrical energy is generally not available. The whole system, represented by the electrical consumers mentioned above, is sourced by an on-board battery. An exception form combustion propelled systems, which are out of the scope of this thesis. The electric battery has a limited capacity and therefore can only support flight and other energy consuming processes for a limited amount of time. After battery depletion, system failure is inevitable and has to be prevented to ensure a safe operation. The topic of battery state observation and management will be covered in later sections of this work.

2.3.3. Consumption Magnitudes and Dynamics

All aforementioned components, except the battery, consume electrical power to carry out their task. The total of these consumptions amounts to the overall energy consumed during the operation of a UAV. The magnitudes of consumption impact by different components was roughly compared above, but will be a subject to later analysis steps in Chapter 4.

In general, it can be expected that the consumption of some components is not only decisive in terms of magnitude but also because of their dynamic behavior. While the consumption of a sensor is assumed to be approximately constant over a complete flight, the consumption of the powertrain will vary significantly over different flight phases.

The battery, as the only available energy source on the mobile UAV has to cope with those varying loads, and has to provide the needed power and overall energy.

2.4. Battery Technology for UAV Utilization

Batteries in general are devices capable of storing and sourcing electrical energy. In chemical processes electrical energy is transformed and stored in the form of chemical energy, which can then be re-transformed to electrical energy when needed. The topics of battery technology and battery management in autonomous robotics were previously discussed by Thomas Schmalz [Sch13] and Vanessa Gries [Gri16] in assigned student works in relation to this thesis. The findings in those documents and the information given by Pop et al. [Pop+08] were the basis for the following sections.

The classic design of a battery cell consists of a positive electrode (cathode), a negative electrode (anode), and an electrolyte. The electrodes do not come in contact with each other, but are electrically connected by the electrolyte.

An externally enabled current flow between the two electrodes, by either a charger or a consumer circuit, results in reduction and oxidation reactions at the electrodes. At the same time, ions inside the electrolyte medium migrate between the medium and the electrodes. These chemical processes allowed to power external electric consumers and are reversible in rechargeable batteries.

Depending on the materials and the design, a battery offers a certain voltage and an overall energy charge capacity. Multiple cells can be combined in series and in parallel to create battery packs with higher voltages and capacities. Different battery designs contain different materials for both the electrodes and electrolyte medium on both sides of the battery, to improve its properties.

2.4.1. General Characteristic Properties

The battery materials used and design specifics applied mostly define the properties of a battery. According to Pop et al. [Pop+08, pp. 11 sqq.] the crucial properties of batteries are:

Nominal Voltage The electric potential difference rating of the battery in volts (V).

Maximum Capacity The overall electric charge capacity of the battery defined as the integral product of current over time, in ampere hours (mAh).

Discharge Rating ("C" Rate) The maximum discharge current of a battery, in proportion to the capacity of the battery.

Cycle Life A rating of the lifetime of a battery, given as the number of charge and discharge cycles before the battery is expected to fall below certain performance evaluation criteria.

Self-Discharge The effect of reversibly losing a portion of the battery's charge due to internal chemical processes during dormant storage.

Specific Energy A measure to quantify the energy density as energy per mass ratio, given in watt-hours per kilogram (W h/kg).

Memory Effect A problem of some battery types, in which the battery delivers only the capacity used during the preceding repeated charge and discharge cycles.

Safety A combination of all factors defining the overall safety of a battery in a certain scenario. Factors include danger of explosion and chemical contact, sensitivity against shock and pressure, and temperature constraints.

Many battery types are available on the market and dozens are subject to research. All of them differ in their chemical compositions or design specifics, and in the above mentioned properties. An in-detail overview is given by Zhang et al. in *Rechargeable Batteries* [ZZ15]. Most of the presented types are highly specialized and not market-ready. Every type has its own advantages, disadvantages, restrictions and dangers.

During the product search for a battery application, the mentioned functional and non-functional properties are relevant and have to be matched to the application task and context. Another factor is the economic aspect as the market price and availability of a product not only depends on the materials used, but also on the scaling effects of mass production and regulatory laws.

In the current customary market, four battery base types are common: lead-acid, nickel-cadmium, nickel-metal-hydride, and lithium-ion batteries.

2.4.2. Importance of Lithium-Ion Polymer Batteries

For most mobile applications today, the lithium-ion battery technology is the recommendable and available choice, as Chen and Sen confirm in "Advancement in battery technology: A state-of-the-art review" [CS16]. Especially interesting is the technology subtype lithium-ion polymer (LiPo). A rechargeable lithium-ion battery featuring a polymer electrolyte. This lithium-ion battery type provides higher specific energy (capacity per weight ratio), making it the ideal choice for weight-critical applications such as UAVs.

Almost all commercial UAV products feature a LiPo battery, profiting off their high specific energy, high potential C-rate and high cycle life. Typical properties of commercially available LiPos are given in Table 2.1.

The main disadvantage of LiPos is the potential danger of overcharge, over-discharge, overheating or physical damage. All of these can lead to catastrophic failure, including electrolyte leaking and explosion. An appropriate application and the utilization of a battery management system in combination with a battery charger specialized for LiPo batteries mitigate those risks.

Table 2.1 – Customary market ranges for LiPo properties

Property	Symbol	Mass Market Range
Nominal Voltage	U_{bat}	7.4, 11.1 and 14.8 V (3.7 V per cell)
Maximum Capacity	Q_{max}	1500 to 12 000 mA h
Discharge Rating		20 to 120 C
Cycle Life		500 to 1000
Self-Discharge		1 to 10 % per month, at 20 ℃
Specific Energy		90 to 250 W h/kg

2.4.3. Life Cycle of LiPo Batteries

The life of a battery is characterized by repeated charge and discharge cycles. Due to irreversible physical and chemical impairment every battery type suffers from decreasing performance, over the course of their lifetime. At some point in its life, the battery reaches a state of callable performance that is below certain levels, and the battery has to be decommissioned. This evaluation is known as the state-of-health (SoH) of a battery.

One of the main advantages of the lithium-ion polymers is the relatively long lifetime. The case of failure or aging of a battery over the course of its cycle-to-cycle use was not considered as an influencing factor for experimentation in the scope of the thesis project. This does not, however, imply that the unique state-of-health of one battery can be ignored and generalized.

The following sections will detail the LiPo life cycle that consists of charging, discharging and storage phases. Prior to that the term “state-of-charge” as a measure of the current battery charge will be introduced.

2.4.3.1. State-of-Charge

According to Pop et al. [Pop+08, p. 3] the state-of-charge (SoC) is defined as the currently available charge inside a rechargeable battery, stated in comparison to its maximum possible charge given the prevailing state-of-health.

Various methods to determine the current SoH and SoC of a battery exist. The remaining charge cannot be measured directly, instead proxy measurements have to be carried out and results have to be compared against known battery parameters, in order to make assumptions. Different methods for such proxy measurements are presented below.

The ability to probe and observe a battery also depends on the physical combination of battery pack and the metering components, often called the battery management system. An uncoupled and temporarily disconnected solution on the consumer side is not able to continuously observe the battery and its absolute state. Merging the active metering component with the battery pack presents certain challenges and increases the price of the battery. Such a permanent combination is commonly called a "smart battery". A detailed overview of the challenges of SoC indication and the smart battery design is given by Pop et al. in *Battery Management Systems* [Pop+08].

Proxy measurement and battery state determination can either be based on continuous observations or on the combination of absolute conditions.

Continuous Charge Observation All differences aside, the fundamental similarity of all batteries is the fact that a certain amount of electric charge is present in them at all times. Relative changes of this amount occur in the form of current flowing in and out of the battery, depending on the charger or load connected. The current flow can be observed and summed up using an integral product over time, to compute capacity changes. Combined with a short-term or long-term memory, good estimates for the overall resulting state-of-charge are possible without fine-grained knowledge about the battery specific properties, as listed in Section 2.4.1.

The method is simple and independent of the battery type, model or rated capacity. It is cheap to implement and offers reliable insight into the energy use of a consumer. The method still has its limits. Aggregated data over charge and discharge cycles needs to be collected, to gain knowledge about the absolute remaining charge inside a battery. The callable energy of a battery depends on factors like the battery temperature or the utilization, and is not necessarily equal to the previously charged amount. Self-discharge processes during storage cannot be accounted for.

Momentary Properties Measurement The momentary indication method is another approach for SoC determination, besides or alongside the continuous observation as described above. Physical, chemical, and electrical properties of a battery are characteristic for the state-of-health and absolute state-of-charge of a battery. The principle of a momentary SoC indication system is, according to Pop et al. [Pop+08, p. 26], defined by the following SoC factors. Some are momentary measurements, and others pre-determined characteristic values.

- Temperature of the battery (Dependent on use and surrounding conditions)
- Measurable voltage (Influenced by temperature, current drain, and others)
- Battery impedance (Computational electrical property as combination of resistance and reactance of the battery, indicator for SoH, depends on chemical conditions)
- Voltage relaxation time (A precise indicator for the absolute SoC of a battery, measured over longer idle times after charge or discharge cycles)

After measurement the values are further processed, error-corrected and filtered, and finally compared against known characteristic values of the battery model. These characteristic values are both pre-determined by the manufacturer and also dynamically adapted due to observed measurements. The presented battery state-of-charge indication method allows for a precise and absolute determination of the remaining applicable charge of a battery. The accuracy of the method, however, greatly depends on the accuracy and error-corrected measurement of the mentioned conditions.

Sufficient sensing and processing solutions are subject to novel product development, thanks to advances and interests in the industry of battery-powered electric automobiles. Commercially available battery management systems are still rare and relatively expensive.

State-of-Charge determination in UAVs The market for UAVs is young and competitive. The typical UAV is much cheaper than an electrical automobile and the design goal of low weight discourages the addition of complex components. Additionally, the need for a precise state-of-health determination is highly situational and depends on the use case. Therefore, most mid to low priced segment UAV models come with a simple solution, or none at all.

The conventional solution comprises an off-the-shelf battery pack and a simple metering component on the UAV side, as described in Section 2.4.3.1. Newer and higher-priced UAVs feature more sophisticated SoH and SoC indication hardware. Bundled smart batteries with momentary properties measurement capabilities are available in first UAV models released over the last few years.

2.4.3.2. Charging Cycle

Charging of a battery is in general characterized by an externally applied voltage, resulting in a current flow and therefore in an increase of stored electric charge. To safeguard the battery against high currents exceeding at least one of its physical and chemical boundaries, a special charger device will appropriately limit the maximum charging current. This is especially important at the beginning of the charging process, when the internal resistance of the battery is low and higher current flows are possible.

Lithium-ion polymer batteries are additionally sensible to high voltages and over-charging. With raising charging level, the battery voltage will converge to the charging voltage and eventually reach critical values, negatively affecting the state-of-health of the battery. Multistage charging methods are able to mitigate those risks, while they still top out at a state-of-charge of 100 %. Advanced methods, like presented by Khan et al. [Kha+16], are able to improve the charging time and charging efficiency.

The conventional multistage method commonly found in commercial chargers is called constant current constant voltage (CCCV). The diagram in Figure 2.4 illustrates a CCCV charging cycle for a single LiPo cell. The method consists of two stages.

The first stage is characterized by a constant charging current (CC) and a linear increase of stored charge in the battery. As the battery charging level rises, the battery voltage rises as well. At approximately 75 to 80 % of the maximum capacity, the aforementioned sub-critical battery voltage is reached and the CCCV charging process transitions into the second stage. The constant voltage stage (CV) fixes the charging voltage at the LiPo-typical maximum voltage of 4.2 V per cell. Because of the fixed charging voltage and the increasing battery charge, leading to an increased battery resistance, the charging current will decrease over time. This results in an overall non-linear monotonically decreasing rate of battery charging, until the full battery capacity is reached [Yan+10].

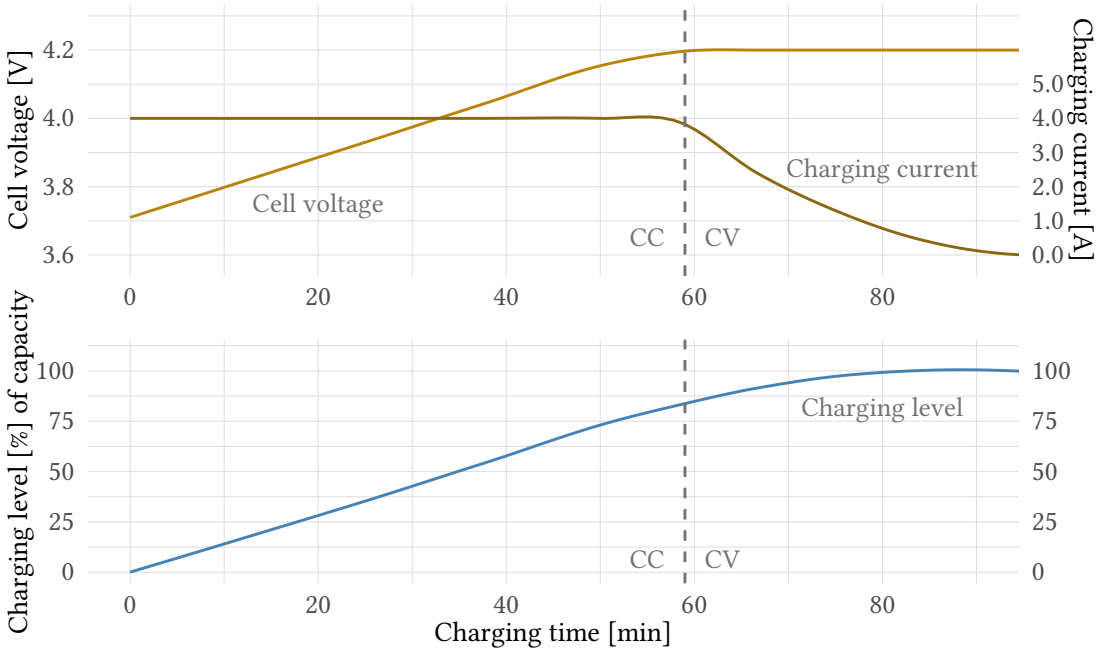

Figure 2.4 – Exemplary plot of battery voltage and the charging current, next to the resulting charging level for a typical LiPo cell. The depicted charging process follows the CCCV method.

2.4.3.3. Discharging Cycle

When a battery powers a consumer, its stored charge is provided to the consumer's electrical components. The battery charge is depleted and the battery might eventually reach full depletion.

Over the course of this process, the battery voltage continually decreases and additionally varies with the cell temperature and the discharge current. The cell voltage drops from up to 4.2 V to as far as 3.5 V over the viable part of the discharge cycle. Towards full depletion, the discharge cycle is characterized by a rapid decrease of the LiPo battery voltage.

As a lithium-ion polymer cell is sensitive to over-discharging, this last portion of up to 10 % of the cycle must be avoided to protect the battery from chemical impairment. Specific values are highly dependent on the manufacturer and model of the battery at hand. High quality products provide a steady voltage over a long range of the discharge cycle [Tra16].

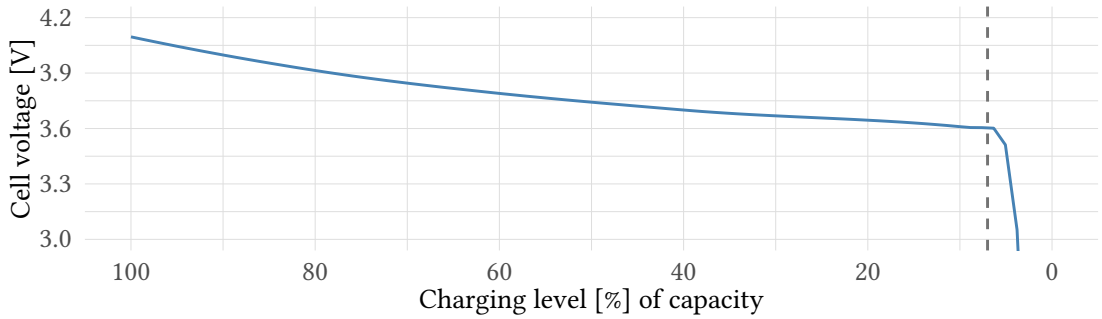

Figure 2.5 – Exemplary plot of the cell voltage over the course of a full discharge cycle for a typical LiPo battery. In the example the viable part of the battery ends at 8 % SoC.

A diagram showing the general tendency of the LiPo battery cell voltage over its full discharge cycle is depicted in Figure 2.5.

A consumer circuit utilizing a battery must be able to operate at non-constant voltages. Additionally, the state-of-charge should be monitored to avoid over-discharging. In professional LiPo battery applications, a battery management system should be applied to monitor the state-of-charge and to maintain a good state-of-health.

3. System Environment Analysis

The research question of this thesis is closely linked to the specifics of the operational environment considered. The utilization of UAVs is multifaceted and may differ in aspects like the number of tasks, the nature of movements, and the possibilities and limitations of the control and coordination system.

In this chapter we will introduce disaster scenarios, discuss the different response challenges faced, analyze the emerging tasks, and look at the derived assignments for robots. Furthermore, we will discuss the systematic structure behind response coordination with the help of UAVs, and present a conceptional layer model comprising the scenario breakdown, missions, maneuvers and UAVs. The chapter ends with a deeper look into the testbed UAVs used during the empirical study (see Section 4.1), the used flight controller software and communication protocol, and the central ground control station system. The presented information on UAV-aided disaster response creates the basis for the development of a purposeful resource management system.

3.1. Challenges of Disaster Response Scenarios

Natural or man-made disasters can emerge without prior signs and in the most diverse locations. This is especially true in the modern world, where many people live in crowded areas or in areas vulnerable to natural disasters, like the flooding zones of the United States or metropolitan areas with heightened earthquake probability throughout Asia. A coordinated response is crucial during or after the incident.

A reliable communication infrastructure is invaluable for reconnaissance, situation analysis, and combat and rescue coordination.

Typical use cases for UAVs are the construction of a comprehensive mobile ad hoc communication infrastructure for coordination [MGK12; Sas+14], and reconnaissance tasks like scouting an area for survivors and debris [MO07].

3.1.1. Disaster Response Aspects

According to Asplund et al. [ANS09] and Lundberg et al. [LA11] the challenges of disaster response are highly dependent upon an already existing reliable means of communication, to enable efficient task-oriented personnel and resource coordination. In "Communication Problems in Crisis Response" [LA11] Lundberg et al. identify five problem areas in the disaster communication environment:

1. Communication infrastructure – Restoration of a spanning network
2. Communication paths – Establishment of service demand fulfilling network routes between participants
3. Situation awareness – Perception and propagation of situational data, as well as execution of appropriate measures and countermeasures
4. Common ground – Clear and open communication on a human level
5. Message format – Task-specific preparation and presentation of data

Communication systems are eminent in providing critical services for major parts of the infrastructure of today's society and industry, e.g., in power grids, economic services, transportation and defense. Uninterrupted and secure communication is often taken for granted, even though the operation of services heavily relies on existing communication infrastructure. Ironically, the increasing complexity and interdependencies of these communication systems make them vulnerable to faults, accidents, and attacks.

In the event of a disaster, preexisting communication services are likely to be disrupted or disabled, e.g., infrastructure integrity and connections are often physically damaged, and cannot be reinstated in short-term. Bullet points 1 and 2 address this need for fast communication infrastructure restoration.

Reina et al. [Rei+15] found that a heterogeneous decentralized multihop ad hoc network fulfills the requirements of a communication network in disaster response scenarios. In literature, the research area of multihop ad hoc networks is broadly covered, Wang et al.

[Wan+16] even present a specific solution for disaster response network reconstruction. Most of the presented solutions expect and allow physical communication nodes to be distributed in the area, to be dynamically repositioned, and to occasionally emerge and disappear.

Reconnaissance is another important aspect of disaster response. The quick and unhindered search for survivors or the mapping of the disaster area for a clear situational understanding are important response actions. These and other reconnaissance tasks are covered by bullet point 3 of the list of problem areas in the disaster communication environment.

A central coordination and mission control unit is commonly available in disaster response scenarios. This is irrespective of the utilized, technically decentralized, communication infrastructure and results out of the need for central data collection and task planning by personnel at a disaster response base [Rei+15]. The task of the central coordination and mission control unit is the collection, preparation, and presentation for task-specific response decisions as required by bullet point 5 of the list of problem areas from above.

Bullet point 4 of the problem areas list is oriented at human relations and cannot be especially addressed by technology. However, the fast restoration of a communication infrastructure and the rapid and flexible collection and presentation of reconnaissance results is indirectly able to ease the effective interpersonal communication.

3.1.1.1. Technical Requirements

For communication infrastructure restoration and reconnaissance alike, we demand the following requirements towards a technical solution:

Instantaneous and Unhindered Restoration of communication infrastructure needs to happen as soon as possible. Potential geographic restrictions, like damaged streets caused by the disaster, need to be quickly overcome or bypassed.

Spanning and Heterogeneous Every radio communication technology has a natural signal propagation range limitation. The created infrastructure therefore needs to consist of multiple distributed communication nodes, interlinked to connect all participants in all parts of the disaster response area.

Purpose-Driven Command and coordination of response teams and the necessity for data communication (e.g. during reconnaissance tasks) depends on the disaster situation and development. The infrastructure and the provided network need to dynamically adapt to those changing communication requirements.

The creation of a distributed ad hoc network as well as the task-oriented execution of individual reconnaissance missions necessitate many independent and flexibly applicable operating agents. A disaster scenario will in general yield many parallel tasks and the utilization and management of agents thus need to be coordinated.

3.1.2. UAV Utilization in Disaster Response

The possibilities and advantages of UAVs, especially multicopters, were introduced in chapter Section 2.2.4. Due to their size and physical characteristics, they can be provided on-site, short-term, and deployed quickly. Their high degree of freedom allows for rapid agile maneuvers even in tight spaces and under harsh conditions. As flying vehicles they are flexible in their three-dimensional path planning, and therefore also capable of avoiding disaster-related road or field damages.

As UAVs are unmanned and relatively small, they pose minimal risks to human lives, which is especially important in the event of an unexpected system failure, which is a looming threat in disaster situations.

The following services can be distinguished for UAVs provision in the context of disaster response utilization:

On-Spot Service Provision Most non-airplane UAV types are capable of hovering in a certain position. Airplanes offer the option of a pseudo-hover by flying in a narrow circle around a fixed point. Another scenario is the planned landing of a UAV at its intended position, e.g., on a rooftop or in open field, not vulnerable to the effects of the disaster. In all these cases the UAV system qualifies as a fixed position service provider for the creation of an ad hoc spanning backbone network for both global interconnectivity and local connection of participants with the network. An analysis of placement strategies for meshed field coverage has previously been presented by the author of

this thesis [DMZ13]. Distributed fixed-position aerial platforms also offer the basis for a global sensing and observation system, beneficial for disaster response efforts.

Path-Dependent Service Provision This classical approach to service provision is characterized by a predefined path to follow. The path is herein either defined by waypoints or by point-to-point trajectories. Another configuration component can be movement speeds and/or arrival times. A moving UAV can quickly provide valuable data about bigger parts of the disaster area for reconnaissance and sensing. This data can then aid in effective and timely decision-making and coordination of next disaster response actions.

Message-Ferrying Service Provision Another rather special and often indispensable service in disaster situations is the establishment of communication between disaster response teams, that are separated by significant spatial distance, rendering a steady network connection infeasible or impossible. In such cases the concept of message-ferrying can be of service. Message-ferrying utilizes an agent, like a UAV, as a physical means of transportation of delay-tolerant data. The data is stored in the memory of the UAV, which moves between distinct exchange points along predefined paths. An algorithm to plan the movement of a ferrying UAV between multiple service-demanding exchange points was presented by Tobias Simon, a close colleague with an associated working group, in "A Self-Organized Message Ferrying Algorithm" [SM13]. The resulting movement principles of a message-ferrying UAV are comparable to the aforementioned path-dependent service provision.

Dynamic Path Service Provision Certain tasks of disaster response cannot be preplanned. In search and rescue missions, a UAV equipped with an infrared camera or gas sensor will adapt its movements according to the measured data, in order to complete the given task. The future movement of the UAV is unpredictable in this case. Dynamic paths and tasks are an inevitable aspect of disaster response actions. However, due to the research goal of this thesis and the limited predictability of dynamic movement in terms of future location and energy consumption, dynamic path service provision will not be a central research object in the scope of this thesis.

Overall, UAVs are an excellent fit for disaster response scenarios. They comply with the requirements listed in the previous section, and are able to providing the distinguished services to address the disaster response problem areas 1, 2, 3 and 5 listed in Section 3.1.1.

3.1.3. UAV Fleet Coordination in Disaster Response

In the previous section, we presented the utilization capabilities of single UAVs. It was shown that the UAV is able to aid in the aforementioned problem areas in the disaster communication environment. The utilization of multiple UAVs in disaster response scenarios is expected to accelerate the communication infrastructure restoration to support wider and more flexible communication needs, and to provide all kinds of reconnaissance services. In the area of sensor-based search and rescue missions, new unprecedented possibilities are provided by UAV utilization. Utilization of multiple UAVs permits the execution of a variety of missions in the scenario within a short time frame. In literature, the described combination of individual systems, to form a more complex new system with increased capabilities and additional functionalities, is called a system of systems (SoS).

Multiple UAVs could be utilized in swarms. Swarming is a special form of inter-UAV coordination and movement, in which a group of UAVs act in a cooperative fashion where all UAVs collaborate upon one task. Swarming introduces additional challenges and is attracting significant research interest, cf. [BSK10; LY15; Sas15; Sas+14]. Energy management and maintenance actions for single UAVs are not especially affected by the constellation of UAVs in groups. On the other side, requirements towards a swarm executing a mission may differ from single UAV utilization, in the dynamics of UAV count fluctuations, e.g., swarm rearrangements under group size flexibility. Those conceivable additional requirements and their potential effects on energy consumption form a new research question and are out of the considered scope of this work.

While some UAVs are utilized for independent missions, others might operate as part of a bigger task, like the creation of the spanning infrastructure network. The breakdown and assignment of all these missions to physically available and applicable UAVs has to be carried out by a well-suited entity. In Section 3.1.1 the demand for a central mission control unit was already justified based on the centralized personnel and resource

coordination in disaster response scenarios. Besides mission assignment, the mission control unit also has to coordinate UAVs in-between missions and before and after utilization. The mission control unit is thus also responsible for hardware and resource management.

The described necessity for management and coordination of diverse entities in disaster response tasks is complex. A generalized but flexible view on the overall system of systems is deemed to be useful for the discussion of next steps in our analysis.

3.2. Conceptional UAV Response Model

In the last few sections, we discussed various details of disaster response scenarios, the emerging tasks, and the benefits and new opportunities of UAV fleet utilization. A mission control unit was motivated.

In this section, a hierarchical layered model is defined for UAV-aided disaster response under anticipation of central coordination. The conceptional UAV response model is depicted in Figure 3.1.

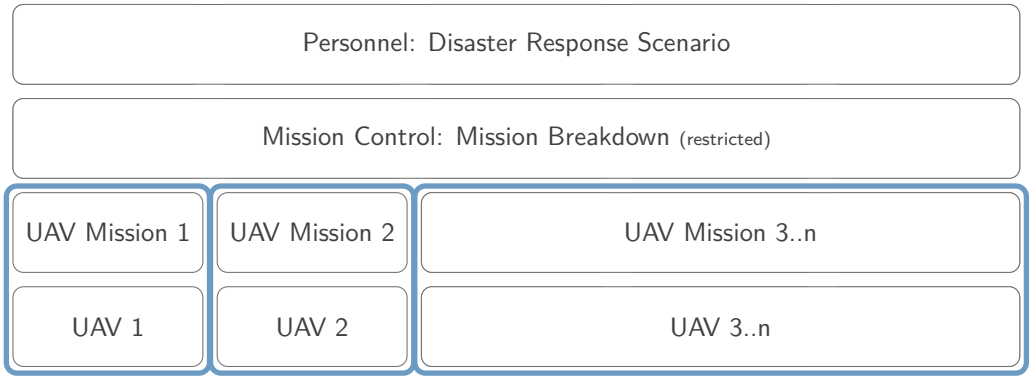

Figure 3.1 – Conceptional model of layered UAV scenario response coordination.

On highest layer, the model is represented by the disaster response scenario, which is characterized as good as possible by the response personnel and updated by personnel or automatically over time. In the following sections we will go into the details of the lower layers, and discuss responsibilities and challenges.

3.2.1. Mission Control Entity

A mission control unit was already motivated with the purpose of central coordination and management of all scenario-derived missions. The first step to that end is the mission breakdown. In a classical approach, which is the vantage point of this analysis, missions intended for UAV utilization have to be broken down substantially. This is founded on the limitations of the UAV flight capabilities and resource constraints, namely its aerodynamic limits and its battery capacity. Therefore, special UAV-tailored missions are addressed in the conceptional model in Figure 3.1.

Additional responsibilities of a mission control lie in hardware and resource management, however those are not yet addressed in the classical conceptional UAV response model and will be the subject of Chapter 5.

3.2.2. Scenario-Derived Missions

The concept of a mission in the scope of UAV-aided disaster response is defined by the combination of a movement and the execution of an operational task like wireless data transmission or reconnaissance. A mission can be of arbitrary size in both the spatial and temporal dimension and is only limited by the field and duration of the disaster response scenario.

We consider the operational task assigned to a UAV to have no significant variable impact on the energy consumption or the preplanned movement trajectory of the UAV utilization. Dynamic path development arising from received sensor data, as discussed in Section 3.1.2, is also excluded from the work on this thesis. Under these considerations the operational task will not have an influential part in this work.

We have to distinguish between the general term “mission”, and the term “UAV mission”. Where the former describes a mission according to the above definition in general, the latter is additionally restricted in length respectively duration to fit the capabilities of a single physical UAV. This differentiation is important, as a long-lasting single mission needs to be broken down substantially into multiple UAV missions to be executable.

A UAV mission overstretching the limitations of the assigned unique physical UAV (mainly because of its limited battery capacity) may end in catastrophic failure, loss,

and damages. Therefore, UAV mission planning has to take safety margins for flight energy consumption into account. However, at this point of the analysis, an insufficient understanding of the flight behavior and energy consumption is available. The planning of UAV missions and additional energy safety margins has to be carried out on rough estimates and will hence tend to over- and undershoot. Safety margins have to be selected generously, cutting overall utilization efficiency. A detailed discussion of safety margins will be given in Section 4.4.1.

3.2.3. Atomic Maneuvers

In the context of this thesis, a mission should be defined as a combination of maneuvers. Based on the UAV services described in Section 3.1.2 fundamental maneuvers can be derived for further examination: the hovering or pseudo-hover maneuver, the point-to-point movement, and movement trajectories of higher order. From an observational flight path point-of-view the higher order trajectories can easily be abstracted as a set of concatenated point-to-point maneuvers. Furthermore, because the main focus of this work lies on the multicopter UAV, which offers near-holonomic behavior (see Section 2.2.3), we can postulate that all maneuvers only depend on the current and target locations, but not on the orientation of the UAV. Concluding, only two parameterized maneuver types need to be differentiated:

1. **Hover maneuver** $M_h(t_c)$ – A flight maneuver type characterized by a fixed position in air and a duration. The maneuver duration is given by the specific command to be executed by the UAV.
2. **Point-to-point maneuver** $M_m(\vec{s_c})$ – A flight maneuver type characterized by a straight trajectory between two coordinates. Movement between those two points is expected to happen at constant speed. The maneuver direction and speed are given by the specific command to be executed by the UAV.

In a mission such maneuvers can be freely concatenated. We consider individual maneuvers to be atomic, meaning they are unambiguous in their definition and cannot be further broken down nor interrupted. We also expect maneuvers to not be of significant duration in comparison to the endurance limitation of a UAV.

3.2.4. Abstract UAV Entities

In the context of the conceptional UAV response model, the complex UAV system can be represented as a simple model, considering only its movement and energy consumption over the course of a mission. A small fixed-weight object invests electrical energy to allow controlled movement above ground in all directions.

Two types of maneuvers were introduced in the previous section. These are noticeably different in terms of control and navigational behavior, however looking at physical forces and energy consumption during these maneuvers, a slightly different distinction is appropriate. Due to the gravitational force, a certain amount of energy is always needed to hold the UAV in air. Additionally, changes in its position will have a negative or positive impact on the energy consumption. The acting forces and the overall energy consumption of our generic simplified UAV abstraction are illustrated in Figure 3.2 and can be divided into two parts:

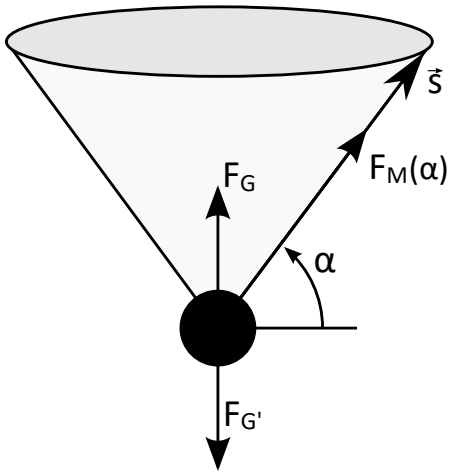

Figure 3.2 – Abstract multicopter model in the context of this thesis.

Altitude Conservation Energy The energy needed to hold the UAV in its position (hover, force F_G). Significant factors defining this energy portion are build specifications like number and efficiency of the motors, material and quality of the propellers, and/or total weight. These properties are assumed to be constant for one UAV system, a realistic assumption at least during one flight.

Displacement Energy The additional energy needed to change the position along a movement vector $\vec{s}$ (point-to-point, force $F_M(\alpha)$). Flying along a point-to-point vec-

tor constitutes the second part of the overall energy consumption. Due to the UAV's holonomic freedom of movement, its climb or descent angle α can be selected as the relevant part of the point-to-point vector. Other vector parts are assumed to not have any considerable influence on energy consumption (cf. Section 3.2.3).

3.2.5. Charging Stations

The charging station is not an essential part of the presented conceptional UAV response model, but an indispensable component of the UAV-aided disaster response system of systems. So far, the utilization of UAVs as mobile, fast and versatile platforms for disaster response assistance was in the focal point of our discussion. In order to provide UAVs for task execution beyond the endurance of the limited battery, a (re-)charging process for UAVs between utilizations has to be established.

Charging happens at designated locations with the necessary conditions, like an adequate energy source or available personnel to handle a manual connection sequence. In Section 2.4.3.2 the need for a special charger device matching the UAV battery type was highlighted. Further factors of charging possibilities in the field are the number of maximum parallel charging processes at one location and the amount of charging locations in the application field.

In real-world applications, the exact nature of the mentioned details might widely vary. For our analysis, we will assume one or multiple charging stations (CS) in the application field. A charging station provides multiple charging spots for parallel service. Charging of a battery installed in a UAV utilized in an automated operation bears the challenges of navigation to and a safe physical connection with a charger [LST13]. Multiple commercially available products provide automated charging capabilities, like the HiveUAV [Hiv18] or the Skysense Outdoor Charging Pad [Sky18]. Concepts to physically exchange the battery of a UAV in an automated fashion, as presented by Michini et al. [Mic+11] or Ure et al. [Ure+15], were not further considered in this work, as they lack compatibility with non-customized UAV models, like our testbed UAVs which will be presented in the next section. The exact sequence of steps leading to the charging and release of a UAV – be it a fully automatic process or manual plugging of connectors – shall not be of further interest in the scope of this thesis.

A charging station is an important necessary part of a UAV utilization project. It is, however, not part of our presented conceptional UAV response model, as it does not play an active role in the response coordination, but rather simply offers a passive necessary service.

The concept of an intelligent charging station (ICS) emerged during the work on this thesis. We define an ICS as a charging station with decision capabilities [Die+16]. The ICS is accompanied by an active component, like a microcontroller, which manages the activities in the local vicinity. The ICS offers waiting and charging spots and coordinates the assignment of these to approaching UAVs. It is also permitted to deny service to requesting UAVs due to capacity overload. Most importantly, the ICS offers interfaces for other systems, to retrieve consolidated data regarding available UAVs and their individual state-of-charge, estimates for future workload, and to select a UAV fit for utilization. A part of those features will be addressed in later concept decisions for our resource management system.

3.3. Boundaries Imposed by the Utilized Systems

The analysis as well as conceptional and implementational work in this thesis are aimed to be generally applicable for all UAVs, with special focus on multicopters. Beyond that, specific analysis steps, as well as necessary assumptions and restrictions, had to be decided on the particular hardware/software system used during the practical work surrounding this thesis. The sample system consists of two different testbed UAVs and a fitting combination of ground control station software. Product selection was based on functional, extensibility, and financial factors.

The deciding factors for product selection, as well as other important hardware and software characteristics of the utilized system, will be discussed in the following sections.

3.3.1. Hardware of Utilized Testbed UAVs

Two different multicopter builds were used in this thesis work to perform empirical analyses. The first one is a commercial “Solo” quadcopter by 3D Robotics [3DR18], which

is used as a reference platform to other commercial products. The second is a non-commercial quadcopter that has been custom-built from common off-the-shelf components. This copter is used for comparison and validation measurements to retrieve more generic insights on flight phase energy consumption in general.

Technical key data of both multicopters is given in Table 3.1. The 3DR Solo has a higher battery capacity, higher operating voltage, but also a higher weight. While the custom-built quadcopter was originally designed for agility and speed, 3D Robotics intended the Solo for autopilot-supported photography applications, hence making it stable and prepared for heavy equipment payloads. The battery capacity of both multicopters is given in milliampere-hours and watt-hours alike. The difference between the two units was discussed in Section 2.3.1 and in most cases they are interchangeable.

Table 3.1 – Comparison of the utilized multicopter systems based on key aspects.

	3D Robotics Solo	Custom-Built
Weight	1800 g	1150 g
Bat. Voltage	14.8 V	11.1 V
Bat. Capacity	5200 mA h	2200 mA h
	76.96 W h	24.42 W h

Both quadcopters employ the same microcontroller and run a firmware tailored to each system to enable autonomous flight. This setup provides the same flight algorithms for both systems, while taking physical differences into consideration.

3.3.1.1. Utilized Batteries and Applied Charging Method

Both testbed UAVs utilize batteries and battery chargers that operate following the CCCV multistage charging method, which was introduced in Section 2.4.3.2. A precedent analysis of our testbed batteries was carried out by Ludwig Breitsprecher [Bre18]. We were able to confirm the expected CCCV behavior and Ludwig Breitsprecher developed a reference implementation of an energy storage model.

The model depicted in Figure 3.3 is a simplified representation of the battery state-of-charge during a CCCV charging process, based on values for maximum capacity, projected full charging duration and parameters for the transition between the CC and CV

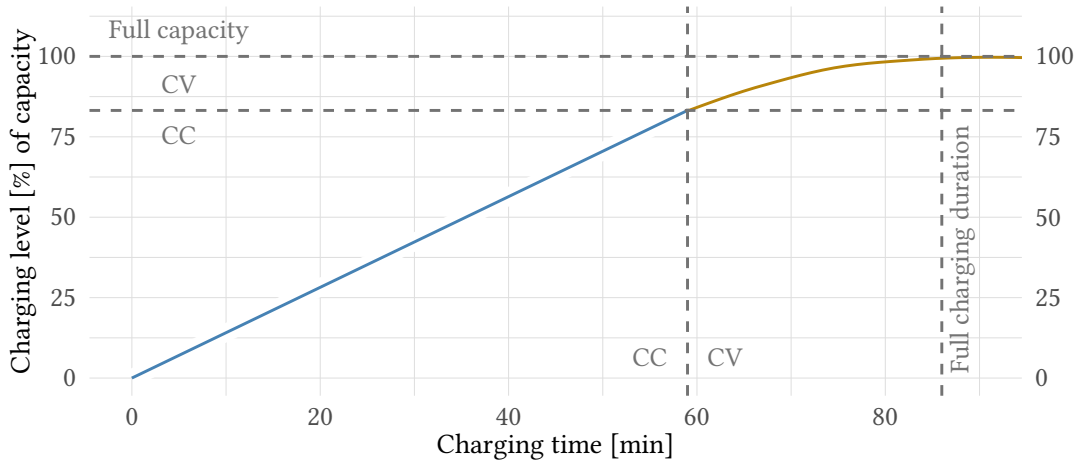

Figure 3.3 – Simplified battery charging model for the 3DR Solo battery, following the CCCV multistage method.

stages. The CC stage is characterized by a linear increase in battery charge, the subsequent second stage (CV) follows a smooth saturation function to eventually reach 100 % SoC after the full charging duration. Starting at a given remaining charge in the battery, the SoC after a certain duration can be estimated by this simplified underlying mathematical model [Bre18].

The simplified CCCV battery charging model for the 3DR Solo battery, derived from laboratory observations, is characterized by the key parameters given in Table 3.2.

The 3DR Solo quadcopter is equipped with a "smart battery" marketed battery pack. The bay-mounted battery is easy to attach and detach and comes with a built-in battery management system, offering detailed state-of-health and state-of-charge information over an SMBus (Revision 1.1 [SBS98]) communication link. The necessity for a high quality SoH and SoC monitoring was discussed and justified in Section 2.4.3.1. The 3DR Solo was specifically chosen because of this property, to ensure accurate and precise energy consumption readings for the planned empirical analysis.

The endurance of a battery during flight highly depends on the details of the mission executed by the UAV. Typical flight times of our testbed UAVs range from 10 to 20 minutes. It would be possible to attach higher capacity batteries for longer flight times. That is especially true for the custom-built quadcopter, which we also equipped with a 3000 mA h and a 4000 mA h battery for testing. These batteries increased the UAV endurance significantly, however part of the additionally gained flight time is negated by the added

Table 3.2 – 3DR Solo CCCV battery charging model characteristics.

	CC Stage	CV Stage
Full Duration	44 min	25 min
Capacity Range	0 to 85 %	85 to 100 %
Nominal/Peak Current	6 A	

weight and inflicted additional consumption. Bigger batteries increase flight time (up to a certain point) while decreasing energy efficiency. The added weight also affects flexibility due to inertia, and adds permanent stress on the airframe and powertrain of the UAV. For the remainder of this thesis, no other batteries were thus used for flight tests and further analysis steps.

3.3.1.2. UAV Flight Controller Firmware

The firmware installed on the flight controllers of both quadcopters is ArduPilot [Ard18a]. Technical details and a description of contributions during the work on this thesis are given in Appendix A.1.5. ArduPilot is an open source development project and offers support for all kinds of UAVs and numerous optional peripheral sensor and actor modules. The core of ArduPilot is a mature configurable flight control system, ensuring stabilization, reacting on remote inputs, and perform flight in different flight modes.

Autonomous flight mode is of special interest for this thesis. This mode enables the execution of maneuver-based missions without manual remote control and is hence the mode used during our UAV-aided disaster response scenarios. In the context of the ArduPilot firmware, missions are defined and provided as lists of commands that represent the concept of maneuvers as introduced before.

3.3.2. Ground Control Station Software

In addition to the firmware on the flight controller, the ground control station software used at the mission control is an important component of the overall system discussed in Section 3.2. The Mission Planner [Ard18b] PC software was used as part of our testbed system, cf. Appendix A.1.4. The GCS software is used to communicate with the UAVs,

configure their parameters, retrieve their telemetry data, or control aspects of their individual flight. The software also offers a graphical frontend to monitor UAVs and to plan command-based missions in a format defined by the ArduPilot project.

ArduPilot commands are characterized by a command type, target or operation coordinates, and optional command type specific data points. An example of a simple command list is given in Source Code 3.1. Interesting parts of each command are highlighted. The first column leads with an incremental command index and the forth column encodes the command type by its internal identifier. The 9th and 10th column represent geographic latitude and longitude, the 11th the altitude dictated by the command. All other columns are related to optional or deprecated command parameters, which are irrelevant for this discussion.

```
QGC WPL 110
0  0  0  22  0.00  0.00  0.00  0.00   0.000000   0.000000  30.0  1
1  0  0  16  0.00  0.00  0.00  0.00  50.683500  10.971500  75.0  1
2  0  0  16  0.00  0.00  0.00  0.00  50.682500  10.971500  30.0  1
3  0  0  20  0.00  0.00  0.00  0.00   0.000000   0.000000   0.0  1
```

Source Code 3.1 – An example command list generated by Mission Planner.

For comparison, the same command list is shown as a screenshot of the planning view of the Mission Planner software in Figure 3.4. Amongst the extensive list of existing command types, only a few are of interest to our application. Those commands with their respective identifiers are namely: navigate to waypoint (16), hover for a certain duration (19), return to launch location (20), land at location (21), and take-off from ground (22).

The previously introduced concept of maneuvers is closely linked to commands. Maneuvers as we defined them in Section 3.2.3 extend commands by the additional information of starting coordinates, while reducing their command types to a minimum pair of different maneuvers, judged by their flight behavior and resulting energy consumption. Table 3.3 shows a comparison between commands and maneuvers.

The combination of ArduPilot flight controller and Mission Planner GCS imposes a certain flight and mission execution behavior on our UAVs. Flight during the execution of

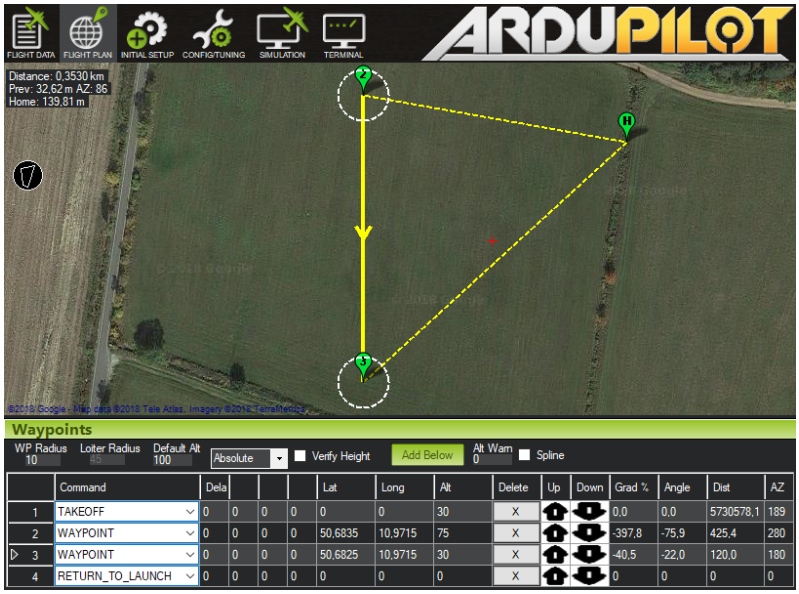

Figure 3.4 – Mission Planner view for the commands list in Source Code 3.1.

autonomous missions is controlled by internally configured parameters. Commands behind those missions do not include execution-specific data, like the flight speed for one single maneuver. Furthermore, ArduPilot commands do not give any option or guarantee with regard to the arrival time or deadline of one command. One exception is the hovering maneuver, which is characterized by a fixed duration. The duration of a point-to-point maneuver solely depends on the flight behavior resulting out of the UAV setup and the flight controller configuration.

Table 3.3 – Comparison between commands as used by ArduPilot and our concept of maneuvers.

	Commands	Maneuvers	
		Hover	Point-to-Point
Types	Over 131	1	1
Starting location	—	—	✓
Target location	✓	✓	✓

3.3.3. Control Communication Protocol

Due to the fast growth of the UAV industry, it is important to consider compatibility issues in UAV communication. The MAVLink [Mei+18] micro air vehicle link message marshalling library has been established to overcome the existing differences. MAVLink is a community-driven message library project for coordination of micro air vehicles. It was first released in 2009 by Lorenz Meier, as part of his work at ETH Zürich, under the LGPLv3 license. For further references and technical details including own contributions, cf. Appendix A.1.6.

MAVLink defines a very lightweight, header-only message set and structure and is widely incorporated in modern flight control firmwares, ground control stations, management software and other ground to UAV communication links. MAVLink has been implemented and extensively tested with established flight control systems such as PX4, PIXHAWK, and AR.Drone. It provides unified communication definitions among different types of robotic nodes, covering through all application disciplines including water, land, and air. All robots supporting MAVLink can be controlled by the same instructions, and collect and supply data in compatible formats. Many UAV vendors are also providing MAVLink capabilities, because of its versatility and simplicity [Mei+11; Coo+12; Arc+15].

The ArduPilot flight control firmware and the Mission Planner GCS software communicate using the MAVLink communication library. Most of the technical details and decisions outlined for ArduPilot and Mission Planner above, like the concept of commands and command types, can also be found in the MAVLink library.

3.3.3.1. Implementation of a MAVLink Maintenance Extension

MAVLink is specifically designed to support point-to-point communication between ground control stations and UAVs. Such a centralized approach is not feasible in all constellations.

In “Towards a Unified Decentralized Swarm Management and Maintenance Coordination Based on MAVLink” [Die+16] we proposed to use MAVLink on UAV-to-UAV communication links and presented a message set to support maintain UAV operation functionality, additionally support for groups and swarming behavior was introduced.

This includes replacement of UAVs or communication with an intelligent charging station (ICS) as introduced in Section 3.2.5 to improve the recharging process. Our addition can significantly reduce the overhead for an operator of a GCS to organize and control UAVs. The proposal forms the technical basis for the following chapters of this thesis.

The MAVLink extension proposal [Die+16] is based on the full definition worked out by the student work by Kati Neudert [Neu14], which was assigned and carried out in the context of this thesis.

The proposal includes detailed descriptions, formal message sequence charts, and a full message set implementation for the following topics:

- UAV management in groups
- UAV management in formations
- Maintenance actions for replacement
- Maintenance actions for recharging
- Maintenance coordination with an ICS
- Geographical regions with properties and restrictions
- Extensions on navigation capabilities
- Swarm management

All MAVLink extension details can be taken from the respective proposal documents and will not be repeated here.

In conclusion, the presented sample system provides typical components that could be used in a UAV-aided disaster response. A general UAV movement and energy consumption model will be derived by the help of the presented testbed UAVs in the following chapter. The discussed details about disaster scenarios, the utilization options and constraints of UAVs, and the conceptional response model will be important in the later development of a resource management system.

4. A Prediction Model for UAV Movement and Energy Consumption

An unmanned aerial vehicle, like most mobile robotic systems, has to rely on a limited electrical battery as its only energy source. Before we can discuss energy usage and transfer the results to a higher UAV fleet management level, we need to look at the movement and energy consumption of individual UAVs. This chapter provides details on the electrical energy consumption of UAVs in general, and the testbed quadcopter models introduced in Section 3.3.1 in particular. Based on the findings in an empirical study, an energy consumption prediction model is derived. Another discussed aspect is the role of uncertainty and the resulting need to include safety margins in the prediction algorithm. Finally, the chapter ends with a parameterized model of the energy consumption, representing the consumption of the 3DR Solo testbed quadcopter.

First experiments and analysis steps towards an energy consumption prediction model were performed by students assisting during the work on this thesis. The bachelor thesis by Niclas Büdenbender [Büd14] was oriented at a low-level energy consumption analysis based on a correlation between motor speed set values and power-draw readings. The work introduced the research field of energy consumption, but no clear maneuver relations were found as the theoretical model behind the UAV flight principles and energy consumption is inconceivably complex. It was furthermore found that a theoretical model is unfitting for the mission and maneuver oriented energy consumption prediction. As a concluding next step, the task of the students work by Peh, Löber, and Brackenhoff [PLB16] was to perform an energy consumption analysis based on anticipated correlations between a flight maneuver and its accumulated power readings. The results of their work were the starting point for the subsequently described analysis.

The characterization of the UAV as a *de facto* black box system should be based on real-world observations, and on the general flight principles of multicopter UAVs. Unlike theoretical models based on mechanical, electrotechnical or aerodynamic properties of

one system, this analysis concentrates on providing a reliable empirical energy consumption profiling methodology for a group of systems.

The work presented in Sections 4.1 and 4.3 have been published in a condensed version at the *SysCon'17* [DKZ17b]. Special aspects of energy consumption estimation uncertainty were the subject of our paper presented at the *VALUETOOLS 2017* [Die+17], which is the base for the in-detail discussion in Section 4.4.

The bachelor thesis by Tobias Krüger [Krü18] is another work originating from the context of the following analysis. A simplified version of the UAV energy consumption prediction model has been implemented in the ground control station software Mission Planner (cf. Section 3.3.2), which was used for flight planning in all practical experiments. The implementation was provided to the Mission Planner development community and all technical details and a source code reference can be found in Appendix A.1.4.

4.1. Empirical Flight Data Analysis

A good understanding of a system is crucial in order to improve it or the systems around it. For the sake of simulation-based optimization, an abstract model of the system, especially of the relevant parts of that system, needs to be available to generate realistic and comparable results. These results are ultimately the deciding factors in the modification, improvement, and optimization process.

An empirical analysis was carried out in order to develop both a generic state-based UAV consumption model, and a parameterization for that model based on data from the testbed UAVs.

4.1.1. Empirical Benchmark Measurements

In Section 3.2.4 we reduced the complex UAV to a simple model for maneuver-based mission execution with focus on energy consumption. First test flights and manual flight data observation and comparison suggests the expected model behavior, following analysis discussion will confirm it. Only the flight angle, as one variable factor, was found

to be of significant impact on the energy consumption of one multicopter UAV over the course of one maneuver, resulting in the aforementioned dependency $F_M(\alpha)$.

The high customizability of UAVs was highlighted in earlier chapters. Relevant invariable factors that are only changeable between flights are the total weight and the speed parameterization of the flight control. Modifications to the UAV setup, such as the materials and components used or the values of other control parameters, are not considered here as they would usually require a new calibration of the model. All mentioned factors are not in the scope of this work.

In order to evaluate the energy consumption of various flight phases, we planned multiple missions, each featuring different aspects and flight maneuvers.

4.1.1.1. Benchmark Flight Missions

After the first few test flights we identified three configurations as benchmarks for our energy profiling. These configurations reflect the major components of the UAV's movements:

1. Energy needed to maintain the current altitude
2. Energy needed for horizontal movement
3. Energy needed for movements with vertical portions

Accordingly, the following three flight patterns were planned as benchmark flights for later empirical flight data analysis.

Steady Hover Benchmark A simple mission is used to obtain a value for the energy consumption in hover mode. To achieve this, the copter is flown to a given position and instructed to stays there for about 10 min, at the configured altitude. For this we chose a flight area with almost no wind in order to avoid any influence of horizontal repositioning.

Horizontal Movement Benchmark We decided to use a squared flight pattern, as sketched in Figure 4.1a, to obtain measurement values for horizontal position change irrespective of any wind influences. In this pattern, the quadcopter is flown from waypoint to waypoint on a straight line without change in its altitude, until the square is completed and the quadcopter returns to its initial position. This setup ensures that systematic impact of wind from any given direction could be averaged out as it affects each flight phase from a different angle differently.

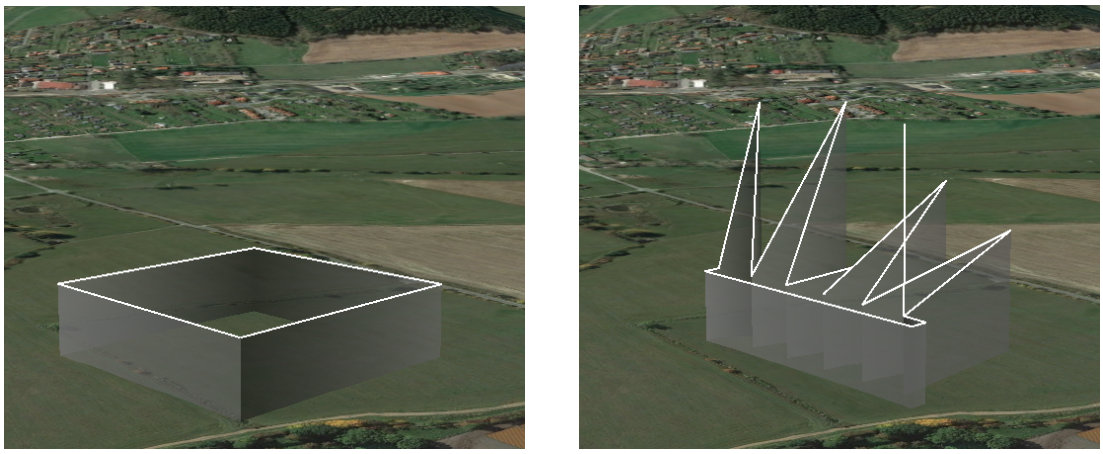

a: Benchmark #2 - Squared Flight

b: Benchmark #3 - Climb / Descent

Figure 4.1 – Two out of three planned benchmark flight patterns to gather measurements for horizontal and vertical movement.

Climb and Descent Benchmark Finally, the vertical position change is evaluated by repeatedly is flying the UAV from one position to another with a different altitude at a given climb angle, as shown in Figure 4.1b. After reaching the position, the quadcopter flies to the next position with its original altitude in order to capture the same angle but for descending movements. This flight pattern is repeated multiple times allowing measurements at different climb angles.

4.1.1.2. Flight Parameterization

We planned a certain minimum flight duration by choosing appropriate coordinates for each used flight pattern. This was to ensure that we gather enough individual measurements for our statistical analysis of the different flight phases. We carried out multiple

flights with each quadcopter for each setup based on this general concept. In total, we performed six to twelve flights for each mission.

Since both systems use the same firmware, they show similar flight characteristics even though the individual flight parameters are different. Whenever a UAV switches from one maneuver to the next at a given waypoint, there is some transient behavior that results in slight deviation in flight characteristics, such as acceleration and deceleration. This has been taken into account in the statistical analysis described below.

It should also be noted, that we did not vary the internal flight parameters between measurement flights. These parameters are numeric settings which influence the details of flight control, such as the maximum speed during automatic horizontal flight or the configuration of pre-processing algorithms for sensor data. Modification of such parameters would potentially change the UAV flight behavior and require a new analysis iteration.

4.1.1.3. Data Acquisition

The ArduCopter firmware collects very detailed logging information throughout a flight. Information regarding the flight control, mission execution, GPS readings, battery depletion and more is sampled every 100 ms. The generated log files can be retrieved from the internal flight controller memory after flight, and are in A comma-separated values file contains values in a table as a series of ASCII text lines organized so that each column value is separated by a comma from the next column's value and each row starts a new line. file format.

Wind was rated negligible in all captured benchmark flights by a preliminary measurement with an anemometer. Additionally, the measurement flights were dispersed over multiple days to account for weather differences. Individual UAV hardware was unchanged during all flights. In order to account for potential state-of-health differences between the individual testbed quadcoter batteries, multiple batteries of the same product type were used, three in the custom-built and four in the 3DR Solo quadcopter.

4.1.2. Statistical Sample Data Analysis

A detailed analysis of 20 selected individual captured flights was performed. This includes log files from both multicopter systems and all of the aforementioned flight patterns.

Details regarding the developed analysis script can be found in Appendix A.1.1.

4.1.2.1. Log File Parsing

The analysis script implements an algorithm of steps to select, filter, and transform the logged data to ultimately compute distinctive analysis results. To that end, the first step is to load each log file into memory and parse for relevant data.

```
1 IMU, 120872091, 0.00199961, -0.005316967, 0.0007880511, -0.4594238,
     0.4295748, -9.636625, 0, 0
2 CMD, 120887098, 9, 1, 16, 0, 0, 0, 0, 51.07728, 10.98858, 20
3 MODE, 120887127, Auto, 3
4 CURR, 120887164, 67, 1234, 214, 5354, 17.03422, 0
5 MAG, 120887200, -59, 166, 413, -89, -13, -16, 0, 0, 0, 1
6 BARO, 120890976, 2.217192, 100994.6, 24.44, -0.07670648
7 GPS, 120947045, 3, 472195600, 1887, 16, 0.70, 51.0772841,
     10.9890496, 0.12, 161.66, 0.07, 0.00, 0.03, 1
8 IMU, 120952054, 0.0003370403, 0.002114687, 0.002921721, -0.5191283,
     0.4812518, -9.787397, 0, 0
9 CURR, 120986942, 67, 1235, 219, 5349, 17.09505, 0
```

Source Code 4.1 – Excerpt from a Log File Showing Random Successive Lines

All log lines are per definition[1] sorted chronologically. All lines are formatted in a A comma-separated values file contains values in a table as a series of ASCII text lines organized so that each column value is separated by a comma from the next column's value and each row starts a new line. (CSV) structure in which different types of log entries are stored in conjunction with type-related data. An example of a typical log file can be seen in Source Code 4.1.

[1]The dataflash log format is documented at http://ardupilot.org/copter/docs/common-downloading-and-analyzing-data-logs-in-mission-planner.html (Retrieved 2018-03-01)

Primary parsing is done based on the type data field, given as the first field in every log line. For the purpose of further analysis the following data types are extracted from the vast amount of all lines:

- **MODE** – Log entries regarding the state of high level system operations
- **CMD** – Log entries on updated mission maneuvers
- **GPS** – Log entries containing positional location data
- **CURR** – Log entries with periodic energy consumption and status data

Furthermore, early log entries with type MSG are processed to differentiate between the different multicopter systems, based on a unique identifier.

All log entries consist of a timestamp and fine-grained discretized sampling data, for different relevant aspects of the covered data types. Most log entry types and data fields are skipped, others are transformed or added to aid in the following steps.

Log entries for the CURR data type are written at a supposed sampling time T_s of 100 ms. A quick analysis of one log data set confirms that the precision of the sampling is quite high, following a normal distribution, with a slight shift in accuracy:

$$T_s \sim \mathcal{N}(105.7, 0.041)\,\text{ms} \tag{4.1}$$

4.1.2.2. Maneuver Separation

The next step in computation is the selection of individual maneuvers and the separation of their steady states between transitions. Each maneuver is described by the start and end timestamp, and the underlying type and ID of both, the previous and active command needed to derive the maneuver path.

As shown in Figure 4.2, the transition between two distinct maneuvers is observable as a clear short-duration change in the average power-draw. Selection of power consumption samples from the flight log is therefore done based on the extracted timestamps, with a guard band of a two-second subtraction on both ends of the transition.

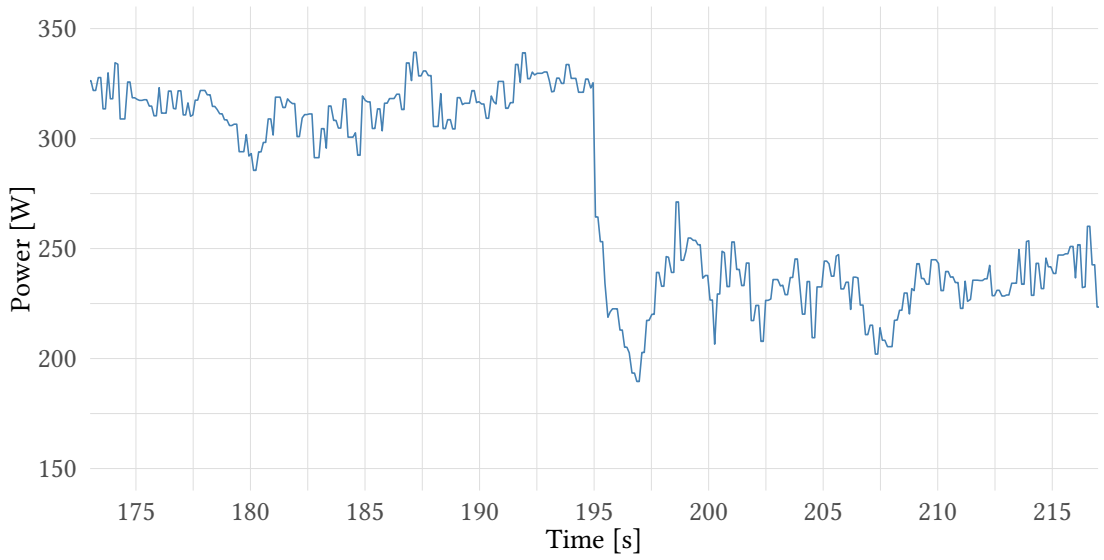

Figure 4.2 – Power measurements during maneuver transition.

4.1.2.3. Single Maneuver Analysis and Reduction

Measurements from within these selected maneuvers are statistically analyzed to compute the power-draw of the system for the duration of one maneuver. This is represented by the stochastic mean value and standard deviation. Additionally, the overall consumed energy is calculated.

For a point-to-point maneuver ($M_m(\vec{s_c})$), the climb or descent angle and distance traveled along this path are computed from both the predefined maneuver command instructions and the raw GPS recordings, for later comparison. The important parameter that is *speed of flight* is not part of the maneuver command, and has to be derived from the start and end GPS coordinates and the time it takes to travel on a linear path between them. The calculated speeds are expected to be of acceptably high precision. The reason for this is the low HDOP (horizontal dilution of precision) throughout all measured flights, as well as the negligible potential GPS position error in comparison to the maneuver distances which is approximately at least 50 m.

The special case of a hovering maneuver ($M_h(t_c)$) is processed quite similarly, but distances, angles, or speed data are irrelevant. The maneuver is characterized by its duration, derived from predefined maneuver command instructions, given by log entries of the CMD type.

4.1.2.4. Concluding the Separation and Reduction Process

The described computations are carried out for all maneuvers of one flight and for all selected flights. Each flight was tagged with information and data regarding the general conditions, which include surrounding weather like temperature or wind, weight additions, and other hardware setup modifications. Later analyses based on these factors are thus possible.

The last part of the statistical analysis concentrates on correlations between different maneuvers based on single parameters. Energy consumption values from all flights and maneuvers are, for example, compared based on their respective flight angle, duration and/or distance. Conclusions regarding the more general energy consumption profile can be derived from these considerations.

4.1.3. Evaluation of Initial Results

The measurements and examinations were done with the Solo quadcopter in general and with the described custom-built copter for comparison. In sum, 124 individual maneuvers were selected after separation and filtering.

In Figure 4.3 the raw power-draw readings of a randomly selected flight are shown, with each distinct maneuver visually separated. A few obvious assertions can be made solely based on the course of the diagram and confirmed with the consolidated data gained in the previously discussed analysis.

1. Every flight maneuver is characterized by an apparent mean power.
2. Maneuver mean power depends on the maneuver parameters.
3. Power draw is fluctuating around the mean value following a certain distribution. First analysis suggests a normal distribution of the individual reading samples.

Besides these, apparent higher-order influences spanning multiple samples of one maneuver are observable in the diagram and will be discussed in detail in Section 4.4.2.1.

In Figure 4.4, the first couple of seconds of the power samples are magnified and presented. The readings represent the initialization and standby phase of the UAV, after

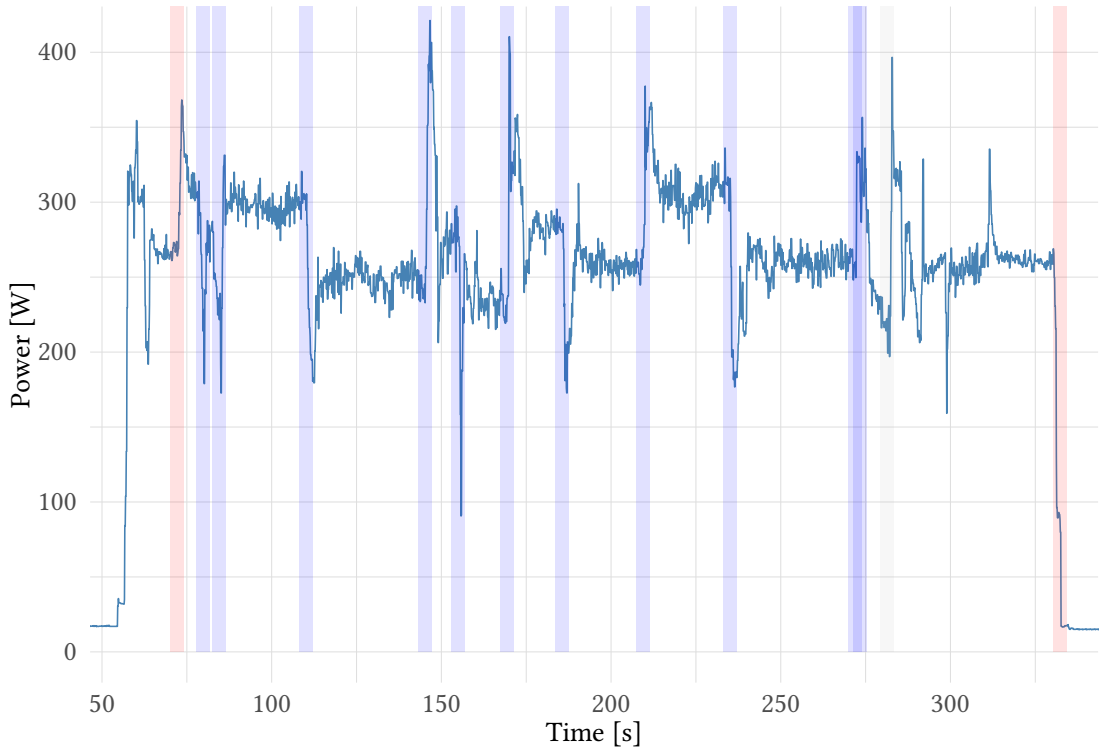

Figure 4.3 – Power readings of one complete benchmark flight. Blue separators characterize maneuver transitions, red separators indicate the beginning and end of automatic flight mode.

power-on and prior to arming, which is when the UAV is cleared to fly and starts turning its propellers. The activities during the initialization phase depend on the UAV build, and potential tasks in this phase include system checks and initial GPS localization.

Both parts of the phase are characterized by a nearly constant power-draw of approximately 16.4 W and 16.0 W, respectively. Compared with the 275 W of power consumption during flight, as illustrated in Figure 4.3, power consumption during the standby phase is negligible.

We planned a set of benchmark flights and executed them to collect measurement data. The described preliminary analysis gives us the needed understanding for a UAV model creation. The model and its properties will be the subject of the analysis and discussion in the next sections.

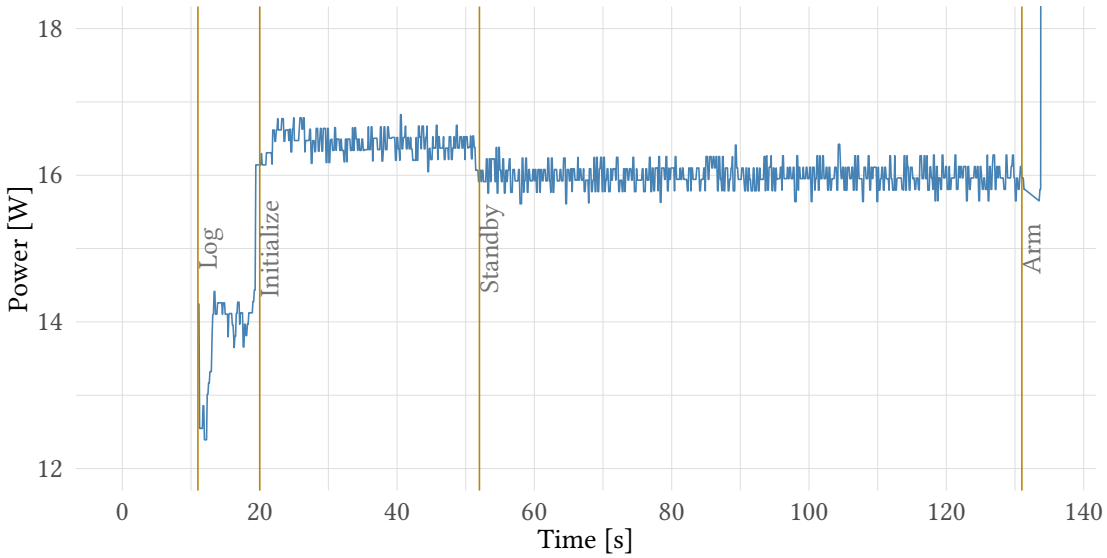

Figure 4.4 – Power readings during an example standby period.

4.1.4. Proof for Normal Distribution of Power Samples

Power samples were assumed to be normally distributed, however for further analysis the property must be proven. A quantile-quantile plot is a visual method to compare a sorted data set against a theoretical data set based on their respective quantiles. If both data sets have the same underlying distribution the resulting graph should show the identity line, irrespective of a sample offset.

In Figure 4.5 close proximity of the imperfect hovering maneuver sample plot to the identity line can be confirmed. The testbed UAV power reading sample data is therefore proven to be normally distributed with $P \sim \mathcal{N}(\mu, \sigma^2)$.

The same method was used to verify normal distribution for point-to-point maneuver sample data. This was to be expected, as external influences affect the UAV and its flight control irrespective of its movement.

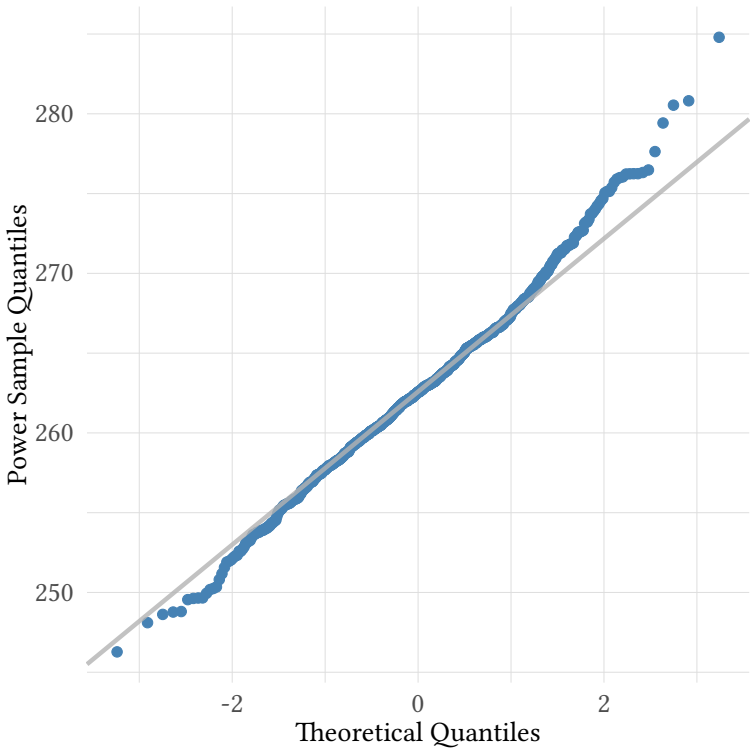

Figure 4.5 – Quantile-quantile plot of power samples from a hovering benchmark flight compared to a normal distribution.

4.2. A State Machine for UAV Energy Consumption Prediction

Our empirical study offers insight into the spatial movement and energy consumption behavior of UAV systems in general, and the utilized testbed quadcopters in particular. In this section we are going to derive a finite state machine model, representing a purpose-specific abstract view off generic UAV systems. As described in the introduction, emphasis during modeling primarily lies in the maneuver execution behavior, and the stochastic energy consumption. Aerodynamic, mechanical, and electrical processes and control cycles have been abstracted.

The initialization point of the UAV system is the moment in which it is powered up and ready to interact and fly. The motors are not active in the Standby state.

During flight, maneuver execution is characterized by a sequence of hovering ($M_h(t_c)$) and point-to-point maneuvers ($M_m(\vec{s_c})$). Transitioning between these happens after every maneuver execution.

Energy is consumed in each of the previously described states. After a certain number of maneuvers, causing a certain degree of battery depletion, the UAV transitions into the Charge state, which can be termed as a "negative consumption" state. Charging happens at the location of a charging station and navigation by the help of preliminary point-to-point maneuver is required. After a successful complete or partial charge, the UAV returns into the Standby state, ready to be redeployed. The described state machine is depicted in Figure 4.6.

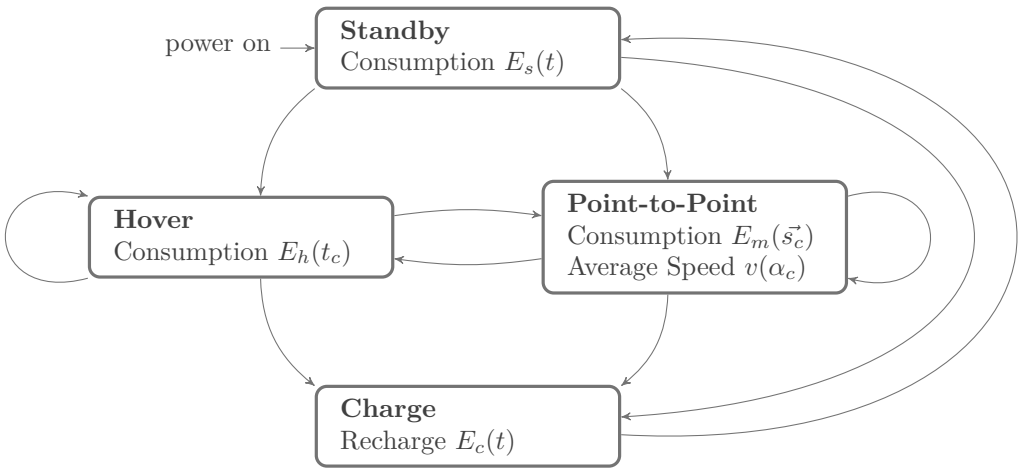

Figure 4.6 – The developed energy consumption oriented UAV state machine, illustrating the inner-state relations and inter-state transitions.

Maneuver transitions are omitted as a separate state, because of their negligible impact as found in Section 4.1.2.2. Transition triggering events are attributed to flight control maneuver execution decisions.

Inside the diagram states, the individual model-relevant functions are included. They represent energy use, recharging, and the spatial movement behavior represented by the flight-angle-dependent movement speed.

4.3. Parameter Inference

The important state-dependent functions derived from the empirical analysis as shown in the state machine presented above are:

- **Function 1** – Standby Energy Consumption: $E_s(t) \approx P_s t$
- **Function 2** – Point-to-Point Maneuver Average Speed: $v(\alpha_c)$
- **Function 3** – Hovering Maneuver Energy Consumption: $E_h(t_c) \sim \mathcal{N}(\mu_h, \sigma_h^2)$
- **Function 4** – Point-to-Point Maneuver E. Consumption: $E_m(\vec{s_c}) \sim \mathcal{N}(\mu_m, \sigma_m^2)$
- **Function 5** – Charging State Energy Recharge: $E_c(t)$

For the purposes of analysis and simulation of active UAV operations, the first and last functions are of little significance. In Figure 4.4 we illustrate that the standby energy consumption (Function 1) is rather insignificant in comparison to active maneuver execution. Recharging (Function 5), especially the recharging duration, will be an influential part of simulation and has been discussed in Section 2.4.3.2.

The flight-angle-dependency of the average flight speed during one maneuver (Function 2), has a direct influence on the point-to-point maneuver duration and therefore its energy consumption (Function 4). This systematic relation will be the subject of Section 4.3.2.

Both energy consumption functions are assumed to be normally distributed. The assumption is obvious, when considering the nature of the described figures, and has been proven by the appropriate stochastic method in Section 4.1.4.

The energy consumption of a maneuver for a certain duration (Function 3) or for a duration resulting from a certain distance traveled (Function 4), is defined as the integral of power flow over the maneuver duration t_c:

$$E(t_c) = E_{t_0 \to t_1} = \int_{t_0}^{t_1} P(t)\,\mathrm{d}t \tag{4.2}$$

Basic mathematics dictates, that the distribution of a sum of normally distributed samples out of one stochastic variable is by itself normally distributed. It may therefore be

concluded that the energy consumption of a maneuver is normally distributed under our assumptions.

In the following sections, the nature, parameter dependence, and mean values of the factors listed in Section 4.3 will be discussed. The variance of all three will be discussed in the subsequent Section 4.4.

4.3.1. Hovering Maneuver Energy Consumption

The testbed Solo quadcopter was used to gather sample data for the power-flow during the hovering benchmark flight, as described in Section 4.1.1.1. In Figure 4.7, next to the original time series plot, the accumulated time series data of one hovering benchmark flight – over a duration of 8 minutes and 48 seconds – is depicted as a histogram of sampled power readings. The histogram shows that the power consumption during steady-state of one maneuver is approximately normally distributed, as proven in Section 4.1.4.

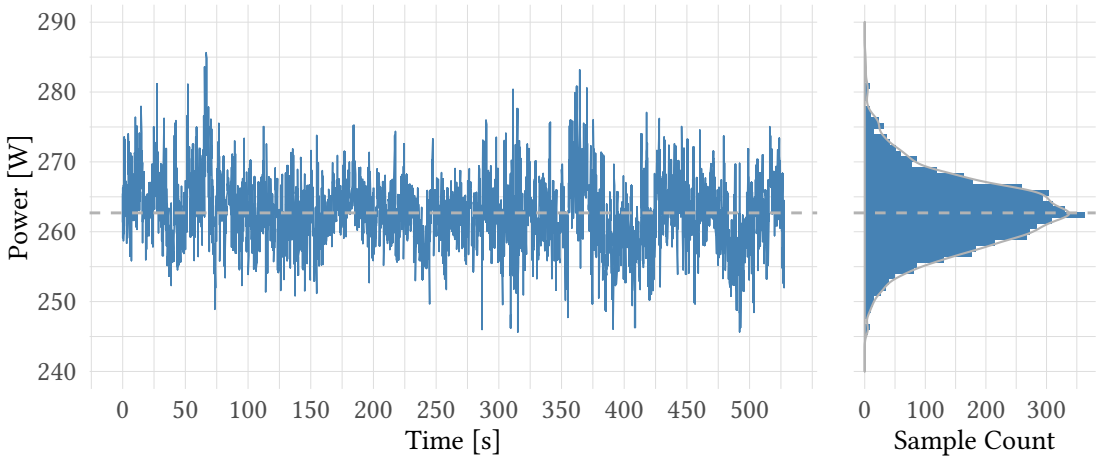

Figure 4.7 – Hovering benchmark flight power readings and the resulting sample histogram.

Every point-to-point maneuver is executed under the same control and stabilization principles and is prone to the same external influences. Energy consumption of point-to-point maneuvers is hence also normally distributed.

4.3.1.1. Evaluation of Sample Data Precision

Data gathered and derived from log entries, as described in Section 4.1.2.1 provides the means to calculate energy consumed by one complete maneuver or a segment of it. Multiple ways allow us to derive the overall consumption over a certain period of time. In this intermediate section we are going to discuss and compare different methods and evaluate their use for further analysis. The overall consumed energy of one maneuver can be derived from the sampled data in any of the following ways, and will be compared with the benchmark flight energy E_{hB}.

Difference taken from total current reading The current flow through the UAV is internally summed up and provided as the consumed charge value `CurrTot`. The value-by-value product of `CurrTot` and the battery voltage at the time, yield the total consumed energy of the UAV. Total energy values can simply be subtracted to obtain the relevant portion of the consumption for a certain duration. For the benchmark flight in question, maneuver energy consumption results in:

$$E_{hB1}(T) = E(t_0 + 528\,\mathrm{s}) - E(t_0) = 47.72\,\mathrm{W\,h} - 10.26\,\mathrm{W\,h} = 37.46\,\mathrm{W\,h} \tag{4.3}$$

The figure `CurrTot` is computed by a component directly connected to the battery, and summed up internally. The internal workings of the component are unknown and cannot be generalized, but amongst the other methods given below, this one is expected to be of the highest possible accuracy. The disadvantage of the reading is its absolute incremental nature and the provided low resolution. Differences for short time durations are therefore afflicted with discretization error. Additionally, this discretization error renders the figure unsuitable calculate statistical data on the energy consumption distribution.

Integral and sample sum from present power reading A typical course of sampled power readings is shown in the left half of Figure 4.7. Thanks to the high sampling rate confirmed in Equation 4.1, integration over samples is justified. Sampled power readings integrated over time should result in a good estimate of the overall energy

consumption. Potential differences to the aforementioned results could originate from the missing knowledge about the continuous signal before sampling.

$$E_{hB2}(T) = \int_{t_0}^{t_0+528\,\mathrm{s}} P(t)\,\mathrm{d}t = \sum_n (x_n T_n) = 38.539\,\mathrm{W\,h} \tag{4.4}$$

As the sampling rate has a high timely precision, it is furthermore acceptable to reduce the integral product to a simple sum of samples, which can further be reduced to the product of the sample mean and the overall duration. The method would be easier to use in the next steps of analysis.

$$E_{hB3}(T) = T_s \sum_n (x_n) = T_s(\mu_{x_n} n) = T\mu_{x_n} = 38.538\,\mathrm{W\,h} \tag{4.5}$$

Conclusion The results show that there is no *de facto* difference between the integration and sample sum methods of calculating the energy consumption from sample readings. More importantly, the results are almost identical to the first method of energy calculation from the internally summarized data. The difference is only 2.88 % and therefore fairly negligible. In light of the aforementioned disadvantages of the first method, further analysis will be carried out based on the sampled readings.

Another advantage when working with the sampled readings is the additional information available in the signal patterns, which will be discussed in Section 4.4.

4.3.2. Flight Angle to Flight Speed Correlation

In Section 4.2 the relation $v(\alpha_c)$ was already introduced as a relevant model part of the point-to-point maneuver and is the subject of this section.

First test flights suggested a clear relation between the climb or descent angle (α) and the average flight speed caused by the flight controller. The difference is easily observed in the field. In scope of the ArduPilot, mission planning level it is not intended to influence the flight speed directly, but rather as a result of of the point-to-point maneuver. The maneuver speed selection depends on the configured internal control parameters, and the stabilization and control algorithms utilized by the flight controller. These are invariant as previously shown in our initial analysis restrictions.

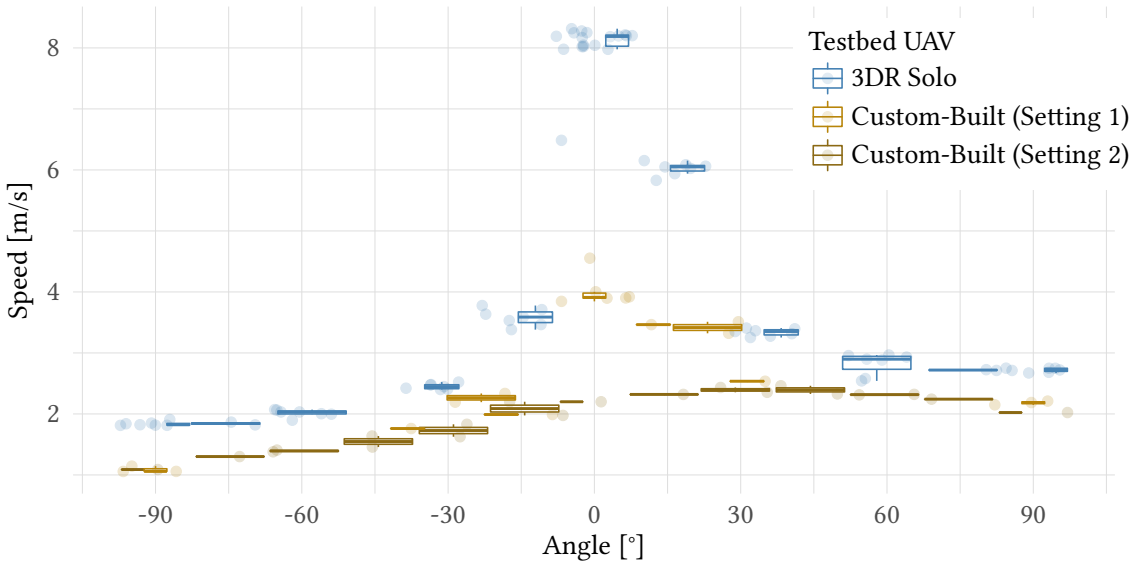

Figure 4.8 – Individual samples and resulting box plot of average speed values during different flight angles.

Combined flight data statistics were generated as described in Section 4.1.2.4. Information about the speed of the UAV during individual maneuvers can now be summarized, and brought into relation with the respective flight angles. Figure 4.8 shows average speed values at different flight angles from all considered benchmark flight maneuvers. Speed selection is clearly dependent on the flight angle, and deviation of values per angle is relatively low. While the 3DR Solo is traveling with 8 m/s at 0°, it is only traveling with 1.2 m/s in a −90° maneuver. A comparison between the two testbed quadcopters also confirms that the different hardware and parameter configuration of both systems has a clear speed selection impact, while having the same general tendency and precision. To confirm the parameterization dependency, a different flight controller setting for the custom-built quadcopter with reduced agility properties was added to the comparison.

In light of the high precision of the values and under consideration of the focal point of this analysis on energy consumption, it was decided to disregard the deviation of the average flight speed per angle as a model factor. Further analysis and simulation will assume a simplified average flight speed, dependent on a UAV specific function and the maneuver flight angle.

The main argument for that decision lies in the algorithm in ArduPilot [Ard18a] behind the flight navigation control. An analysis of the source code (see Appendix A.1.5) disclosed the nature of *Auto Mode* navigation and its impact on speed. Other than for land-based vehicles, positional changes for aerial mobile robots are done indirectly by change of the absolute target location. Navigation in automatic flight mode of ArduPilot is controlled by global target values, namely GPS coordinates. The travel time is therefore directly dependent on the individual maneuver details. Stochastic external influences, like headwind, do not have the propagation effect known from land-based vehicles.

In conclusion we can state that within certain boundaries, traveling speed is a parameter rather than an outcome of navigation control in our testbed UAVs.

4.3.3. Flight Angle to Energy Consumption Correlation

Climb or descent angle (α) was already named as one of the most important factors to affect energy consumption in point-to-point maneuver. In addition to the resulting flight speed, we also expecting a significant impact on the electrical power-draw, due to the maneuver flight angle.

The impact on the energy consumption $E_m(\vec{s_c})$ during a point-to-point maneuver is therefore twofold:

1. The flight angle has a direct impact on the energy consumption per time unit, due to increased or decreased power demand.
2. The flight angle has an indirect impact on energy consumption of a maneuver, due to the angle-dependence of the flight speed and the resulting maneuver duration, as shown in Section 4.3.2.

The trajectory $\vec{s_c}$ can be reduced to its influential components as discussed in Section 3.2.4. By applying the basic physical principles $E = P \cdot t$ and $t = d/v$, and in-

troducing flight angle dependencies, the energy consumption during a point-to-point maneuver can be represented thus:

$$\begin{aligned} E_m(\vec{s_c}) &= E_m(\alpha, d) \\ &= P_m(\alpha) \cdot t(d, \alpha) \\ &= P_m(\alpha) \cdot d/v(\alpha) \end{aligned} \tag{4.6}$$

The resulting point-to-point maneuver energy consumption depends on three components. The fixed maneuver-defined distance d, the flight-angle-dependent flight speed $v(\alpha)$ discussed in Section 4.3.2, and the flight-angle-dependent power-draw $P_m(\alpha)$. The remainder of this section is dedicated to a better characterization of the latter-most factor.

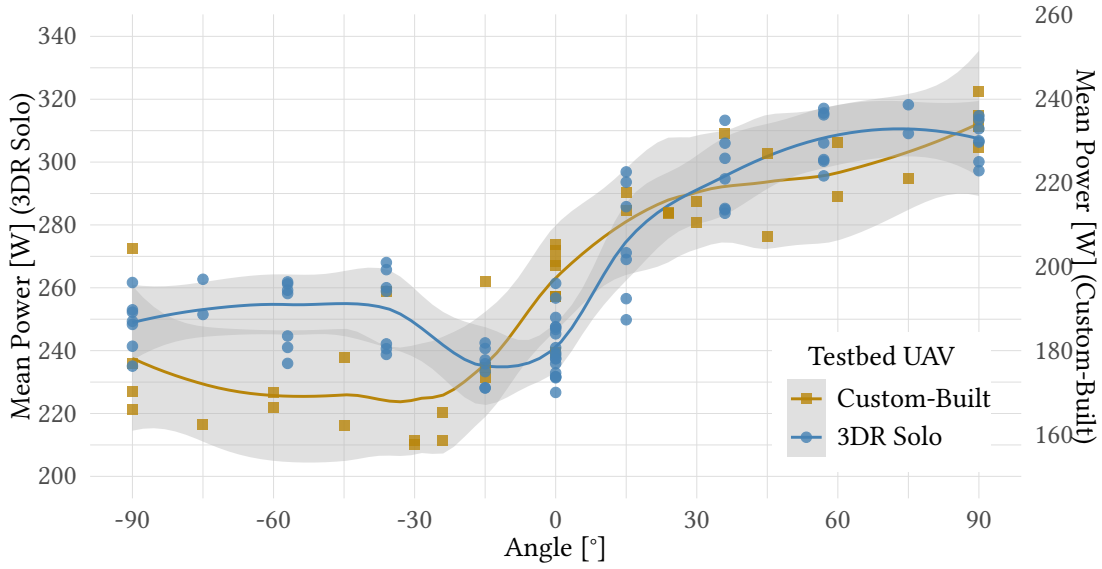

Figure 4.9 – Average power readings in relation to climb and descent angle, showing a comparison between both testbed UAVs. The custom-built copter values are normalized.

Figure 4.9 shows the mean power-draw from all the considered benchmark flight maneuvers, arranged by their respective maneuver climb or descent angle. Values for both testbed UAVs are differentiated for comparison. Trend lines in the diagram give the first impression of an angle-power-dependency.

Values calculated for the custom-built quadcopter are roughly three-fourth of those of the 3DR Solo. One of the most evident hardware differences in the comparison between

the two testbed UAVs in Section 3.3.1 was the used battery pack of three-cell (3S) versus four-cell (4S) battery size. The close proximity of the resulting data to the three-forth ratio is a coincidence resulting from the diverse physical and hardware properties of the UAVs.

By comparing flight-angle-dependent power-draw data, from both testbed quadcopters, we can assert that the general dependence tendency and value deviation are very similar. Aside from that, there are clear differences. The overall power-draw differs by a fraction of approximately three-by-four between our custom-built and the 3DR Solo quadcopter. Angle-to-power trend differences can be seen in the results for angles of decent. We assume that the reasons for this are the differently configured control parameters, or the construction and material differences like the overall weight.

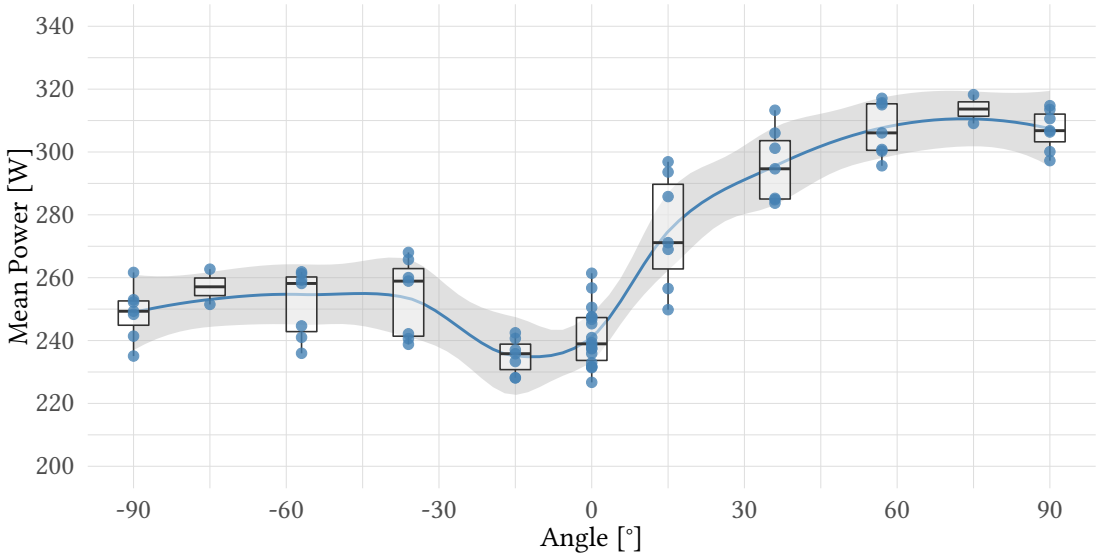

Figure 4.10 – Distribution of average power readings in relation to climb and descent angle, shown only for the 3DR Solo testbed UAV.

The following analysis will concentrate on the more densely covered 3DR Solo quadcopter. A specialized diagram version of Figure 4.9, only showing data for the 3DR Solo, is depicted in Figure 4.10.

The mean power-draw values for one angle from all flights are in close proximity. Deviation is approximately equal among all measured maneuvers. It is clearly visible that more power is drawn at climbing angles than at angles of descent, which was to be expected. Steeper angles, however, do not show a proportional effect on the power-draw,

contrary to our expectations. In fact, power-demand at ±90° is even lower than at close-by sloped angles. We see the reason for this behavior in the previously discussed flight speed being controlled by the flight controller and selected significantly slower than at 0°. While the quadcopter is traveling with 8 m/s at 0°, it is only traveling with 1.2 m/s at a −90° maneuver.

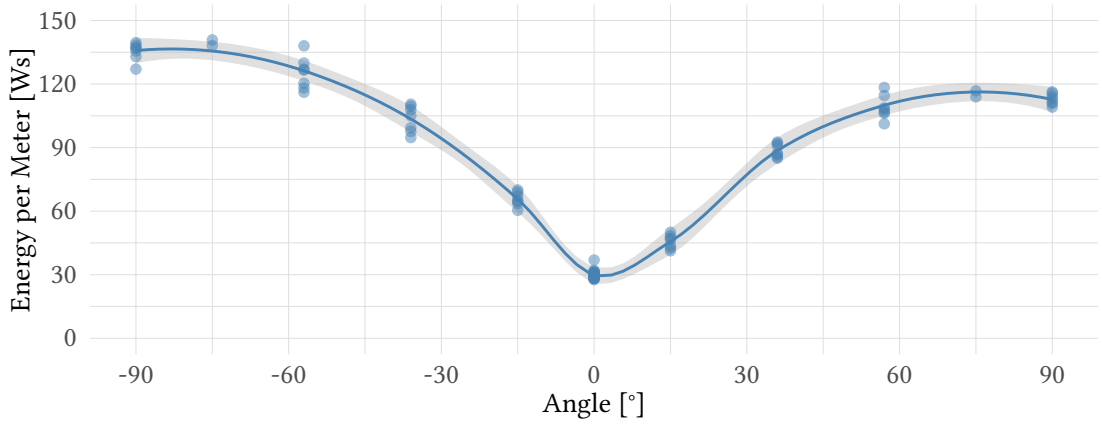

Figure 4.11 – Average power demand per meter covered at different climb and descent angles.

To mask the influence of UAV speed on the overall power-draw and to emphasize the maneuver progress of the UAV, Figure 4.11 illustrates a first approximate of the energy needed to surpass one meter of the point-to-point maneuver trajectory. This is based on the flight angle and the available power-draw samples, as derived in Equation 4.6.

The diagram shows an even stronger influence of the climb or descent angle on overall energy consumption per distance than on pure power-draw, while ignoring the time component included in previous diagram data. Beyond that, the diagram cannot be used to give insight into the stochastic nature of energy consumption of a distinct point-to-point maneuver. The results of this section are an understanding of mean power-draw and mean energy consumption during a point-to-point maneuver. The stochastic deviation of these values and the data needed to forecast probable energy consumption of a maneuver are the subject of the following sections.

4.4. Estimation Uncertainty

A precise estimate of gross energy consumption is indispensable for the simulation and planning of these UAV maneuvers. However, a system under imperfect conditions is always influenced by outside factors, and therefore suffers from stochastic uncertainty. The effects of the resulting fluctuations in the overall power-draw during one maneuver, of factors like wind, on movement and navigation adjustments, were already visible in the earlier sections.

In safety-critical systems planning with a mean or median estimate is insufficient. The UAV has a limited overall battery capacity, and will fail mid-air when the battery is depleted before reaching a safe landing spot, for instance at a charging station.

If one maneuver is planned under consideration of a mean consumption estimate, the UAV consumption will in reality vary close to this value. In Section 4.3 it was found that the energy consumption follows a normal distribution. In 50 % of all cases, the UAV will consume less energy than the mean value suggests. In the other half of all cases the consumption will exceed the assumed amount. A UAV maneuver scheduled close to the battery depletion level will, therefore, result in a premature battery depletion and system failure, in as far as 50 % of all cases.

4.4.1. Consideration of Safety Margins

Hardware failure due to energy depletion is not acceptable and a serious safety hazard. However, the sample space of a normally distributed stochastic variable is theoretically unbounded, and can take values far from its mean, no matter how improbable. Safety margins need to be included in the estimation of energy consumption to ensure the possibility of successful mission completion. Educated safety margin selection based on the mission characteristics and a stochastic model of the multicopter energy consumption, is important to find a good trade-off between multicopter utilization efficiency and failure probability.

In statistics the term “quantile” denotes values of the range of a random variable, dividing its distribution into equal parts of probability [For+10]. Based on the principle

of quantile division, the quantile function is a tool in probability statistics for quantile determination.

For a given continuous random variable Z, and a probability $p \in [0, 1]$, the quantile function Q yields the value z_p, at which the cumulative probability for the range $(-\infty, z_p]$ is less than or equal to the targeted probability p:

$$Q(p) = z_p \quad \text{under} \quad p \coloneqq P(Z \leqslant z_p) = F(z_p) = \int_{-\infty}^{z_p} f(z)\,\mathrm{d}z \tag{4.7}$$

The quantile function $Q(p)$ is the inverse to the distribution function $F(z_p)$. Also worth mentioning are the survival and inverse survival functions. While the distribution function and the quantile function address the probability that a random variable takes a value less than or equal to z_p, the survival function $S(z_p)$ and inverse survival function $Z(p)$ yield results for the probability of a value greater than z_p:

$$S(z) = P(Z > z_p) = 1 - F(z_p) \quad \text{and} \quad Z(p) = Q(1 - p) \tag{4.8}$$

This inverted view on probability is interesting for our analysis of energy consumption, because the probability of consumption overshoot and the resulting system failure is of high importance.

The quantile function and the inverse survival function are especially interesting for the next steps in the energy consumption estimation. They provide the means to calculate energy consumption values under safety margin inclusion, according to certain probability requirements.

Introduction of a safety margin in the energy consumption estimation process increases the probability that a UAV will sustain maneuver execution. An increase in quantile selection has a direct inverse impact on system failure probability. However, the assumption of higher energy consumption per maneuver has a negative impact on the overall schedulability. Heightened maneuver estimates lower the expected overall range or duration of the UAV mission and therewith its (potential) efficiency.

4.4.2. Duration-Dependent Variance Inference

In order to support efficient use of resources available to one UAV, and to assist with the timely execution of maintenance processes under an overall low risk of system failure, consumption estimates based on safety margins have to be used. In Section 4.4.1, we discussed the concept of quantiles, the quantile function Q and inverse survival function Z. They allow for systematic energy consumption estimation under a postulated failure probability requirement. Both Q and Z depend on the characteristics of the probability density function f, and therefore on the mean and variance of the energy consumption distribution.

The mean value of power-draw during maneuver execution ($\bar{P}$) was discussed in Section 4.3.1 and Section 4.3.3 and the calculation of the overall energy consumption of one maneuver was found to be directly proportional, $E = \bar{P} \cdot t$. Variance of the energy consumption distribution is yet unknown.

4.4.2.1. Characteristics of Signal Variance

Like for the mean, the goal is to infer the variance property of the energy consumption normal distribution from the power sample readings. By understanding the systematic relation between power-draw and energy consumption, the energy consumption for diverse maneuvers may be predicted, based on analysis results from a gross amount of power samples and the maneuver parameterization in question. Figure 4.12 shows a sample power readings plot for comparison. The three main challenges in energy consumption variance inference are:

1. Energy variance depends on maneuver duration (analog to the mean estimate)
2. Relative energy variance decreases with increased maneuver duration
3. Power time series samples are not statistically independent
   (explained and discussed below)

The first challenge becomes clear, when we think about the directly proportional relation between energy consumption and power-draw. In addition, the second challenge is easily understood by the following example.

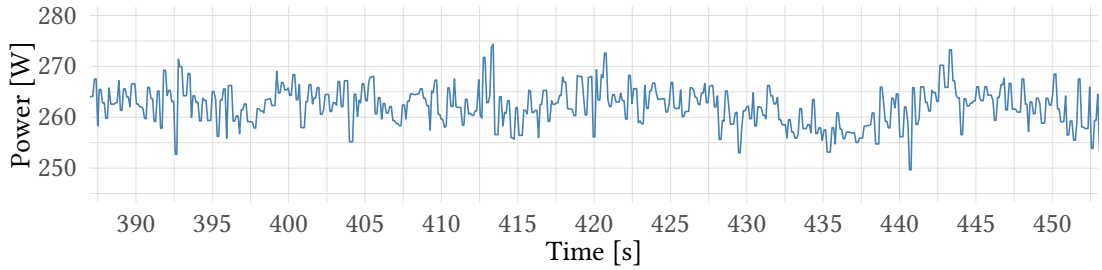

Figure 4.12 – Power readings during one example maneuver.

Imagine a sampling experiment over a fixed duration, covering k samples. The mean value of measured power readings is calculated for a single experiment trial, and summed up to result in a characteristic energy amount. Due to the stochastic nature of the base data, subsequent trials will result in slightly different trial consumptions. After the execution of sufficient trials, the pool of trial consumptions will create a normal distribution for $E_k \sim \mathcal{N}$ by itself.

Imagine extending the experiment duration from k to $k+1$ samples. Due to the nature of the normal distribution of individual samples, each draw from the sample space will likely be in close proximity to the sample mean value. Adding the sample $k+1$ to the resulting energy amount of all trials will therefore support the tendency to reduce the relative deviation of the overall energy consumption distribution E_{k+1}, so that:

$$\frac{\sigma_{E_k}}{k} > \frac{\sigma_{E_{k+1}}}{k+1} \tag{4.9}$$

Ott et al. [OL10, p. 185] discussed the described characteristic as the "standard deviation of the sampling distribution of the sample mean", characterized by

$$\sigma_x = \frac{\sigma}{\sqrt{k}}. \tag{4.10}$$

However, this is not applicable to the problem at hand. Due to the effects of higher order sample dependency of the time series as mentioned in the third challenge, a simple variance inference depending on the sample count is not sufficient. The method is able to describe the tendency of the expected result and a trend for the standard deviation of the energy consumption, as postulated in the second challenge.

4.4.2.2. Time Series Model Selection

The claim in the third challenge in Section 4.4.2.1 is essential for the next step in our analysis. The deviation of power-draw measurements originates not only from stochastic error and noise, but also and more importantly from external factors like wind. These systematic influences have short-term effects on the measurement series beyond one single sample, and need to be considered for a realistic energy consumption prediction as they have considerable effect on its deviation.

In stochastics, especially in time series analysis theory, an autoregressive integrated moving average model (ARIMA) is used to analyze and understand time series data, and to predict future development. The ARIMA model is a parameterized combination of an autoregressive model (AR), a process of subtracting non-stationary differences (integrated/I), and of a moving-average model (MA). A parameterization of the general model is depicted in the form of ARIMA(p, d, q), indicating a regressive model of order p, the execution of d integration steps, and a moving-average model of order q. Brockwell and Davis [BD91] have discussed the ARIMA model and its components, coefficient estimation and use, in-detail.

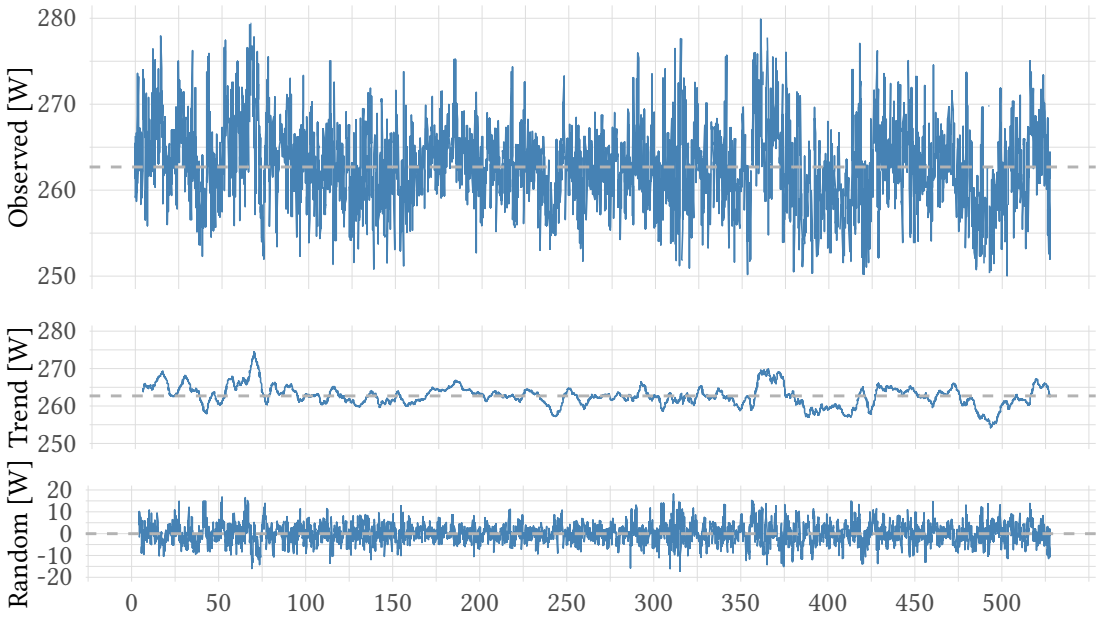

Figure 4.13 – Decomposition of additive time series data into its trend and random components, shown for one example hovering maneuver.

Single maneuver power readings are stationary and non-seasonal, meaning that they only consist of a trend component and an irregular random component. The separation into those two parts is visualized in Figure 4.13, based on power-draw readings from one example hovering maneuver. Therefore, no integration steps (I) are needed in the applied ARIMA model.

In order to determine a matching configuration of the remaining autoregressive (AR) and moving-average (MA) model parts, we carried out an analysis using the autocorrelation and the partial autocorrelation functions. The resulting autocorrelations per sample shift (lags) are shown in Figure 4.14. In the correlogram, we see that a large amount of lags exceed the significance bound. In the partial correlogram only the autocorrelation for the first few lags reaches outside the bounds. The correlogram indicates the moving-average model order, while the partial correlogram indicates the autoregressive model order. Smaller orders are generally preferred. According to these findings, the recommendations by Brockwell and Davis [BD91] is to discard the moving-average component from our model.

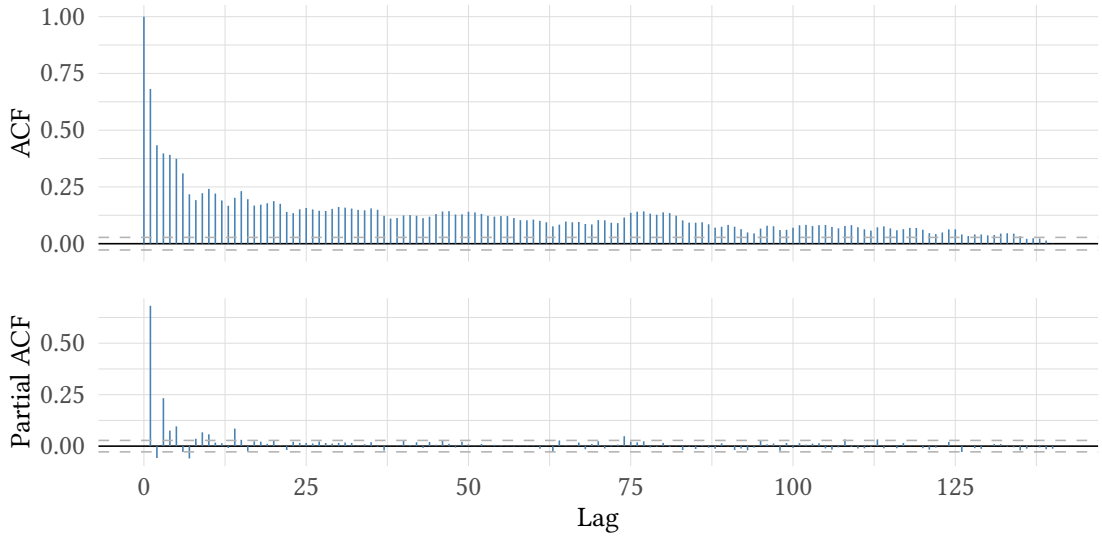

Figure 4.14 – Correlogram and partial correlogram of the stationary example time series.

In conclusion, the power-draw time series can be represented by an ARIMA$(p, 0, 0)$ model, or simply by an autoregressive model of order p. In the above example, the partial autocorrelations for lags 1 to 10 and 14 exceed the significance bounds, hence a AR(14) or even AR(10) model may be used to describe the example time series. In general the

use of a larger order model is mathematically and computationally less efficient, but will not worsen the prediction abilities of the model.

4.4.2.3. Variance Inference based on Autocorrelation Lags

Decomposition of the power-draw time series data, and determination of a fitting ARIMA model in the previous section provide the means to predict power-draw behavior of the observed UAV system. An autoregressive model for power-draw also enables the inference of connected characteristics, like variance of the energy consumption distribution.

Let $x_1, \ldots, x_n$ be the individual equidistant samples of one distinct stationary time series realization out of a common population of time series data, normally distributed with $X \sim \mathcal{N}(\mu, \sigma^2)$. The integral product under the signal is represented by

$$S = \sum_{i=1}^{n} x_i \quad \text{with} \quad \mathrm{E}[S] = \sum_{i=1}^{n} \mathrm{E}[x_i] = n\,\mu \tag{4.11}$$

as was proven in Section 4.3.1.1.

The variance of any random variable is mathematically equal to the covariance of the variable with itself:

$$\mathrm{Var}[S] = \mathrm{Cov}[S, S] \tag{4.12}$$

We can benefit from this alternative representation for our problem and bring the variance in relation with findings from the previously discussed autoregressive model. The autocorrelation function (ACF) introduced and applied in the previous Section 4.4.2.2 yields autocorrelation lags, which are:

$$\gamma(h) = \mathrm{Cov}[x_{i+h}, x_i] \tag{4.13}$$

Equation 4.12 can be transformed to take the autocorrelation knowledge of the time series into account:

$$\begin{aligned} \mathrm{Var}[S] &= \mathrm{Cov}\left[\sum_{i=1}^{n} x_i, \sum_{j=1}^{n} x_j\right] \\ &= \sum_{i=1}^{n}\sum_{j=1}^{n} \underbrace{\mathrm{Cov}\left[x_i, x_j\right]}_{\gamma(i-j)} \end{aligned} \tag{4.14}$$

Extraction of the sums of constant factor is allowed as a consequence of the definition of covariance. Analogous to Equation 4.13, the latter covariance factor is equal to $\gamma(i-j)$.

It is important to understand the ranges of indices i and j, and their relation to the lag index h. The matrix in Equation 4.15 illustrates the ranges as 1 to n of both variables, and gives their relative distance $|i-j|$ restricted by the matrix ranges. The relative distance $|i-j|$ can be derived from the matrix, and is equal to $|h| \in [0, n-1]$.

$$|i-j| \quad \begin{matrix} \\ \mathrm{i} \\ \downarrow \end{matrix} \begin{matrix} \mathrm{j} \rightarrow \\ \end{matrix} \begin{bmatrix} 0 & 1 & 2 & & \\ 1 & \ddots & \ddots & \ddots & \\ 2 & \ddots & \ddots & \ddots & 2 \\ & \ddots & \ddots & \ddots & 1 \\ & & 2 & 1 & 0 \end{bmatrix} = |h| \tag{4.15}$$

Further rearrangement of Equation 4.14 under the consideration of the matrix structure and the autocorrelation lags, results in the formula for variance of integral product S under a signal of n samples:

$$\mathrm{Var}[S] = n \underbrace{\gamma(0)}_{\mathrm{Var}[X]} + 2 \sum_{h=1}^{n-1} (n-h)\,\gamma(h) \tag{4.16}$$

The former term represents the n elements of zero lag, and the latter comprises the two triangular remaining halves of the matrix multiplied by their actual lag value $\gamma(h)$.

The parameter n originally represented the sample count of the analyzed time series. For consumption prediction n has to be selected according to the prediction time frame and the original time series interval, so that

$$n = \frac{T}{\Delta t} \tag{4.17}$$

yields the respective count of samples for prediction. Such scaling is needed as the autocorrelation lags are coupled with the original sampling interval.

Equation 4.16 allows us to calculate the variance of the integral product over a stationary, non-independent, and equidistant time series. The result is a normal distribution with

$$S \sim \mathcal{N}(n\mu, \mathrm{Var}[S]). \tag{4.18}$$

Finally, the theoretical result of S, given as "power times sampling step", has to be transformed to the actual energy unit for E, given as "power times time":

$$\begin{aligned} E &= \Delta t \cdot S \\ E &\sim \mathcal{N}(T \cdot \mu_P, \Delta t^2 \cdot \mathrm{Var}[S]) \end{aligned} \tag{4.19}$$

4.4.2.4. Maneuver Grouping for Variance Inference

We are now equipped with the means to generate a forecasting function for the variance of one distinct time series. During the benchmark flights discussed in Section 4.1.2, dozens of individual time series data sets were collected. The underlying maneuvers have distinct differences in their flight parameters, as summarized in the reduced UAV state machine diagram in Figure 4.6. Grouping identically parameterized maneuver time series data sets during the autocorrelation analysis will increase the validity of the analysis, while reducing the negative impact of single errors.

Let $X_1, \ldots, X_m$ be independent and identically distributed (i.i.d.) realizations of a normally distributed random variable X, with mean μ and variance σ^2. Every realization represents an equidistant and stationary time series with

$$\mathrm{E}[X_s] = \mu \; \forall s. \tag{4.20}$$

One possible realization was grounds for the discussion in Section 4.4.2.3 and lead to Equation 4.16. To utilize data from multiple data sets $X_1, \ldots, X_m$, we enhance the autocorrelation lag generation by determining the average of individual results. The autocorrelation lags computed for a group of m i.i.d. time series data sets are therefore given by

$$\gamma_G(h) = \frac{1}{m} \sum_{k=1}^{m} \mathrm{Cov}\left[x_{i+h}^k, x_i^k\right], \tag{4.21}$$

where $x_1^k, \ldots, x_n^k$ are the individual samples of the realization X_k.

The generated lags are expected to be of higher quality, as they are less affected by random interference expected from single maneuver time series data.

4.5. Multi-Maneuver Prediction

The energy consumption for one maneuver depends on the specifics of the individual UAV, as well as on maneuver characteristics like the climb or descent angle. The most influential factor is the maneuver duration, with a directly proportional effect on the mean consumption, and a strong monotonic relation with the variance of the consumption.

Let $M_i, i = 1, \ldots, p$ be independent but consecutive maneuvers of a mission assigned to a UAV. For each maneuver M_i with duration T_i and mean power-draw μ_{P_i}, the expected energy consumption E_i is normally distributed with

$$E_i \sim \mathcal{N}\Big(\underbrace{T_i \mu_{P_i}}_{\mu_i}, \underbrace{\Delta t^2 \, \mathrm{Var}[S_i]}_{\sigma_i^2}\Big), \tag{4.22}$$

as shown in Equation 4.19, and can be simplified as the energy consumption mean μ_i and variance σ_i^2.

The sum of independent normally distributed random variables is, according to Forbes et al. [For+10, p. 144], also normally distributed with the combined mean and variance:

$$E \sim \mathcal{N}\left(\sum_{i=1}^{p} \mu_i, \sum_{i=1}^{p} \sigma_i^2\right) \tag{4.23}$$

The resulting distribution of E characterizes the combined consumption over the course of the given p maneuvers. The distribution is also grounds for characteristics like a quantile value for combined consumption under certain safety margin requirements.

4.6. A Prediction Model for the 3DR Solo Quadcopter

Over the course of this chapter, we highlighted the challenges of defining an energy consumption model for UAV systems, the base for energy consumption prediction. To that end, an extensive empirical study was carried out to collect and analyze data from both testbed UAVs. As a result, a state machine representing the essential states of the UAV, with a focus on mission-based energy consumption, was presented. In combination, the resulting state-based mathematical model and the generated UAV specific values define the foundation of mission-specific energy consumption prediction in future simulations as well as real-world applications.

In this section we present a concrete model parameterization for the 3DR Solo quadcopter testbed UAV. The model follows the discussed parameterization process and real-world behavior simplifications.

The state machine diagram in Figure 4.15 shows an improved version of the general state machine depicted in Figure 4.6 on page 61, including the systematic findings from throughout this chapter.

For actual measurement and analysis value representation we decided to work with lookup tables (LUT), combined with linear interpolation, for the prediction of results for discrete input values, e.g., certain climb or descent angles. The decision is grounded

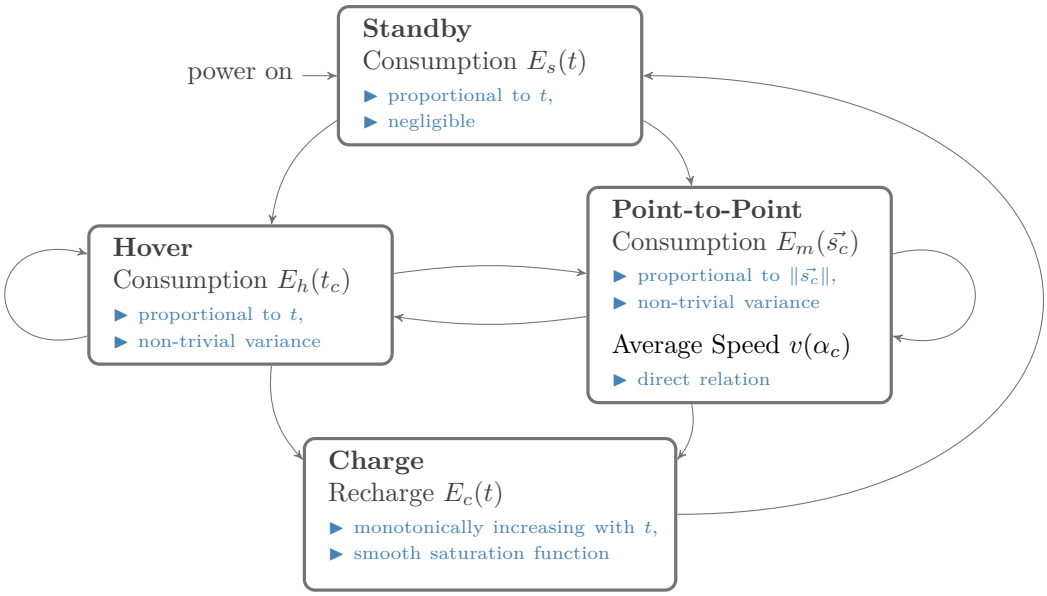

Figure 4.15 – Our energy consumption oriented UAV state machine, illustrating inter-state transitions, inner-state relations, and relation characteristics.

in the minimization of practical effort to parameterize it, and in the close proximity of the sampling range, leading to precise interpolations. For a generic input value x and a function f, the interpolated LUT-aided result will be y, depicted as:

$$f : x \overset{LUT}{\longmapsto} y = f^{LUT}(x) \tag{4.24}$$

The mapping function depends on the lookup table and linear interpolation as follows:

$$y = f^{LUT}(x) = LUT(x_0) + \frac{LUT(x_1) - LUT(x_0)}{x_1 - x_0}(x - x_0) \quad \text{with} \begin{matrix} x_0, x_1 \in LUT \\ x_0 \leqslant x \leqslant x_1 \end{matrix} \tag{4.25}$$

Besides parameterization details, concrete values for energy consumption over realistic maneuvers are shown as examples. The battery capacity of the 3DR Solo quadcopter battery of 76.96 W h may be used as a basis for comparison.

Standby State – Energy Consumption

The energy consumption of the 3DR Solo quadcopter during standby, with non-turning motors, was analyzed in Section 4.1.3. The power draw P_s was found to be almost constant and the consumption to be systematically insignificant, so that it may be simplified to:

$$E_s(t) = P_s \cdot t = 16.0\,\mathrm{W} \cdot t \tag{4.26}$$

Example: *How much energy does the testbed 3DR Solo quadcopter consume during a 30 minutes standby period?*

$$E_s(30\,\mathrm{min}) = 16.0\,\mathrm{W} \cdot 30\,\mathrm{min} = 8.0\,\mathrm{W\,h} \tag{4.27}$$

Point-to-Point State – Average Speed

The average flight speed per maneuver was found to be in direct relation to the climb or descent angle α_c. Based on averaged values for multiple maneuvers of specific angles, we presented characteristic average speeds of the 3DR Solo in Figure 4.8.

In Appendix A.2.1 a LUT for angle-speed dependence is given, so that the speed selection by the 3DR Solo flight controller may be estimated by $v = v^{LUT}(\alpha_c)$.

Example: *How fast does the testbed 3DR Solo quadcopter move on a point-to-point maneuver trajectory with a 45° climb angle?*

$$v^{LUT}(45°) = LUT(34.8°) + \frac{LUT(57.9°) - LUT(34.8°)}{57.9° - 34.8°}(45° - 34.8°) = 3.106\,\mathrm{m/s} \tag{4.28}$$

Hovering and Point-to-Point States – Energy Consumption

The energy consumption mean in maneuvers was found to be proportional to both the duration and the distance:

$$\begin{aligned} E_h(t_c) &= P_h \cdot t_c = 262.7\,\mathrm{W} \cdot t_c \\ E_m(\vec{s_c}) &= P_m^{LUT}(\alpha_c) \cdot d_c / v^{LUT}(\alpha_c) \end{aligned} \tag{4.29}$$

The mean power draw during a hovering maneuver was discussed in Section 4.3.1 and measurements suggest a mean value of 262.7 W for our testbed 3DR Solo quadcopter.

The mean power draw of a point-to-point maneuver ($P_m^{LUT}(\alpha_c)$) depends on the climb or descent angle and is given for our testbed 3DR Solo quadcopter by the LUT in Appendix A.2.2.

The discussion of deviation in Section 4.4 found the energy consumption variance to depend on the maneuver duration and implicitly on autocorrelation lag values. The needed lag values for our 3DR Solo quadcopter were computed following Equation 4.21, resulting in a lookup table of averaged lag values per benchmark climb or descent angle. The resulting LUTs for hovering and point-to-point maneuvers are presented in full in Appendix A.2.3.

Variance inference for actual energy consumption prediction is henceforth done utilizing Equation 4.16, with the produced lag values and the maneuver duration as input data.

Example: *How much energy does the testbed 3DR Solo quadcopter consume on average during a five minutes hovering maneuver?*

$$E_h(5\,\mathrm{min}) = 262.7\,\mathrm{W} \cdot 5\,\mathrm{min} = 21.89\,\mathrm{W\,h} \tag{4.30}$$

Example 2: *How much energy does the testbed 3DR Solo quadcopter consume on average, during a point-to-point maneuver with 45° climb angle and a 500 meter distance?*

$$\begin{aligned} E_m(\vec{s}\,) = E_m(\alpha, d) &= E_m(45°, 500\,\mathrm{m}) \\ &= P_m^{LUT}(45°) \cdot 500\,\mathrm{m} \,/\, v^{LUT}(45°) \\ &= 300.7\,\mathrm{W} \cdot 500\,\mathrm{m} \,/\, 3.106\,\mathrm{m/s} \\ &= 13.45\,\mathrm{W\,h} \end{aligned} \tag{4.31}$$

Example 3: *How much energy consumption has to be planned with for the previous example, when a safety margin for the lower 95 % of all cases should be guaranteed?*

Computation of variance is done using Equation 4.16 and under utilization of the LUT for autocorrelation lag values:

$$\mathrm{Var}[E_m(45°, 500\,\mathrm{m})] = 3.325^2 \tag{4.32}$$

The resulting normal distribution for energy consumption follows Equation 4.19 and is the base for quantile computation according to Section 4.4.1:

$$\begin{aligned} E_m(45°, 500\,\mathrm{m}) &\sim \mathcal{N}(13.45, 3.325^2)\,\mathrm{W\,h} \\ z_{0.95} &= 18.92\,\mathrm{W\,h} \end{aligned} \tag{4.33}$$

Charge State – Recharge

Recharging of the 3DR Solo battery was not specifically addressed in this chapter on energy consumption. Still, charging and the charge state are part of the state machine and part of the UAV life cycle.

In Section 2.4.3.2 and Section 3.2.5 we discussed and analyzed the charging behavior of batteries in general and practical experiments by a student are presented in Section 3.3.1.1, including a parameterization for the 3DR Solo battery CCCV charging process.

Example: *The battery of the testbed 3DR Solo quadcopter remains with 25 % of battery state-of-charge. How long will it take to charge up to 75 % and 100 %?*

The first case of 75 % target capacity can be calculated following the linear charging characteristic of the CC stage, as given by the simplified CCCV charging model for the 3DR Solo battery in Table 3.2:

$$\begin{aligned} T_c(25\,\%, 75\,\%) &= (75\,\%\,C - 25\,\%\,C) \,/\, I \\ &= 2600\,\text{mA h} \,/\, 6\,\text{A} = 26\,\text{min} \end{aligned} \tag{4.34}$$

In the second case, both the CC and CV stage of the simplified charging model have to be considered. The time calculation can be divided into the two portions and summed up to reach the final result. The full CV stage duration is taken from Table 3.2.

$$\begin{aligned} T_c(25\,\%, 100\,\%) &= T_c^{CC}(25\,\%, 85\,\%) + T_c^{CV}(85\,\%, 100\,\%) \\ &= 32\,\text{min} + 25\,\text{min} = 57\,\text{min} \end{aligned} \tag{4.35}$$

In the examples, the declining current and therefore less effective charging process during the CV stage is clearly visible. The latter 15 % in the second example take the same amount of time as the 50 % capacity difference charged in the first example.

5. Resource Management and Maintenance Requirements

UAVs are powered by a battery with a capacity for flights lasting for 15 minutes and more, depending on the hardware utilized. The concept of a mission was defined in Section 3.2.2 and a mission in the context of disaster response scenarios is generally expected to last longer periods of hours or days. A resource management system has to plan and coordinate maintenance processes to solve this conflict. It is inevitable for a comprehensive and timely utilization of UAVs in disaster response.

Over the course of this chapter, we will discuss different resource management aspects, derive resulting maintenance tasks, and work out the most influential parameters to achieve yet to be defined optimization goals.

Throughout the chapter, requirements will be derived and specified. Requirements are assigned with unique identifiers, following the scheme "[REQ-*category*-*index*]". Every requirement is assigned to a *category* classifying it as one of three categories. A functional requirement 'F' describes a functionality or system service, a non-functional requirements 'N' specifies the operation and quality goals of the system. A domain requirement 'D' characterizes bounds or restrictions of the application domain upon the system operation. The *index* is a three-digit number increased per requirement.

Identifiers will be reused in later sections to refer to the individual requirements.

5.1. Separation of Mission Planning and Resource Management

Scenarios as described in Section 3.1 dictate the extent of potential UAV utilization. The amount and nature of missions, emerging from the characteristics of a scenario, are not

easily derived and have been subject to related research. The specifics of how a scenario is divided into individual missions, that will in sum facilitate all scenario goals, and the planning of those missions are out of the scope of this work.

In Figure 3.1 on page 35 a preliminary view on the layered conceptional response model without resource management layer was given. The scope of this work is the resource management layer as a subordinated layer to the scenario response planning level. Resource management has to have lower planning priority as opposed to the scenario breakdown to ensure effective scenario response utilization. Even without knowing the details of exact scenarios, the following requirements are straightforward for our resource management layer to be interfaced with the upper level.

These base requirements address the importance of a resource management layer for the enablement of UAV-aided disaster response:

[REQ-F-101] Utilization of UAVs in disaster scenarios shall be accompanied by processes of resource management to achieve near-optimal performance with restricted means.

[REQ-F-102] Resource management shall not be part of the scenario breakdown and mission planning process to achieve separation of concerns.

[REQ-F-103] Resource management shall facilitate the uninterrupted execution of missions as part of the overall scenario to not compromise scenario response.

[REQ-F-104] Resource management shall not alter nor delay mission execution.

[REQ-F-105] The resource management layer shall not break the layer-to-layer communication interface compatibility to the scenario response planning layer.

[REQ-F-106] Resource management shall relieve the higher layer from all mission duration limitations induced by single UAV limitations.

[REQ-F-107] Resource management shall be able to react to changed, terminated or added future missions and mission maneuvers.

It is quite obvious, that a fusion of mission planning and resource management aspects would have measurable impact on the performance of the UAV-aided scenario response system. There are two reasons to exclude this option in the decision space of this work.

First, the aim of this thesis is to support UAV utilization in disaster scenarios. In these scenarios, missions are task-driven and defined based on expert knowledge. The consideration of necessary maintenance tasks incurred by resource management has to be out of the scope of this scenario-oriented planning process, to allow unrestricted and unhindered disaster response actions. Separation of mandatory resource management planning and effective scenario-oriented mission planning is an important requirement.

The second reason for a clear separation of the two planning processes lies in the complexity of the unification of those. Scenario-wide mission planning under consideration of the resource management processes for individual UAVs in a global and up-front manner poses vastly different challenges and would define a new research question for a subsequent thesis.

To be able to focus on the central research question the following constraints were drawn. They address the utilization domain of disaster scenarios and the disaster area, as well as the utilized UAVs, to simplify our analysis of strategies:

[REQ-D-301] The disaster area is assumed to portray steady weather conditions without significant wind.

[REQ-D-302] Resource management shall not attend to scenario-specific needs (like peripheral hardware devices).

[REQ-D-303] The overall utilization shall be based on one single UAV model with homogeneous configuration of entities.

[REQ-D-304] Resource management shall not induce restrictions or require preliminary modifications with regard to the utilized UAVs.

5.2. Restrictions on Mission Characteristics

Resource management shall enable and support the utilization of UAVs in disaster scenarios, which after mission breakdown means the uninterrupted execution of individual missions. Missions therefore have to fulfill certain requirements to be manageable. The following requirements are defined for missions and expected as a result of mission breakdown by the mission control:

[REQ-D-305] Missions are assumed to be long-lasting or continuous in duration to necessitate resource management.

[REQ-D-306] Single maneuvers are atomic and non-interruptible by resource management.

[REQ-D-307] Single maneuvers are considerably shorter than the flight time of a single UAV to allow maintenance processes in-between maneuvers.

These domain requirements originate from the environment analysis of the response model in Section 3.2.

5.3. Resources and Mandatory Management Processes

The task of resource management is characterized by processes that enable and ensure consistent resource availability for mission execution. Limited resources in geographically separate locations have to be appointed, deployed and applied to aid in that effort. Those processes pose certain challenges regarding the required knowledge, their timely scheduling, and the overcoming of shortages and restrictions. The following sections address different resources, related management aspects, and resulting challenges of those.

5.3.1. Resource Overview

Resources of UAV-aided disaster scenario response actions are namely of three categories:

- UAVs – The amount of physical UAVs utilized during the scenario
- UAV energy – The electrical energy available to a single UAVs on ground or in the field, at a certain point in time
- Ground storage energy – The amount of electrical energy available at charging stations for operation and recharging processes.

The last item on the list is either restricted by an exhaustible energy storage or unlimited due to a connection to the global power grid. The gross amount of electrical energy

needed for a scenario depends on the scenario complexity and will increase with the scenario duration. The ground energy resource availability is deemed to be less important for further discussion of resource management processes, and will only be considered as a base requirement and during the evaluation of gross energy demand. This does, however, not ignore the location of individual charging stations, which can improve management processes if well selected.

The energy stored by a single UAV is limited by the battery capacity. During UAV utilization, energy consumed can be assigned to one of two portions: energy consumed during mission execution and energy consumed to perform maintenance flights. Maintenance flights, even though required in order to sustain mission fulfillment, do not contribute to the progress and success of a mission. Additionally, maintenance flight duration has a direct negative impact on the potential duration of mission execution, due to the fact that both are sourced out of the limited overall operation time. Minimization of the maintenance energy portion is therefore expected to increase overall efficiency of UAV utilization, and thus decrease the amount of UAVs needed to support the uninterrupted advancement of the scenario.

The total amount of physical UAVs is seen as the most important resource metric. The provision of hardware for and during a disaster response scenario is potentially critical. Acquisition of additional UAV entities is also critical from an economical stand point. Minimization of energy used for maintenance flights, and thus extension of mission execution, is expected to aid in the minimization of needed physical UAVs to support all missions in a scenario.

5.3.2. Management Aspects

The task of resource management is to provide resources and to react to changing resource demands of the application scenario. The main goal is to enable and support the uninterrupted execution of all missions defined by a scenario. Timeliness is an important aspect of resource management. Missions should not be delayed or rendered impossible due to resource limitations.

In Section 4.3 the stochastic nature of UAV movement and energy consumption was analyzed and described in an abstract model. This probabilistic model can be used to

predict future developments and therefore help make resource management decisions. Stochastics dictate that a certain outcome is never guaranteed for processes under the influence of uncertainty. Another task of resource management is therefore to balance the trade-off between resource wastage and safety. This includes, for instance, maneuver scheduling delays or the loss of UAVs to hardware failure inflicted by battery depletion.

These aspects result in the following requirements:

[REQ-F-108] Resource management shall work with a realistic prediction model to forecast the spatial movement of individual UAVs.

[REQ-F-109] Resource management shall work with a realistic prediction model to forecast the energy consumption of individual UAVs.

[REQ-F-110] Resource management shall plan maintenance processes to enable and support UAV utilization in the application scenario.

[REQ-F-111] Resource management shall consider stochastic uncertainty during forecasting of UAV movement and consumption behavior.

[REQ-F-112] Resource management shall consider stochastic uncertainty during maintenance process planning.

[REQ-F-113] Resource management shall be able to handle the event of unexpected UAV failure.

The possibility of spontaneous hardware or software failures was previously discussed as a serious threat to successful disaster response. The mitigation of such failures lies in the responsibility of the UAV product development team and can be analyzed and modeled using methods from the research field of failure analysis. This requires a preceding examination of the failure modes and probabilities of UAVs in general, and of our testbed UAVs in particular. Without a realistic failure model, an inclusion in following analysis and evaluation steps is meaningless and will not contribute to our research question. In addition, we expect the probability of spontaneous failure to be considerably lower than the probability for battery-depletion-related failure at the end of a flight resulting out of bad resource management planning. Because of the these reasons, we will not consider spontaneous failure in later steps and the concluding evaluation. Requirement [REQ-F-113] still holds true as a requirement towards a resource management system.

5.3.3. Challenges of Resource Management

In order to fulfill the requirements towards an effective resource management system and strategy, the following challenges have to be overcome:

Knowledge of the field state The location and state of all UAVs in the field is not global knowledge. In real-world, a communication interface is needed to propagate data and to interact with communication partners. Data regarding the state of individual UAVs, like spatial movement or the energy storage, has to be communicated to a central resource management entity. Transmission of data related to resource management has to be scheduled and processed. A good picture of the situation in the field is grounds for efficient resource management.

Predictability of future needs With a good knowledge of the mission, location, and state of UAVs, and an abstract prediction model, future progression can be predicted. This is the basis for prediction of future needs and planning of according maintenance processes by the resource management layer. A precise prediction model is available as the result of the analysis presented from Sections 4.2 to 4.5.

Viability under restrictions Resources are limited by nature. The remaining energy of a UAV is the most pressing limitation, which has to be managed. However, there is also a limitation of UAVs themselves, as mentioned before. The total amount of available entities applicable in the field is likely to be restricted by economic factors or logistics. UAVs are either executing a mission, out of service and recharging, or in transition between those states. While the number of concurrent UAVs in mission depends on the scenario and is expected to be constant over long time spans, the other two states are solely related to resource management and can be subject to optimization. A good management strategy should be able to appropriately schedule UAV utilization and maintenance, to reduce the maximum amount of concurrently utilized UAVs in an application scenario.

To cover all resource management aspects under the given challenges, maintenance processes have to be scheduled and executed.

5.4. Maintenance Processes

The key issue of resource management is the limited energy capacity of individual UAVs. Restoration of the energy stored in a battery is typically done by recharging, a lengthy process involving additional external hardware. Recharging typically happens at a charging station, as introduced in Section 3.2.5. As recharging is not feasible during mission utilization, physical replacement is needed to sustain mission execution.

Battery recharging is actually the most important factor of the UAV utilization, which is obvious by comparing average flight times of approximately 20 minutes against the average recharge cycle of approximately 60 minutes. This downtime of a UAV could only be avoided by a mechanical replacement of its battery, an option that is not taken into account in our model. The decision is also related to Requirement [REQ-D-304].

Additional UAV entities are therefore needed to enable replacement and to compensate for temporal downtimes of charging UAV. Depleted UAVs have to be recharged to restore operational readiness and to support continuous execution of missions with a limited amount of overall UAVs.

Ultimately, these management-imposed actions require spatial movement of UAVs, leading to further resource demands along with the demand of the mission. Maintenance of resources comprises the following processes to enable the resource management goals:

Replacement The process of replacing one UAV by another to sustain mission execution (cf. Section 6.2.3).

Charging The process of recharging a depleted or partly depleted battery of a UAV, taking place at a charging station (cf. Section 6.2.2).

Provisioning The process of selecting a UAV as the replacing or fulfilling UAV for mission execution, and the coordination of its timely arrival by planning according flight maneuvers (cf. Section 6.2.1).

Returning The process of returning a replaced UAV after mission execution to a charging station for recharging (cf. Section 6.2.1).

Resource management requirements to support these maintenance processes can be summarized under the following three topics.

5.4.1. Utilization Observation

The considered system of systems is a combination of centralized and decentralized control aspects. While every UAV stabilizes itself and navigates autonomously, the coordination of inter-UAV tasks and the assignment of missions is centralized with the ground control station as the deciding component. A regular transmission of UAV state data is needed to support observation of the system of systems state by the GCS. The following requirements are defined with regard to the inter-node communication between UAVs, CSs, and GCSs:

[REQ-D-308] Resource management has to be able to handle communication link limitations between nodes (capabilities, reach, throughput, loss).

[REQ-F-114] Energy resources in UAVs and charging stations shall be monitored and recorded for later statistical analysis.

[REQ-F-115] Energy consumption of UAVs during utilization shall be categorized as either mission or maintenance consumption.

[REQ-F-116] A UAV shall transmit a consolidated representation of its current state to the GCS, including progress in its mission and its state-of-charge.

[REQ-F-117] A UAV shall transmit its consolidated state data after every maneuver is executed.

[REQ-F-118] A UAV may transmit its consolidated state data in a regular cycle.

[REQ-F-119] The ground control station shall receive, interpret, and store consolidated state data by all UAVs.

[REQ-N-201] The regular transmission of consolidated state data (Requirement [REQ-F-118]) may happen at rates between 0.5 and 30 s to improve GCS side interpolation and visualization for response personnel.

Observation in a simulated environment is almost unrestricted, the real-world system is faced by limitations that are harder to overcome. The listed requirements are reasonable

for simulation purposes but more importantly realistic in the context of a communication system in real-world applications.

5.4.2. Continuity

It has been established that the replacement of a UAV near its battery depletion is needed for continued mission execution. Replacement should not interrupt consecutive atomic maneuvers but rather happen at the time of maneuver-to-maneuver transition. The planning and coordination of maintenance processes ensuring continued operation of the overall mission is the duty of the ground control station.

Continuity defines the uninterrupted and unterminated support of all scenario missions and hence the enabling of the UAV-aided scenario operation.

[REQ-F-120] The GCS shall plan the time and location of UAV-by-UAV replacement.

[REQ-F-121] UAV replacement shall happen at the transition between atomic maneuvers.

[REQ-F-122] A UAV shall be able to send its mission and mission-related data to another UAV that is close by.

[REQ-F-123] A UAV shall be able to receive mission and mission-related data from another UAV that is close by.

[REQ-N-202] Mission breakdown shall not be restricted to achieve continuity.

5.4.3. Recirculation

Depleted UAVs need to be recharged, to be eligible for recurring use in the scenario. This step permits a long-lasting scenario response with a limited number of UAVs.

Recirculation defines the process of re-enabling a depleted or partly depleted UAV for scenario utilization through recharging at a charging station, including necessary navigation.

As recharging is only possible at charging stations located at designated areas, the movement to and from these has to be coordinated as part of resource management. Full

depletion and unexpected losses of UAVs before reaching the charging station can be avoided by applying the introduced model for energy consumption prediction. However, depletion-related failure is still possible due to the stochastic nature of energy consumption.

[REQ-D-309] Recharging of UAVs is not feasible during flight.

[REQ-D-310] Allocation of a replacement UAV at the point of replacement is not possible without a prior provision process.

[REQ-D-311] Provision of a replacement UAV is not feasible without spending of time and energy, because of Requirement [REQ-D-312].

[REQ-D-312] A mission does never directly intersect with the location of a charging station and its charging and waiting spots.

[REQ-F-124] A replaced UAV shall fly to and land at a charging station for recharging of its battery.

[REQ-F-125] A charging station is assumed to offer a limited number of waiting and charging spots for all UAVs in the mission.

[REQ-F-126] Assignment of charging spots to waiting UAVs shall happen according to the first-in-first-out principle.

[REQ-F-127] The charging process increases the stored charge in the UAV battery and may be interrupted before reaching the maximum 100 %.

[REQ-F-128] A fully or partly recharged UAV is eligible for assignment by the GCS to execute a mission or to replace a UAV.

[REQ-N-203] The planning of UAV replacement shall happen such that premature depletion and UAV loss during the subsequent flight to a charging station has a probability of no more than 2 %.

[REQ-N-204] The planning of UAV replacement shall happen such that premature depletion and UAV loss during mission execution is improbable, with a theoretical probability of no more than 0.5 % of all performed maneuvers.

Requirements with regard to the UAV loss probability are set based on commonly used low-risk percentages. The achievable percentage and meaningful thresholds will be discussed in the evaluation chapter in Section 8.4.

5.5. Improvement of Efficiency

Based on evaluation results, different strategies and strategy settings can be compared, and conclusions about superior solutions under defined conditions can be drawn. In the case of our distributed system of UAVs, resource demand minimization (see Section 5.3.1) under the general condition of an uninterrupted execution of all UAV missions is the optimization goal.

The following requirements are defined for the goal of resource management strategy evaluation:

[REQ-D-313] Optimization potential is generally restricted by the base requirements of the disaster scenario.

[REQ-F-129] The implementation of replacement and recharging specifics shall be exchangeable.

[REQ-F-130] The time and location of a UAV replacement shall be selectable based on different strategies to minimize the energy consumption and duration of maintenace processes.

[REQ-F-131] The selection of a replacing UAV shall be based on different strategies to minimize provisioning spendings and maximize mission utilization of UAVs.

[REQ-F-132] Parameters of replacement and recharging strategies shall be adjustable.

In this chapter, we derived and discussed requirements towards a resource management system for UAV-aided disaster scenario response. The requirements form the base for our system presented in the following chapter. Identifiers as given per requirement will be used to reference requirements linked to individual design aspects.

6. Resource Management Concept and Design

In the previous section, we presented the requirements for resource management in UAV-supported disaster scenarios. Those requirements encompass the basic goal of management and maintenance processes, contain the boundaries of the underlying system, and establish deliberately made restrictions. Based on these goals and restraints, and the system environment as introduced in Chapter 3, we will introduce and discuss our design for resource management in this chapter.

6.1. Insertion of a Resource Management Layer in the Conceptional Model

A block diagram showing a hierarchical model of UAV-aided disaster response coordination was introduced in Figure 3.1 on page 35. The diagram illustrates the involved layers of scenario definition, mission breakdown, and UAV assignment during utilization from a conceptional viewpoint.

In order to fulfill Requirements [REQ-F-101] to [REQ-F-103], demanding a transparent and non-interrupting resource management system for UAV utilization, we introduce a new refined conceptional response model, illustrated in Figure 6.1.

The improved hierarchy inserts a new layer for resource management. The layer poses as a separation between scenario-derived missions and physical mission-executing UAVs. The higher layer for mission breakdown is no longer restricted by resource constraints and missions are henceforth also unrestricted in their duration. The lower layer of UAV assignment and energy management now falls into the jurisdiction of the newly introduced management layer. The layer offers particular possibilities to cope with the

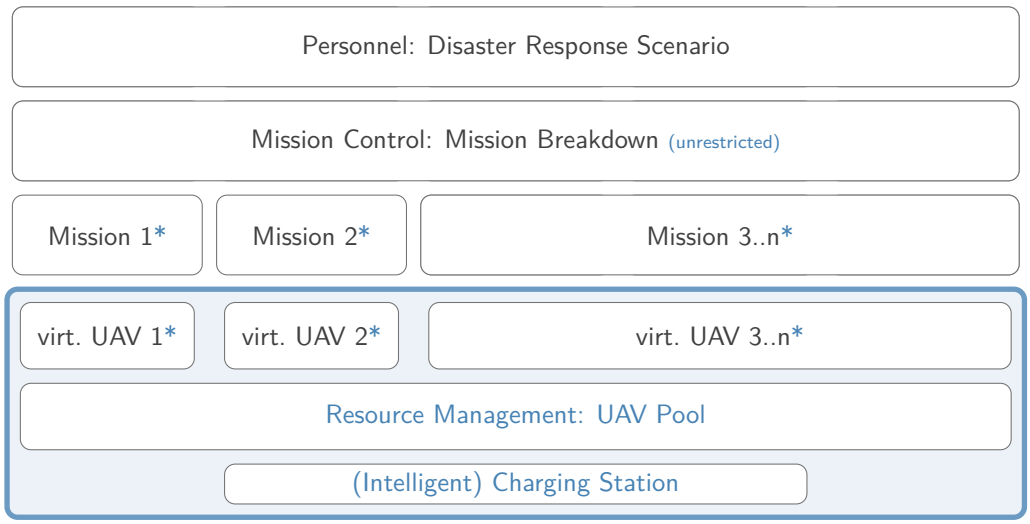

Figure 6.1 – Conceptional model of the layered UAV scenario response coordination (cf. Figure 3.1), improved version extended by a resource management layer.

increased flexibility of the higher layer, while enabling the fulfillment of a wide set of the previously defined requirements.

The new resource management layer encapsulates all related tasks, like replacement planning or recharging coordination. To that end, the resource management layer also possesses a deeper knowledge of hardware/UAV specifics, like the energy consumption model discussed in Chapter 4, or the energy storage model discussed in Section 3.3.1.

6.1.1. Virtual UAVs to Preserve Compatibility

In comparison to the classical conceptional model, the improved model replaces specific mission-assigned UAVs by a pool of managed UAVs, which execute missions in a cooperative manner. In order to comply with Requirement [REQ-F-105] to not break compatibility with the higher layers of the classical model, we introduce the concept of virtual UAVs as part of the improved model. Virtual UAVs are conceptionally seen as similar to physical UAVs, with the special characteristic of not being limited by an exhaustible battery.

Virtual UAVs effectively fulfill Requirement [REQ-F-106] to mask the limited operational duration of exhaustible UAVs by mimicking a non-exhaustible UAV executing a mission.

Resource management is subsequently responsible to assign a real UAV to undertake the operations of the virtual UAV. Furthermore, the resource management system is responsible to perform all needed maintenance processes to preserve the illusion of an uninterrupted execution of the complete mission.

6.1.2. Inclusion of an Intelligent Charging Station

The improved conceptional model now also considers the charging station for automated UAV recharging, as discussed in Section 3.2.5. It is an important part of the resource management system to support recurrent UAV utilization, and is a crucial part of the UAV life cycle.

In the classical conceptional model, the absence of an automated resource management system meant that human personnel had to overlook and potentially manage the recharging of UAVs, in-place or at a dedicated charging station. The resource management system in our improved model is responsible for automatic recharge planning and execution, including the communication of a physical landing and charging location and the charging oversight.

The inclusion becomes especially interesting because of the option of multiple spatially distributed charging stations. Only with a resource management system in place can recharging processes be planned and executed by considering all factors, like the flight distance to different charging stations along the mission path, or temporal capacity overload at one charging station. The latter is not further considered in this thesis.

An intelligent charging station (ICS), as we described it in Section 3.2.5, is capable of easing the management effort, by providing a part of these services, relieving the resource management system from detailed aspects in the vicinity of the ICS. All UAVs on site will be managed locally and aggregated status data and actions are provided to the central resource management system.

Outsourcing these centralized management tasks as decentralized tasks per ICS offers advantages, both technically and systematically. Local management on the basis of local knowledge avoids unneeded global communication chatter, reduces the complexity of the global resource management system and enables technical and functional advances of the ICS technology. The interface definition between global resource management at the mission control unit and ICS entities increases the flexibility and modularity of the overall system.

From a logical viewpoint, the utilization of ICSs does not offer new functionality for resource management on the global scale and will not have to be separately considered in the remainder of this chapter.

6.2. A Replacement-and-Recharging-based Management Concept

Resource management in UAV utilization has to deal with one major challenge: Continuity of long-lasting missions under utilization of short-duration applicability of UAVs. Continuity was introduced and described in Section 5.4.2.

We decided to implement UAV replacement and recharging as the continuity strategy. This was defined by Requirement [REQ-D-304] to not be limited to compatible or accordingly modified UAV models, and by Requirement [REQ-N-202] to not limit the characteristics of missions to be executed.

Because of the potential option of spontaneous hardware or software failure (Requirement [REQ-F-113]), the potential alteration of missions (Requirement [REQ-F-107]), and the influence of stochastic uncertainty on most utilization aspects (Requirement [REQ-F-111]), a global and complete pre-planning resource management is not feasible.

The replacement-and-recharging-based management concept comprises two parts of the overall UAV life cycle and the life cycle synchronization between multiple UAVs. All three are subject to specific configuration and offer resulting optimization potential, and are discussed in the following sections.

6.2.1. Single-UAV Utilization Phases

The life cycle of a single UAV operation consists of two parts. The first half is the utilization phase shown in the simplified state diagram in Figure 6.2. Preceding and subsequent states, which close the life cycle, are explained in the following section.

Utilization is characterized by flight and energy consumption in the field, including flights inflicted by energy management. It comprises the provisioning phase, the mission execution phase, and the concluding return phase.

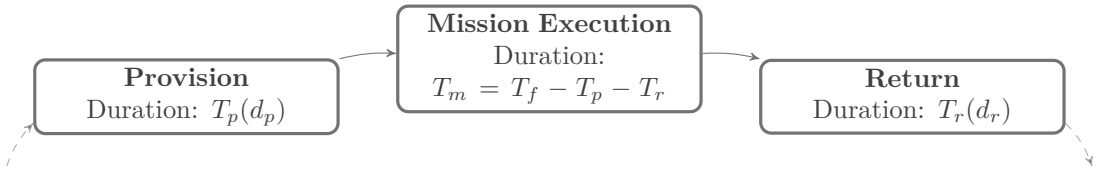

Figure 6.2 – The UAV utilization phases of the overall life cycle.

The first and last utilization phases are not beneficial to the scenario or mission, but rather are the necessary support for our replacement-based continuity concept. Their duration T_p/T_r, and therefore energy consumption, depends on the distance between the origin of the UAV and the location of mission start, respectively on the distance between the location of mission end and the recharging location. The mission execution phase is mainly defined by the details of the scenario-derived mission.

Mission execution duration T_m, meaning the time a single UAV can operate as part of a mission, is however limited by the potential overall flight time T_f and directly lessened by the provision and return times.

Optimization potential based on a minimization of T_p and T_r are discussed later on in Section 6.4.2.

6.2.2. Single-UAV Recirculation Phases

The second half of the life cycle, highlighted in Figure 6.3 illustrates the recirculation efforts. It is characterized by time spent off the operation field in the vicinity of a charging station.

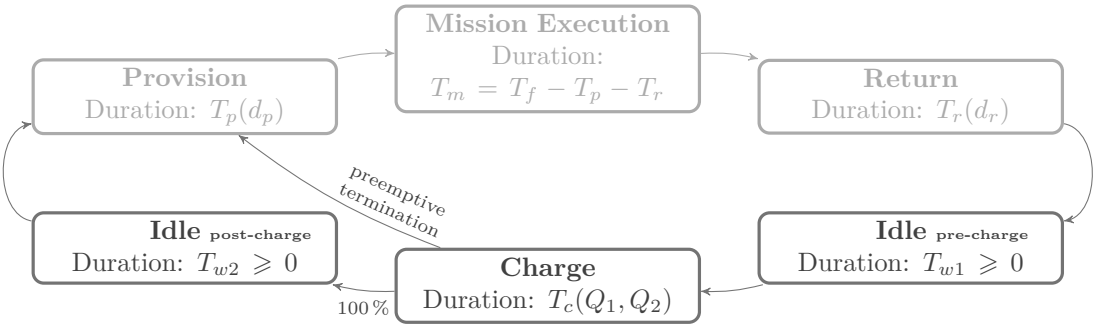

Figure 6.3 – The UAV recirculation phase of the overall life cycle.

Recirculation is divided in the determining charging phase, and preceding and subsequent idling phases. Duration of both idling phases may be zero. The one after recharging depends on the UAV demand, e.g., resulting out of planned replacement processes. The one prior to recharging depends on the availability of free charging spots at the charging station, which were assumed to be limited in Requirement [REQ-F-125].

Time spent in the charging phase (T_c) directly depends on the initial (Q_1) and final (Q_2) state-of-charge of the UAV battery. The charging process of a battery was discussed in Section 2.4.3.2. The initial state-of-charge is the result of consumption during a preceding utilization phase of unknown duration. The final charge will eventually reach the targeted 100 % of the battery capacity if the charging phase is not preemptively terminated by a replacement assignment.

The recirculation phase does not offer obvious optimization potential with regard to energy management. Both idling phases are indirect effects of other factors and an acceleration of the charging process is assumed to be unfeasible within the bounds of the particular hardware. We expect indirect optimization potential with regard to the overall mission-wide UAV demand by exploitation of the non-linear nature of the charging process and preemptive termination and assignment decisions. The approach will be discussed in Section 6.5.2.

6.2.3. Multi-UAV Mission Continuity Cycle

The mission execution phase is the only phase accountable for productive use of the UAV and its energy resource in the context of the scenario goal. All other phases are solely required by resource management in terms of maintenance processes.

A simplified view on the previously described life cycle of UAVs is shown in Figure 6.4. The diagram differentiates between the maintenance use of single UAVs in the bottom half and the productive use represented by "Mission Execution" as part of both the bottom and upper half. In the upper half the diagram illustrates how our concept of replacement and the exchange of mission data can assure the continuous execution of a long-lasting mission by successive use of short-duration UAVs.

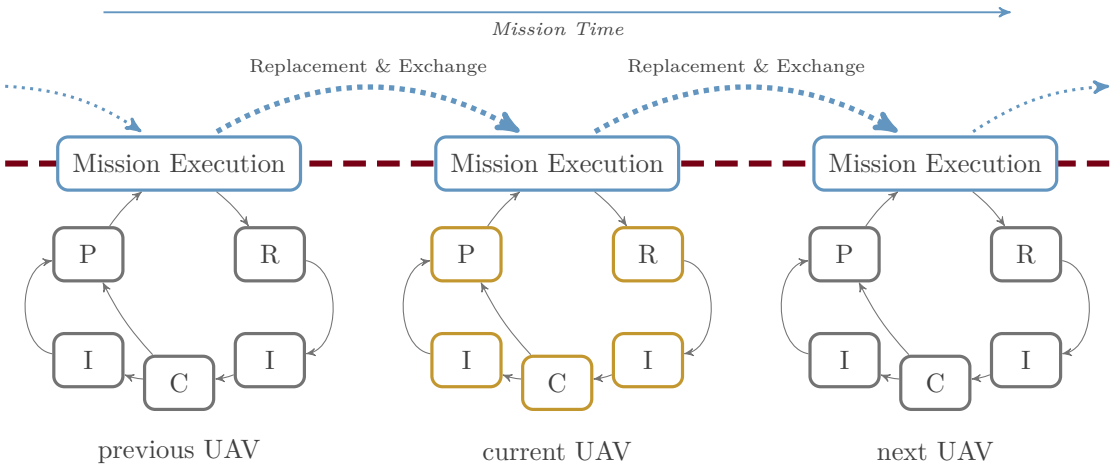

Figure 6.4 – The multi-UAV mission continuity cycle resulting out of the individual life cycles of a UAV as depicted in Figure 6.3. Individual life cycles are shown below the dashed line, continuous execution of one mission by multiple UAVs is shown in the upper part.

The steps performed during the "Replacement & Recharging" transition of a mission between one executing UAV and another fulfill the previously defined Requirements [REQ-F-122] and [REQ-F-123]. These steps are:

1. Wait for both participating UAVs to arrive at the replacement location
2. Exchange mission details and potential additional data
3. Continue in the respective life cycle phases:
    - Replaced UAV: Transition into return phase and fly to charging station
    - Replacing UAV: Transition into mission execution phase and advance the mission

The sequence is straightforward and easily implemented and tested. The replacement and recharging procedure is assumed to be of insignificant duration, judging by the average duration of typical maneuvers. The critical aspect of the replacement process

is the selection of a good replacement time and location, as well as the selection of a good replacing UAV. Good selections are characterized by an efficient use of resources, both with the view on the single replacement as well as on global resource demand. Heuristics for such decisions will be discussed in Section 6.4 and Section 6.5.

6.3. Discussion of a Theoretically Optimal Solution

Before we go into the details and challenges of replacement and recirculation planning and their optimization potential, we want to discuss theoretical lower bounds of resource demands.

The following discussion will look at optimal conditions, which are impossible in a real-world application. The resulting solution will merely point out lower resource demand bounds and hence act as means for comparison and evaluation of realistic imperfect solutions and improvement ideas. Results will also reduce the search space for heuristic configurations.

With the UAV life cycle in mind, the time delay of almost every maintenance phase can be reduced or eliminated by certain assumptions or arrangements. The following phases are subject to modifications in the optimal solution:

Provision and Return Both phases depend on the distance between mission and the responsible charging station. The distance between those depends on the mission planning and charging station positioning. In the optimal case, the scenario is planned in such a way that the distance between charging station and the nearest waypoint of a mission are relatively close. Also, this waypoint would be the best exchange location under the selected replacement strategy. This can be achieved by resource-aware mission planning and optimal charging station placement. Therefore, it is justified to expect both durations to be reasonably small, compared to the overall utilization time:

$$T_p \ll T \quad \text{and} \quad T_r \ll T \tag{6.1}$$

Pre-charge Idling Waiting before being able to charge is the consequence of a limited amount of provided charging spots at the charging station and the thus inflicted

stand-by time. In an optimal solution a sufficient amount of charging spots is provided at all times, resulting in no pre-charge waiting times.

$$T_{w1} = 0 \tag{6.2}$$

Post-charge Idling After a UAV was fully charged, it is eligible for provision and mission execution. Waiting time till a UAV is requested for provision is anticipated in a real-world application. In an optimal solution, all resources are used efficiently, meaning that missions are scheduled such that all non-charging UAVs are immediately used in a subsequent mission, thus eliminating post-charge waiting times.

$$T_{w2} = 0 \tag{6.3}$$

The remaining two phases can either not be specifically optimized, or their optimization would not be meaningful:

Charge The process of recharging at a charging station cannot be eliminated as it is an essential requirement for utilization. It is furthermore not possible to accelerate the charging process beyond the limitations of at least one of the chemical, physical and electrical properties of the UAV battery. Under expectation of perfect utilization, the charge phase always recharges the UAV battery from 0 to 100 % state-of-charge. The charge time T_c is therefore assumed constant.

Mission Execution Any kind of restriction or reduction of the production phase is meaningless. On the other hand, the previously discussed minimization of the provision and return phase increase the potential duration of the mission execution phase. In an optimal solution, flight time is almost completely spent in mission and nearly the whole life cycle time is spent in either mission execution or in charging phases:

$$T_m \lesssim T_f \quad \text{and} \quad T_m + T_c \lesssim T \tag{6.4}$$

The remaining relevant phases of the UAV life cycle in the optimal solution are presented in Figure 6.5. Our discussion of an optimal solution does not address uncertainties due to deviation.

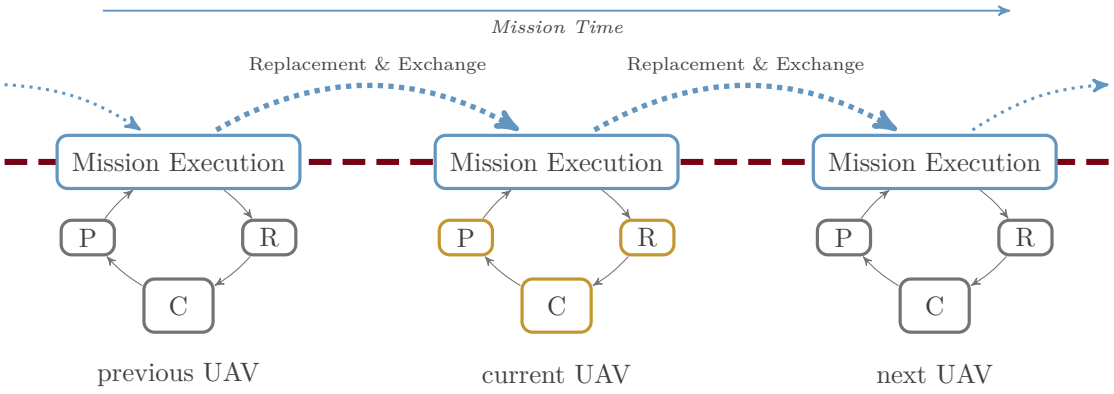

Figure 6.5 – The multi-UAV mission continuity cycle from Figure 6.4 reduced to the relevant phases in the optimal solution. The bottom half shows life cycles of individual UAVs, the upper half shows the continuous mission execution by these UAVs.

Recharging takes considerably longer than the mission execution phase, enabled by one full charge of the UAV battery. In an optimal solution, UAV utilization time is not wasted in idle phases, rather are they always immediately recirculated for mission execution. With the assumed perfect scheduling, every mission is therefore supported by a natural number of UAVs, one in the mission execution phase, all others in their charging phase or the provision/return phases.

The resource demand in an optimal solution under the discussed assumptions is easily calculated. The number of needed UAVs depends on the charging time for a full recharging of the battery to 100 % and on the mission execution time resulting out of the charge.

Example: *How many of the testbed 3DR Solo quadcopters are needed to support a continuous hover mission in 100 meters distance and 45° elevated from the closest charging station?*

The mission execution time per single UAV results from the energy available for mission execution:

$$E_m = E - E_p - E_r = 76.96\,\mathrm{W\,h} - 2 \cdot 2.69\,\mathrm{W\,h} = 71.58\,\mathrm{W\,h} \tag{6.5}$$

The battery capacity E is taken from Table 3.1, E_p and E_r are computed using the testbed UAV energy consumption prediction model given in Section 4.6. Using the same model, the provision/return, mission execution, and the charging durations are equal to:

$$\begin{aligned} T_p = T_r &= 100\,\text{m} \,/\, v(45°) = 0.54\,\text{min} \\ T_m &= E_m \,/\, P_h = 71.58\,\text{W h} \,/\, 262.7\,\text{W} = 16.35\,\text{min} \\ T_c &= 69\,\text{min} \end{aligned} \tag{6.6}$$

The ratio of overall life cycle duration to effective mission execution utilization is therefore:

$$(T_p + T_m + T_r + T_c) \,/\, T_m = 5.3 \tag{6.7}$$

In consequence, at least six 3DR Solo UAVs are needed to support the uninterrupted execution of the example mission. The example only consists of a single mission close to the supporting charging station and the calculation was done assuming no uncertainty. A real-world scenario will require more UAVs to support basic scenario continuity.

Beyond basic continuity coverage, optimization steps can improve utilization performance and reduce resource demand. The influence of uncertainty and the anticipated change of mission details at later points of the scenario response exclude the option of a full pre-planning. Resource management planning represents an online optimization problem. Different heuristics can be applied to address this problem and to achieve an optimized resource demand.

6.4. Strategies for Replacement Scheduling

Replacement of one UAV by another presupposes their mutual presence at an agreed upon location and time.

As traveling to a certain location costs time, the replacement location needs to be arranged beforehand and communicated between both participating UAVs. While the replacing UAV is provisioned from a passive phase at a charging station and can freely be instructed, the other UAV is actively executing a mission. Requirement [REQ-D-306]

demands that all mission maneuvers are atomic and cannot be interrupted. Accordingly, the replacement of a UAV must happen in-between the pre-defined maneuvers (cf. Requirement [REQ-F-121]). Possible replacement locations are therefore the counted number of future maneuver transitions up to the limits of the UAV battery endurance or the mission. As mentioned before, this upper bound has to be additionally shortened due to the fact that the return phase amounts for a distance-related time and energy consumption that needs to be warranted. The formula for overall energy consumption can therefore be denoted as

$$E(k) = \sum_{i=1}^{k} E_M(i) + E_R(k) \tag{6.8}$$

with $E(k) < E_B$ where $k = 0, \ldots, n$ is the amount of future maneuvers and n the maximum number of maneuvers. E_M stands for the energy needed for maneuvers, E_R for the energy to return after maneuver k, and E_B represents the state-of-charge of the UAV battery.

The replacement time as well as the preliminary provisioning time for the replacing UAV can be calculated by the flight speed portion of the energy consumption prediction model ascertained in Chapter 4.

Energy consumption deviation has to be considered during the consumption prediction, in order to guarantee maneuver execution without exceeding the depletion level of the battery. To that end, we introduced and defined the concept of safety margins in Section 4.4.1 and extended the concept for multiple maneuvers in Section 4.5. The choice of appropriate safety margin quantiles, applied during energy consumption prediction, was stipulated in Requirements [REQ-N-203] and [REQ-N-204].

The selection of one of the potential maneuver transitions as the replacement location has quantitative implications with regard to the resource management and thereby influences the overall utilization efficiency and resource demand. In the following sections we present three selection heuristics with their advantages and disadvantages. A quantitative analysis and comparison of all three will be carried out in Chapter 8.

An example mission consisting of multiple maneuvers is shown in Figure 6.6. The example flight and maneuver-related energy consumption values originate in a fictional

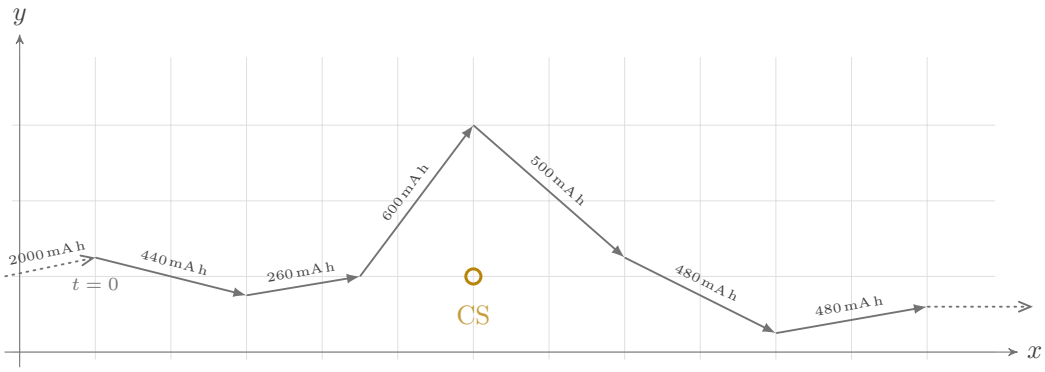

Figure 6.6 – Top view of an example mission consisting of multiple point-to-point maneuvers and a charging station. Depicted energy consumption values per maneuver are exemplary.

scenario and are of exemplary nature. Altitude levels for the individual waypoints are left out for the sake of simplicity. One charging station is available in the field. The example solely consists of point-to-point maneuvers for presentation as hovering maneuvers would not change the selection criteria.

It should be noted, that we draw conclusions regarding the utilization based on the energy consumption. Other measures – like maneuver distance, maneuver travel time, or even higher-level maneuver prioritization – could alternatively be applied. We decided to work with energy consumption as the evaluation criterion in our resource management directed analysis.

From a global perspective, heuristics may only choose different trade-offs between safety and efficient use of energy. The obvious extreme solutions of such heuristics are the exchange at the latest possible point, to maximize efficiency, and the exchange after a single maneuver, which would quite obviously be too inefficient but maximize safety. The following heuristics explore some possible alternatives that have been developed over the course of this thesis.

6.4.1. Latest Opportunity Heuristic

With the goal of maximum UAV battery utilization, this strategy will plan the replacement at the latest possible maneuver transition, similar to a naïve greedy strategy.

Starting at the current point in time of mission execution, the remaining battery charge is compared against the consumption for $k = 0, \ldots, n$ next maneuvers plus the consumption for the flight to the nearest charging station during the return phase. The amount of maneuvers is incremented, until the accumulated mission consumption exceeds the battery capacity. The path with the highest number of maneuvers, which does not exceed the battery capacity, is selected as the solution. The replacement is planned accordingly.

The heuristic can be defined as follows:

$$f_{LO} = \max_{k} \sum_{i=1}^{k} E_M(i) \tag{6.9}$$

In Figure 6.7 the example mission is given with indefinite maneuvers. All maneuvers are assigned with an exemplary consumption, which in reality would be predicted based on maneuver details and our energy consumption prediction model. For the sake of clarity no special computation of safety margins is included, as such would over-complicate the example but not influence the heuristic tendency.

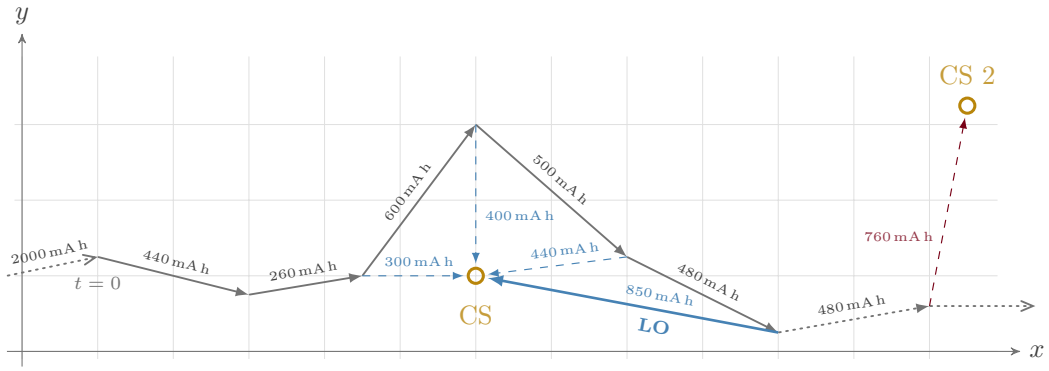

Figure 6.7 – The latest opportunity heuristic shown on an example mission.

In the figure, multiple potential replacement and return paths are depicted. Table 6.1 shows the mission and return consumption, and the summed up overall consumption for all these paths, indexed by letters. The remaining battery charge after the individual paths is computed in the last column.

The predicted consumption for path 'E' exceeds the remaining battery charge and the path is therefore not a feasible solution. Predictions for all other paths are inside the

Table 6.1 – The latest opportunity heuristic shown on an example mission. Numeric results for Figure 6.7. Every return path is assigned a letter for reference.

Path	Consumption [mA h]			Remaining [mA h]
	Mission	Return	Σ Demand	from 5200 mA h
A	2000 + 440 + 260	300	3000	2200
B	⋯ + 600	400	3700	1500
C	⋯ + 500	440	4240	960
D	⋯ + 480	850	5130	70 ◁
E	⋯ + 480	760	*5520*	*-320*

bound of the remaining battery charge. Path ‘D’ is the solution with the least remaining charge and is therefore the best candidate under the latest opportunity heuristic.

6.4.2. Shortest Return Heuristic

In the discussion of a theoretically optimal solution in Section 6.3 we pointed out that the maintenance flight performed during the return phase leads to unwanted consumption. Time and energy spent in the return phase is lost for the mission execution phase. In the likely case that the nearest candidate for replacement is a UAV stationed at the very same charging station, a long return distance is even more undesirable, as its consumption is reflected in the provision phase of the replacing UAV.

The shortest return heuristic copes with the issue by selecting the return path with the least consumption:

$$f_{SR} = \min_k E_R(k) \tag{6.10}$$

The path choice ranges between all feasible paths as discussed in the first heuristic. Figure 6.8 illustrates the same example as before. However, due to the new selection heuristic, path ‘A’ is now the accepted solution.

In comparison to the latest opportunity heuristic, energy and UAV utilization time is not unnecessarily spent on long-distance return and provision phases.

However, the shortest return heuristic suffers from the theoretical problem of local minima as only one of multiple factors is considered. The maneuver transition with the shortest return distance is chosen for replacement, irrespective of other factors. This behavior can result in undesired short mission execution phases and an overall increased number of short-distance return and provision phases. Consequently, the heuristic will result in a non-minimal maintenance utilization of UAVs over the course of a long-lasting mission.

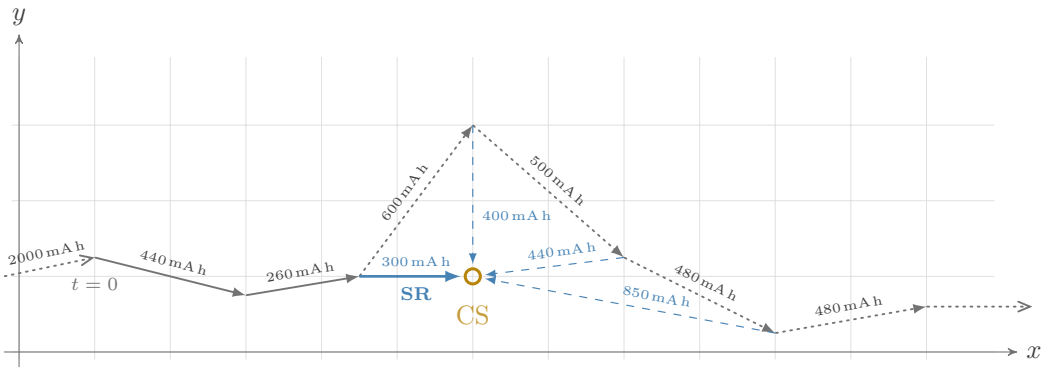

Figure 6.8 – The established example mission shown with the respective solutions for the shortest return heuristic.

6.4.3. Bi-Objective Heuristic

Where the latest opportunity heuristic suffers from unhandled wastefulness, the shortest return heuristic suffers from excessive maintenance utilization of UAVs. Each heuristics supports one extreme, however a more efficient medium solution might exist for one of the intermediate maneuver transitions. We are looking for a trade-off solution that features a high ratio between the energy spent in mission execution to the energy spent in the returning maintenance flight.

The optimization problem can be solved using a bi-objective optimization approach. We chose the method of the weighted sum [Mie98, p. 78] to find a trade-off solution. To do so, we scalarized the bi-objective optimization problem, meaning we transformed Equations 6.9 and 6.10 into a single scalar-valued function. Be aware that f_{LO} is a maximization problem, while f_{SR} is a minimization problem. To optimize both in a common

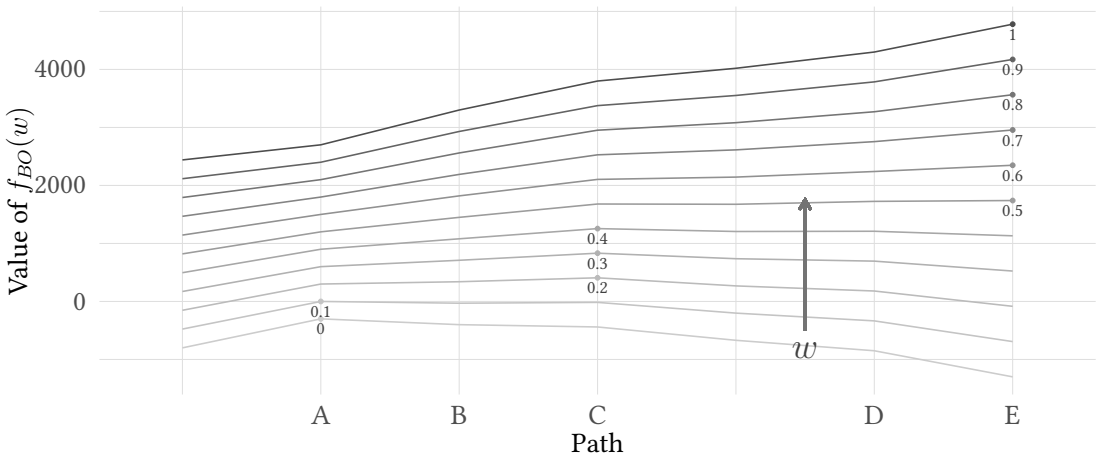

Figure 6.9 – Influence of weight w on the resulting optimal path selection. The course of f_{BO} is shown for eleven w values. The maximum per value is marked by a dot.

direction, f_{SR} is negated and thereby transformed into a maximization problem. We define the following weighted equation for our optimization problem:

$$f(k) = w \sum_{i=1}^{k} E_M(i) - (1\text{-}w) E_R(k) \tag{6.11}$$

The weighting method applies coefficients to the individual functions, to control the trade-off decision. For simplicity a combined weight $w \in [0, 1]$ is used in the denoted equation. The resulting optimization problem for the bi-objective heuristic is given as:

$$f_{BO}(w) = \max_{k} \left(w \sum_{i=1}^{k} E_M(i) - (1\text{-}w) E_R(k) \right) \tag{6.12}$$

It is worth highlighting that both previous heuristics are included in the bi-objective approach:

$$f_{BO}(w) = \begin{cases} -f_{SR} & w = 0 \\ f_{LO} & w = 1 \end{cases} \tag{6.13}$$

The trade-off weight w can be chosen within its range to control the influence of the two parts. In Figure 6.9 the course of the function f_{BO} for values of w is shown for the established example from Figure 6.6. The maximum values per weight are highlighted. Optimal paths for $w = 0$ and $w = 1$ are, as expected, identical to the previously found extrema. The results for $w = 0.2, 0.3,$ and 0.4 are interesting, as the function reaches its maximum at an intermediate maneuver transition. Path 'C' is therefore a good trade-off flight path in the examined example.

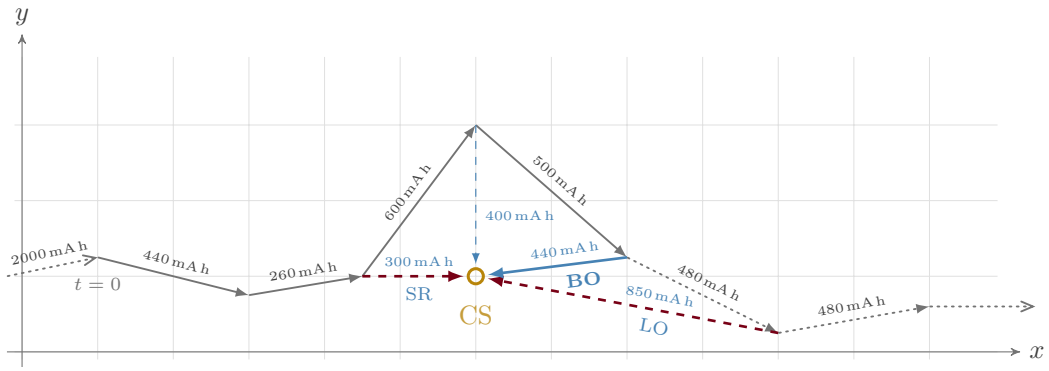

Figure 6.10 – The established example mission shown with the trade-off solutions for the bi-objective heuristic (path 'C').

The strategy is able to find intermediate maneuver transitions with a good trade-off between a long utilization in mission execution and a short return distance. Selection of the right value for weight w is not trivial and will be subject of later evaluation. By choosing the right trade-off, we expect a longer utilization of a single UAV, and therefore an increase in resource management system efficiency and reliability.

6.5. Strategies for Replacing UAV Selection

The previous section concentrated on the scheduling of the replacement and exchange location. The main focus of the discussion was the UAV currently executing a mission, and its return to a suited charging station, under consideration of energy efficiency.

The replacing UAV was only shortly mentioned. We assumed that an idling and fully charged UAV is always available at the relevant charging station and would be the appropriate candidate for replacement. This is in reality not always the case and the section overcomes this simplified assumption.

UAVs are limited in amount and distributed in the field. When not in utilization, a UAV is located at a charging station, either in the charging phase or the precedent or subsequent idling phase of its life cycle. Temporal spikes or disadvantageous synchronization in UAV demand enable the possibility of local shortages in applicable UAVs. The resource management system cannot expect an idling and fully charged UAV to be available at a charging station at all times. It is the responsibility of the mission control to provide an appropriate replacing UAV, and to coordinate its timely navigation to the replacement location. The mission control can benefit from its local memory of regularly updated global node states, as defined in Requirement [REQ-F-119].

Figure 6.11 serves as an example constellation based on the established mission example. Path 'C' was chosen as the return path for the replaced UAV. Charging stations 'CS 1' and 'CS 2' are potential providers for a replacing UAV. The highest-charged UAV per charging station is denoted with its current state-of-charge in percent, as it would not make sense to use another one. A resource aware and energy efficient decision has to consider the state of UAVs at the charging stations, and the distance and resulting energy consumption of the provisioning paths 'M' and 'N', respectively.

In this section, we will present two strategies for the GCS to find and appoint an appropriate UAV as the replacing partner in the replacement and exchange process.

6.5.1. Shortest Provision Approach

The strategy offers a simplistic two-step solution to the outlined problem above. Its advantage is its simplicity, as it solely decides based on the current state of UAVs.

The present charge of a UAV is considered as the key deciding factor for long utilization. Therefore, fully charged UAVs in the idling phase of their life cycle are generally

preferred. Charging UAV are seen as less suited for utilization and are only considered in the second step. A solution is found as follows:

- First a search for the closest idling fully charged UAV is performed.
  - If a candidate was found, it is selected as replacing UAV.
  - If multiple candidates were found, a random selection decides about the replacing UAV and ensures uniform utilization among UAVs.
- If no idling candidate was found, the second step of the strategy searches for the highest-charged UAV and selects it for replacement.

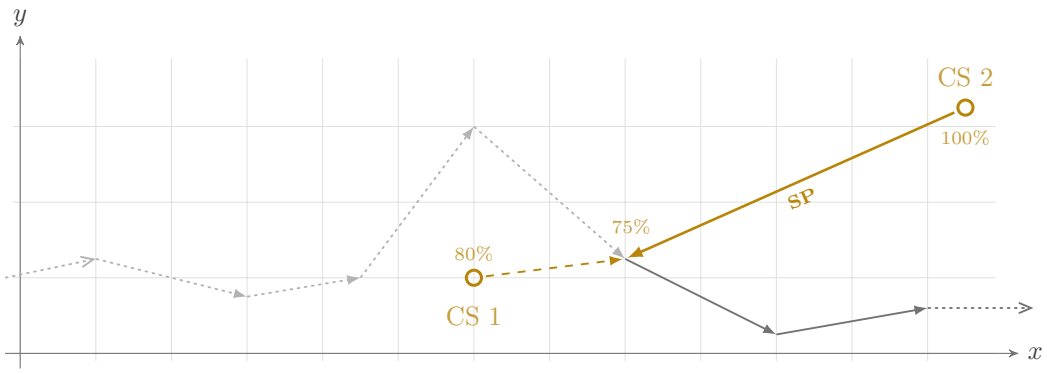

Figure 6.11 – The replacing node decision problem illustrated on the established example. The Shortest Provision Approach with the resulting applicable charge.

The approach is always able to find a candidate. However, in a system under load, the idling UAV produced by the first step might be far away and the second step will seldom be employed.

In the example constellation from Figure 6.11 the shown fully charged UAV at 'CS 2' is easily identified as the appropriate replacing UAV.

The strategy does neither consider nearby high-charged UAVs nor the energy consumed during the provisioning flight nor events that may occur between the times of selection and provision.

6.5.2. Applicable Charge Approach

In the previous strategy, the main aspect for replacing UAV selection is the battery state-of-charge of potential UAVs at the moment of selection. However, under the reviewed issues and with the goal of efficiency improvement, the optimization goal is refined in this strategy. In order to enable maximum mission execution and therefore a high life cycle efficiency, the optimization problem can be defined in a simple manner, as

$$f_{AC}(t_p, l) = \max_m \left(E_{B,m}(t_p) - E_{P,m}(l) \right) \tag{6.14}$$

where t_p is the predicted provision time, $l = (a, b, c)$ represents the replacement location, and $m = 1, \ldots, q$ is an index for all charging and idling UAVs in the field. The energy consumption for the provisioning flight E_P for UAV m depends on the distance to the replacement location, the battery state-of-charge E_B of UAV m depends on the remaining time before provisioning in case of a still charging UAV.

The strategy maximizes the battery charge applicable in mission utilization after provision by searching through all q UAVs irrespective of their current location, and by use of the developed movement and energy consumption prediction model from Chapter 4. The model is used to estimate the time of provision and the state-of-charge at that moment. The state-of-charge at the times of planning and provisioning have no direct relation with the selection, as only the remaining charge at the replacement location is considered. The charging process may get preemptively terminated, as explained in Section 6.2.2.

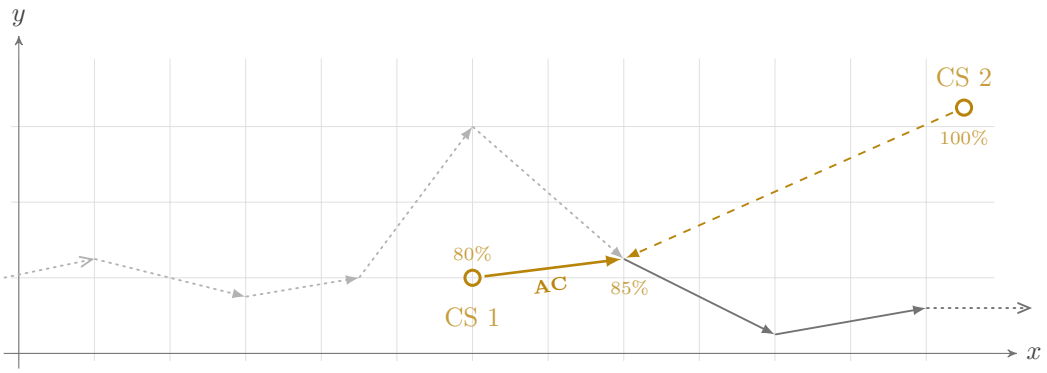

Figure 6.12 – The replacing node decision problem solved by the Applicable Charge Approach.

Applied to the example constellation, in Figure 6.12 we rate both UAVs following Equation 6.14 and select the UAV with the maximum value. We can assume the traveling time and energy consumption on the shorter path to be notably smaller then from 'CS 2'. The currently charging UAV at 'CS 1' is the better replacing UAV candidate as it is able to provide a higher charge when taking over the mission at the replacement location.

A later evaluation of both replacing UAV selection strategies will be interesting to learn about the UAV count and energy efficiency differences on a global system scale. In the same way, an evaluation of the presented replacement scheduling strategies will have considerable effects on overall disaster response performance and reliability. Chapter 8 will conduct and discuss a detailed evaluation.

7. A Discrete Event Simulation Framework for UAV Fleet Management Strategy Evaluation

In Chapter 5 we discussed the requirements for UAV fleet resource management. We then analyzed different design aspects and discussed various strategies for parts of the management and maintenance design in Chapter 6. Such strategies should schedule UAVs in a way that optimizes non-functional system parameters such as utilization, energy use, and mission reliability.

Development and evaluation of strategies has to be done based on models and simulations before their real-world validation. A modeling and simulation-based systems engineering approach [GDT14] saves considerable investments in both time and monetary costs, while providing a high flexibility, and transparency into processes and performance values. Additionally, a real-world experiment, consisting of dozens of UAVs would not have been possible during this dissertation project, because of both financial and spatial limitations.

Existing UAV simulation frameworks, such as ROS/Gazebo, Microsoft AirSim or Drone Flight Simulator, primarily focus on the physical behavior, movement, and control of single UAVs. In this chapter we present a simulation framework for mobile robotic systems developed during the work on this thesis. It pays special attention to resource management and energy maintenance strategies, including realistic UAV system behavior, UAV replacement and recharging processes. The framework offers the flexibility to simulate general and specialized "nodes", and a specialized UAV node to imitate the behavior of our testbed UAV is fully implemented and provided in the current framework state.

The goal of the simulation framework is to evaluate and optimize management processes and maintenance scheduling strategies according to Chapter 6.

An earlier version of the simulation framework was presented in [DKZ17a]. This chapter describes individual aspects of the simulation framework in more detail and includes functionality that have been added since then.

Development of the framework started in May 2016, and constant additions and improvements resulted in the state of the simulation framework used today. The source code is publicly available and was declared open source under the *Academic Public License*. References and further details are documented in Appendix A.1.2.

Besides development effort by the thesis author, contributions were made by students in student works. Ludwig Breitsprecher [Bre18] implemented the intelligent charging station (cf. Section 6.1.2) as part of his Bachelor thesis. The research project by Michael Sommer [Som18] concentrated on the implementation of the shortest return heuristic (cf. Section 6.4.2), various improvements, and general bug fixing under the supervision of the author of this thesis.

7.1. Software Design, Architecture, and Functionality

In this section we will address the conceptional software design and software requirements. These are not to be confused with the resource management system requirements previously presented in Chapter 5.

The major goal for the development of the simulation framework was the need for an environment to simulate and evaluate different coordination and management strategies in UAV fleet utilizing scenarios, like disaster response scenarios. However, the scope for the simulation framework is broader. During early software design discussions, we agreed on a set of architectural design decisions to enable the support for other forms of communication nodes. Besides UAVs, the simulation framework should support utilization of other forms of mobile robots or even non-robot communication network nodes, like driven vehicles or equipped search-and-rescue dogs. The special design challenge of the requirement was the support of potentially vastly different movement and resource

conditions, under the same core principles of an interactive and resource-constrained node entity in the simulation space.

The simulation is designed to take more specific communication aspects into account. Besides the basic existence of a communication link, aspects like the exact radio technology, communication protocols or realistic signal propagation under environmental influences, should be applicable.

Before we can concentrate on the implementation, simulation, and evaluation of strategies for resource management, the basics of mission assignment and UAV utilization with realistic flight behavior have to be addressed in the simulation framework.

7.1.1. System Base Components

The basis of the simulation framework is characterized by distributed communication nodes and the concept of mission assignment and execution. The following components and processes ought to support the basic execution of missions in a scenario, after mission breakdown. The architectural design follows the classical conceptional UAV response model previously presented in Section 3.2.

Mission Control The mission control shall be implemented as a central entity with control over all nodes and missions. As the mission breakdown is out of the scope of this thesis, pre-defined missions shall be supplied to the mission control for further assignment. A mission control entity is responsible for the overall mission goal fulfillment and therefore has to have knowledge of the current state of all nodes.

Nodes, UAVs and Multicopters The support for communication nodes shall be flexible in both movement and behavior to potentially represent all types of mobile robots. Actual implementation for our analysis has to concentrate on a specific UAV model with the functionalities and restrictions discussed throughout the earlier chapters. A concrete parameterized model for a UAV should be based on our 3DR Solo testbed quadcopter and shall present the movement behavior derived in Chapter 4. A mission assigned by the mission control has to be operated autonomously by the executing node, under its characteristics and limitations. Missions assigned to the individual nodes have to be repeated

indefinitely if not otherwise specified. The software architecture has to account for the variety of tasks, while still offering a powerful common interface for coordination and management.

Communication Control and data communication between UAVs and the mission control unit is a basic requirement for the simulation framework. For a first iteration, sufficing under the research goal of this thesis, simple communication links with perfect reception and unlimited range can be applied but more complex signal propagation models and communication protocols should be applicable at a later point.

7.1.2. Resource Management Components

With the base system for simulation and mission execution in place, the following components add functionality for realistic energy consumption simulation and prediction, for replacement and recharging processes, and for different replacement and recharging strategies. The design follows the enhanced conceptional UAV response model developed in Section 6.1.

Mobile Energy Storage In general, a limited energy source is not required for a common node, like a stationary ground unit. For UAVs the electric battery was presented as the only energy storage in the scope of this work, and has to be implemented accordingly. In simulation, processes of battery use have to be represented and linked to the node behavior. Additionally, the same functionality shall also offer functionality for future energy prediction. To that end, a precise energy consumption and consumption prediction model as discussed in Chapter 4 is needed as a component.

Charging Station To complement the previous design decision, a charging station shall also be part of the implementation concept. A charging station can be abstracted as a non-interactive element with a fixed position. UAVs are only allowed to start a recharging process in the vicinity of a charging station. Besides the implementation of a normal charging station, the concept of an intelligent charging station shall be supported. In either cases the process of battery recharging a UAV has to be implemented following a realistic model.

Replacement and Recharging The process of replacement and recharging planning and execution was discussed in detail in Chapter 6. The simulation framework has to support all steps along the presented UAV life cycle. This includes, but is not limited to the negotiation of the replacement location and time, the timely arrival of both UAVs, the exchange of mission data, and the return and recirculation of the replaced UAV. Special attention has to be spent on the replacement and recharging strategies and potential fault and failure cases. From an implementational point of view, this is the most complex aspect of the simulation framework.

7.1.3. Strategy Evaluation

The introduced simulation framework has to support different replacement strategies, according to Section 6.4 and Section 6.5. The outcome of simulation runs will be numerical performance results, characterizing the costs, efficiency and reliability of the simulation setup.

These results can be compared for different combinations and parameter values to define maintenance strategy recommendations to check which heuristic performs best. However, as each simulation run will be a stochastic experiment depending on uncertainties captured in the model, many evaluations with different random sequences will have to be carried out and the samples need to be treated with statistical rigor. Further computations and comparison are thus best done in independent numerical tools like R. The simulation framework should therefore be able to exchange data, i.e., write status data into a parsable log file format or read varying parameter settings.

7.1.4. Visualization of Spatial Movement

Presentation of the behavior and model debugging require a graphical visualization of the mission and the maintenance processes. A visualization will also be beneficial during the development and validation of new features of the simulation framework itself. It should be possible to accelerate the visualization of the node movement w.r.t. real time to comprehend and verify long-term behavior rapidly.

7.1.5. Non-Functional Software Design Goals

The demanded wide support for exchangeable components and processes poses as a special challenge in software design. To cope with these challenges, the development of the simulation framework concentrated on the following aspects of good software architecture design:

Modularity A modular interchangeable hierarchy of components for different aspects of the simulation is needed. This can, for example, be justified on the example of vastly different types of nodes or the claim to support multiple exchange and replacement strategies. Modularity in mind helps to design scalable systems and allows for later additions, like the aforementioned sophisticated communication implementation.

Flexibility The created simulation framework should be usable for current and future research questions. In order to support and ease the implementation and execution of diverse scenarios under varying evaluation criteria, flexibility of the simulation framework is a crucial design goal.

Scalability While first testing and debugging executions of the simulation framework did consist of only a few nodes, later simulation runs in productive use have to include dozens of nodes, executing different missions, increasing the load of needed communication and management effort. The software design has to implement scalability to support low and high simulation setup complexities.

7.1.6. Reuse of Crucial Aspects in Real-World Application

The goal of the simulation framework, as in modeling and simulation-based engineering in general, is to simulate systems and processes that cannot be easily tested in the real-world. The intellectual core of the simulation framework are the components for energy consumption prediction and the coordination of replacement. With a view on modularity, another design goal during the development of the simulation was the opportunity to extract these components at a later point for real-world integration and application in a demonstrator. To that end, we pursued a development in C++ to be in

line with the testbed UAV firmware ArduPilot and the ground control station software Mission Planner, as described in Section 3.3.1.2.

First steps towards a full real-world demonstrator setup are evident in the student works by Harig [Har15], Will [Wil16], and Krüger [Krü18].

7.2. Realization as a Discrete Event Simulation

For our purpose of resource management strategy implementation and evaluation, the communication and coordination between UAVs can be reduced to simple timed interactions. The movement and behavior of UAVs is highly dependent on time-continuous processes, which could just as well be represented by complex sets of differential equations at a detailed physics level. However, for the purpose of resource management for missions with atomic maneuvers, only the resulting state of the UAV after an executed maneuver is of interest. The continuous processes can thus be reduced to timed events with summarized impacts and new UAV state results. The previously introduced models and processes for movement and energy consumption behavior justify a pure stochastic discrete event system representation [Zim08]. A simulation framework implementation following the discrete event simulation paradigm simplifies the program structure and greatly speeds up the computations.

Instead of programming a framework from scratch, we searched for an existing environment that could be extended and adapted for our needs. The simulation environment OMNeT++ [VH+18; Var99], a discrete event simulation library and framework, was found to fit our needs. It is highly extensible and provides a wide variety of components. OMNeT++ is especially oriented at network simulations and provides components and libraries for a wide variety of communication network aspects.

The support of ad-hoc networks, the easy representation of network node movement, and the overall high customizability of simulation model aspects made OMNeT++ an excellent base for the presented simulation framework. User-defined structures and algorithms are developed in standard C++ 11 classes and functions, and OMNeT++ simulation functionality is simply added as an included programming library. The gained flexibility enabled the unbounded development of mixed-domain system like ours.

The OMNET++ 5.0 add-on components OpenSceneGraph and osgEarth are utilized by our simulation to offer a three-dimensional presentation of our scenario field and nodes in a setting with real-world map data and projected three-dimensional building models. Even though these features are not essential for the generation of evaluation results, they helped in the development and testing phase, and support better visualization for UAV system operators.

At the time of this writing, the utilized software versions were OMNeT++ 5.4.1, OpenSceneGraph 3.5.3 and osgEarth 2.7.0.

7.3. Implementation Details and Technical Decisions

The developed simulation framework follows the architectural and functional design decisions discussed in the first half of this chapter. In the second half we want to go into the technical details of implementation, focusing on structural software design decisions and the near real-world behavior representation.

7.3.1. Structural Framework Components

Development of a software with the described complexity demands a good and extendible design. The additional aim to provide a modular framework for diverse simulations and evaluations underlines this need. The following pages will introduce the structural components provided by the framework, with a special focus on UAV fleet resource management.

7.3.1.1. Mission Control

This component represents the entity to manage the UAVs and other nodes in centralized scenarios. It is capable to perform maintenance related tasks and reorganize nodes and redistribute missions.

Missions to be executed by nodes as part of the overall scenario are loaded from files of the `waypoints` file type. These files contain lines of maneuver commands with comma-separated command parameters. The specific structure of the files is generated by Mission Planner inside its Flight Planning pane. An example of such a file was shown in Section 3.3.2. Mission Planner provides all features to easily define and edit missions for UAVs and also transfer these to the real-world UAV. By using the same file format, not only the mission definition process can be simplified, the same mission can also be executed both in the real-world and the simulation environment without translation efforts.

7.3.1.2. Node Hierarchy

The simulation framework supports different kinds of nodes, from stationary devices to airborne vehicles. Nodes as shown in Figure 7.1 create a hierarchy for a wide range of robotic systems. The abstract class `GenericNode` defines the common base for all nodes, consisting of properties like the geographic coordinates or a current operational state representation. Further base classes `StationaryNode` and `MobileNode` are derived from the `GenericNode` with additional properties. The `ChargingStation` is implemented as a direct specialization of the `GenericNode` because of its special properties in energy maintenance processes.

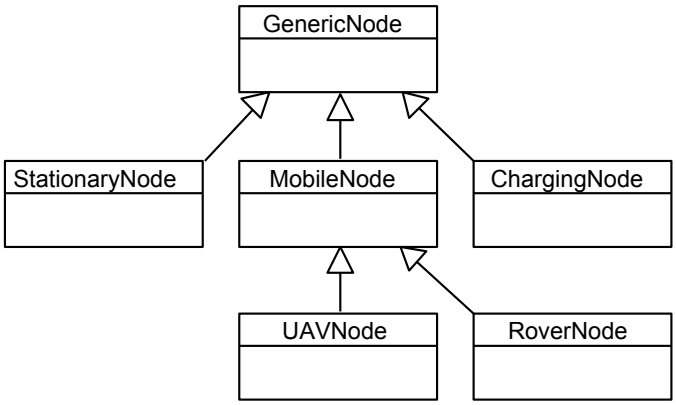

Figure 7.1 – Class diagram of the provided node hierarchy structure.

The shown hierarchy represents the currently implemented set of node types. Further specialized classes can be derived by the framework user. All methods needed for the intended simulation framework execution are either provided by `GenericNode` or

`StationaryNode`/`MobileNode`, or are abstract methods to be implemented by full classes.

Inheriting from the `MobileNode`, the `UAVNode` is a specialized example and is the main node to be used in further analyses. The `UAVNode` will henceforth represent our abstract UAV model from Section 3.2.4. The UAV node has concrete implementations for the behavioral functions and contains and utilizes the energy consumption profile and prediction model as described in more detail below.

7.3.1.3. Commands

The Mission Planner software communicates with compatible UAVs using the MAVLink communication library, cf. Section 3.3.3. Table 7.1 lists all MAVLink commands considered and supported by the simulation framework as part of a `waypoints` file.

Judging by the movement behavior of the UAV, every command execution is comparable with either a hovering maneuver or a point-to-point maneuver according to our abstract definition of a maneuver in Section 3.2.3.

Table 7.1 – Overview of the supported MAVLink commands.

MAVLink Command	Description
WAYPOINT	Position change to specific coordinates
LOITER_TIME	Hold position for a certain duration
LOITER_UNLIM	Hold position indefinite
LAND	Land at the current coordinates
RETURN_TO_LAUNCH	Move to and land at the launch coordinates
TAKEOFF	Ascend to a certain height at the current position

Additionally, in accordance with our publication [Die+16], the CHARGE command was implemented. The command was especially defined for maintenance considerations and instructs the UAV to stay in position (e.g., connected to a charging station) as long as the battery is recharging. The command terminates when the full charge state or a defined intermediate percentage has been reached.

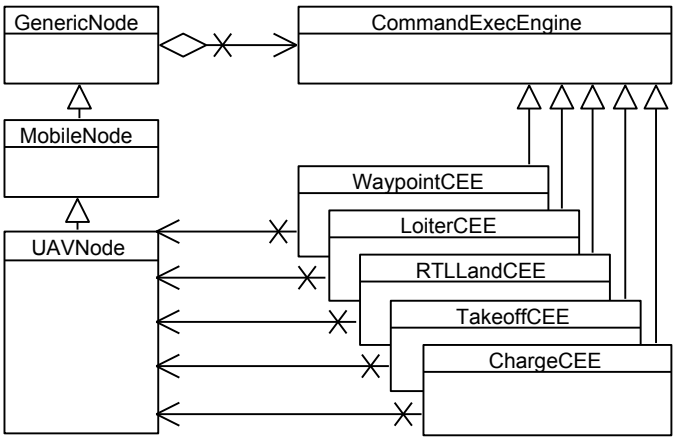

Figure 7.2 – The implemented structure for command execution engines.

7.3.1.4. Command Execution Engine

The behavior of a node is highly dependent on the current operation state of the node. The state of the node is linked to the command that the node is currently executing. These states are represented for each UAV by the supported MAVLink commands shown in Table 7.1. Each command has a specific impact on the node in terms of functionality, restrictions and behavior.

To cope with this tight dependency, the behavioral software design "state pattern" was implemented. Figure 7.2 shows the design and relations of the implemented structure following the commands definition from above.

The UAV node implements all methods needed to simulate the behavior of the UAV. Command-specific details of these methods are however outsourced to various command-specific subclasses of the abstract `CommandExecEngine` class. A UAV owns exactly one command execution engine object as a member and passes down all state/command-specific computations. The command execution engine object is exchanged upon command completion.

It should be noted that the class `CommandExecEngine` is associated with the `GenericNode`, but all shown full implementations are associated with the specialized `UAVNode` class. This ensures that all derived nodes can utilize the concept of commands and command execution engines, while, at the same time, specific nodes will be associated with matching execution engines, able to interact with the associated specialized node

class. To allow direct access from command execution engines to all members of the respective node class, the command execution engines are defined as C++ friend classes of the corresponding node class.

The concept allows for a wide range of different node and command types, the behavior and functionality of a node is not restricted by the simulation framework and can be reused and extended by the user.

7.3.2. Communication and Interaction

So far the structure of a typical simulation setup is defined by a mission control entity and by multiple UAVs or charging nodes in the simulation field. The simulation framework implements and provides simple communication and coordination means between them. The behavior of nodes relies on the existence of a mission, represented as a list of commands to be executed. The mission control will then distribute missions among the existing nodes for execution. Nodes without a mission will stay in an idle state.

Nodes assigned to missions will start executing the assigned commands autonomously and will report status data back to the mission control regularly, e.g., upon maneuver completion. As mentioned in the last section, the command to be executed decides about the execution engine used by the node. The node will be able to update its data (e.g., its position) independently of the active execution engine, and report status information (e.g., the estimated time until maneuver completion).

The communication between mission control and field nodes is implemented using the communication features provided by OMNeT++.

7.3.3. UAV Energy Consumption Simulation and Prediction

The ability to simulate realistic UAV energy consumption is one of the base requirements of the simulation framework. Furthermore it is required to be able to support look-ahead predictions of energy consumption for future maneuvers, to support resource management processes, as described below. This double tracked use of an energy profile is a unique property of the presented simulation framework. The implemented energy profile follows the mathematical model developed in Chapter 4. It should be noted that

the two use cases must be kept separated to avoid using identical values for estimation and execution. Otherwise the stochastic nature of the system would be biased.

The limited energy capacity and the energy consumption of nodes are implemented in multiple parts of the presented structure. Figure 7.3 depicts a simplified view of the involved classes and methods. Energy consumption is a common functionality for all nodes and hence part of all command execution engines. A limited energy source, in the form of a battery, is on the other hand only relevant to a part of nodes not connected to a constant power supply. The battery class is thus modeled as a member of `MobileNode`.

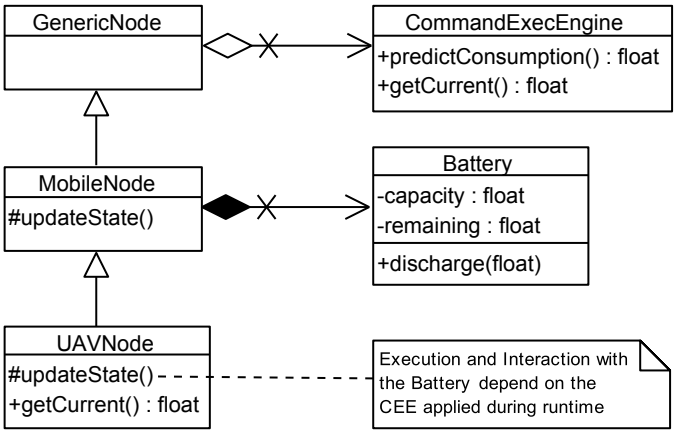

Figure 7.3 – Simplified class diagram of the energy consumption profile and prediction implementation.

The parameterized energy consumption profile for the 3DR Solo quadcopter presented in Section 4.6 is provided through the specialized UAV node class. Addition or substitution by another energy profile is easily supported by the framework. Attention went into the definition of the profile in source code, as a separated file, using the same parameters and lookup tables as discussed in Chapter 4.

The functionality to simulate and predict energy consumption is visually represented by the proxy function `getCurrent()` in Figure 7.3. The respective part of the simulation framework provides many more sophisticated functions, e.g., to draw a random consumption from the underlying normal distribution or to retrieve a deterministic consumption under safety margin considerations.

7.3.4. Maintenance and Replacement Processes

The specification of maintenance processes can vary between different scenarios, from centralized solutions involving a single mission control to self-organized multi UAV systems with cooperative maintenance and node replacement decisions. The current implementation state of the simulation framework components provides the flexibility and extendibility to build simulations of different kinds of scenarios.

A key feature for maintenance processes is the aggregation of combined knowledge about the status of multiple UAVs in the field. As discussed in the previous paragraphs, information like the remaining battery capacity and the energy consumption for future maneuvers (and hence the gross remaining time of operation) is know by the individual UAVs. This data can be transmitted to other UAVs or a mission control to aid in the maintenance process decision making. Methods and data members to store, retrieve and transmit this data are implemented by the simulation framework in all nodes.

The mission control simulation component provides an internal representation of all managed UAVs in the form of a lookup table. The table consists of a snapshot view of all UAVs, containing the current state, the currently executed mission and future maintenance needs.

7.3.5. Failure Handling

Unexpected failure of single UAVs, as specified by Requirement [REQ-F-113], is not part of the implemented framework logic. However, failures resulting out of an over-discharged battery needs to be handled. As discussed in Section 4.4.2.4, the consumption of a maneuver or of a set of maneuvers can exceed the applied safety margin and hence lead to early depletion of the battery.

Resulting failures of a UAV in air would reduce the overall amount of available UAVs and hence render an endless simulation with the aim of stationary evaluation results impossible.

To decouple the two analysis aspects failure probability and stationary evaluation, a middle path was chosen. The simulation will identify and record events of early depletion. Additionally it will allow over-discharge of the battery during maintenance flights,

to support uninterrupted scenario execution. Depletion of a UAV during mission execution is handled and recorded separately. The over-discharged UAV will not disappear from the scenario and will start charging from zero capacity when reaching a charging station. We do not expect any significant side effects from this design decision, as every depleted UAV will anyhow have to go through a long-lasting recharging process.

Later evaluation has to consider measures from both aspects to assess the effectiveness and applicability of a strategy during real-world application.

7.4. Mass Simulation and Performance Data Processing

The simulation framework provides the means to collect performance data, and store it in files at the end of a simulation run. Those files can then be further processed to analyze the general system performance and to evaluate and compare different system configurations.

Tables 7.2 and 7.3 list the aspects that are recorded for UAVs and charging stations. Stored values are aggregated sums over the whole simulation time, separated per UAV/CS and simulation run. The latter is crucial for mass simulations.

Our discrete event simulation base OMNeT++ provides a powerful system for mass simulation automation. As described in the OMNeT++ documentation on "Parameter Studies" [VH+18, Section 10.4], simulation parameter settings can be given as lists or ranges, resulting in mass simulation of all combinations. Additionally, the `repeat` parameter causes every combination of parameter settings to be simulated multiple times, under different random number seeds. These seeds ensure that random aspects of the simulation, like parts of our energy consumption model, behave differently across simulation repetitions. By comparison and consolidation of performance data from different simulation runs, we are able to analyze the effects of parameter changes, while averaging out stochastic influences.

The selection of simulation run parameter ranges and step sizes can happen manually and in reaction to observed behavior and optimization goals. Automated more effective and efficient methods to select and adapt parameter settings under given optimization

Table 7.2 – UAV node performance data collected during simulation.

Type	Aspects	Description
Time	Mission Maintenance flight Charge Idle	Time in seconds spent in the given life cycle phases.
Energy	Mission Maintenance flight Charge	Energy in milliampere-hours consumed and charged in life cycle phases.
Overdraw	Mission Maintenance flight	Energy in milliampere-hours consumed beyond the battery capacity.
Count	Missions Mission m. Maintenance m. Charge phases Idle phases Overdrawn life cycles	Amount of missions executions Maneuvers executed in mission execution Maneuvers executed in provision & return Summed up charging processes Summed up idling phases of UAVs Life cycles that ended in battery overdraw
	Fail	Indicator for known failure state of a UAV

criterions and restrictions are available in the form of simulation-based optimization heuristics. The topic and potential heuristics were discussed and analyzed in a preceding work by the author [BDZ15].

We developed an analysis script in the statistical computing language R, to process the mentioned recorded performance data files. The script executes multiple steps of preprocessing, then calculates and plots various evaluation results. The use cases of the script will be covered in the following chapter on resource management system evalu-

Table 7.3 – CS node performance data collected during simulation.

Type	Aspects	Description
Energy	Usage	Energy [mA h] transferred into UAVs
Count	UAVs	Total amount of UAVs serviced

ation. The project is publicly available under an open source license, more details and a repository URL can be found in Appendix A.1.3. The repository also includes exemplary performance data files.

7.5. Software Quality and Functional Verification

The current software architecture is driven by modularity and scalability. Most design steps were discussed with colleagues or among developers, to create a flexible base for later framework use. The same method was used during the definition of the software behavior. Implementation was then done by one developer and the method of peer-review involving another developer was used to ensure that common mistakes or missed cases were uncovered. General development incorporated the new features and containers of C++11 to benefit from their added safety and error prevention. The frequent use of C++ exceptions and evaluate assertions is another concept established in the development process to catch illogical, unwanted, or illegal behavior.

Memory-related issues are among the most frequent C++ programming errors. They are generally hard to detect and track down. Good software design and modern C++ concepts, like the RAII programming technique or C++11 smart pointers, help to reduce that risk. The simulation framework was frequently tested with the memory checking tool (Memcheck) provided by Valgrind[1], the instrumentation framework for building dynamic analysis tools. The tool uses dynamic recompilation to insert additional instructions in the behavior of the checked program, allowing for memory usage analysis. Memcheck tracks validity and addressability of accessed memory along the program execution and detects the use of uninitialized memory and memory leakage. Results of the analysis of framework simulation runs were the starting point of program code improvements.

The developed framework offers a set of structural elements and functions to build a scenario simulation setup from. This involves the aforementioned movement and energy consumption prediction model, or the different replacement scheduling and replacing UAV selection strategies. Evaluation of the behavior of these aspects was an important task along the whole development process. A systematic functional verification was

[1] Valgrind (v3.13.0) official webpage: http://www.valgrind.org

furthermore the task of the student work by Michael Sommer [Som18]. We are confident that the framework, especially tested scenario simulation setups, behaves in accordance with the discussed real-world derived models and the strategy definitions, defined in the previous chapters.

8. An Application Scenario for Resource Management Evaluation

The existence of a resource management system in a UAV fleet utilization, like the UAV-aided disaster response, is indispensable to enable an uninterrupted continuous coverage of all instructed tasks. A corresponding concept was presented in Chapter 6, however, the verification and optimization of the system and its individual aspects is not feasible in a real-world application. Therefore, a model-based simulation using the simulation framework presented in Chapter 7 will serve as a proxy for the thorough system evaluation.

This chapter introduces an example application scenario, presenting a realistic disaster situation and a meaningful UAV response setup. The scenario will be used to verify the resource management system, and to evaluate and optimize various aspects. A discussion of the results will underline the applicability of the resource management system and the underlying optimization potential. While given numeric results are specific to the presented application scenario, general findings, identified trends, and recommendations are valid for other scenarios with similar arrangements.

8.1. Scenario Description

Our fictional disaster scenario resembles an imaginable situation. A forest fire developed in the woods around Kickelhahn hill south-west to the small city Ilmenau, located in Thuringia, Germany. In the north-west, the forest ends at the village Manebach, the Hotel Gabelbach is located in the south-eastern part of the forest. Danger to human life has to be assumed in the case of a disaster, as the Kickelhahn hill permits many outside activities and is popular among families and hikers. Figure 8.1 shows an annotated cartographic map of the region.

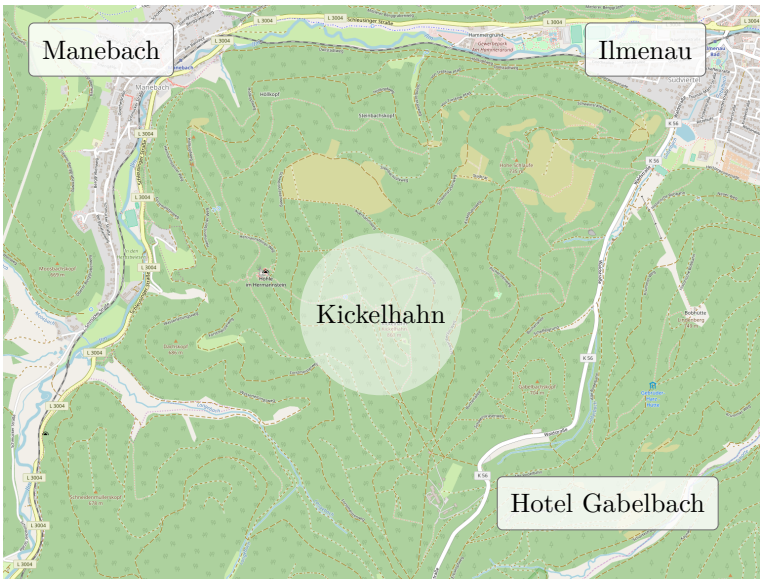

Figure 8.1 – Cartographic map of the application scenario region, showing the surrounding inhabited areas, major fortified roads, and all hiking trails. Source: OpenStreetMap. Map center: N50°39.943′ E10°52.855′

After the fire with unknown origin started spreading, disaster response personnel was alarmed and arrived at the scene. Fire fighters are in position to contain and extinguish the spreading fire. Special attention goes to the protection of human life and of the endangered real-estate. Required response actions involve:

- Identification and repeated observation of the affected area
- Search for trapped humans
- Search for pockets of embers
- Construction of a communication infrastructure

These and more actions need to be executed independent of existing roads and the spreading fire. Results are the basis for further response actions and dispatch of personnel.

The described scenario fits well with the definition of a disaster scenario as described in Section 3.1 and the listed response actions motivate the utilization of UAVs, as previously discussed in Section 3.1.2.

The response coordinator decided to utilize multicopter UAVs to aid in the disaster response. The mission breakdown resulted in a number of missions to provide the means

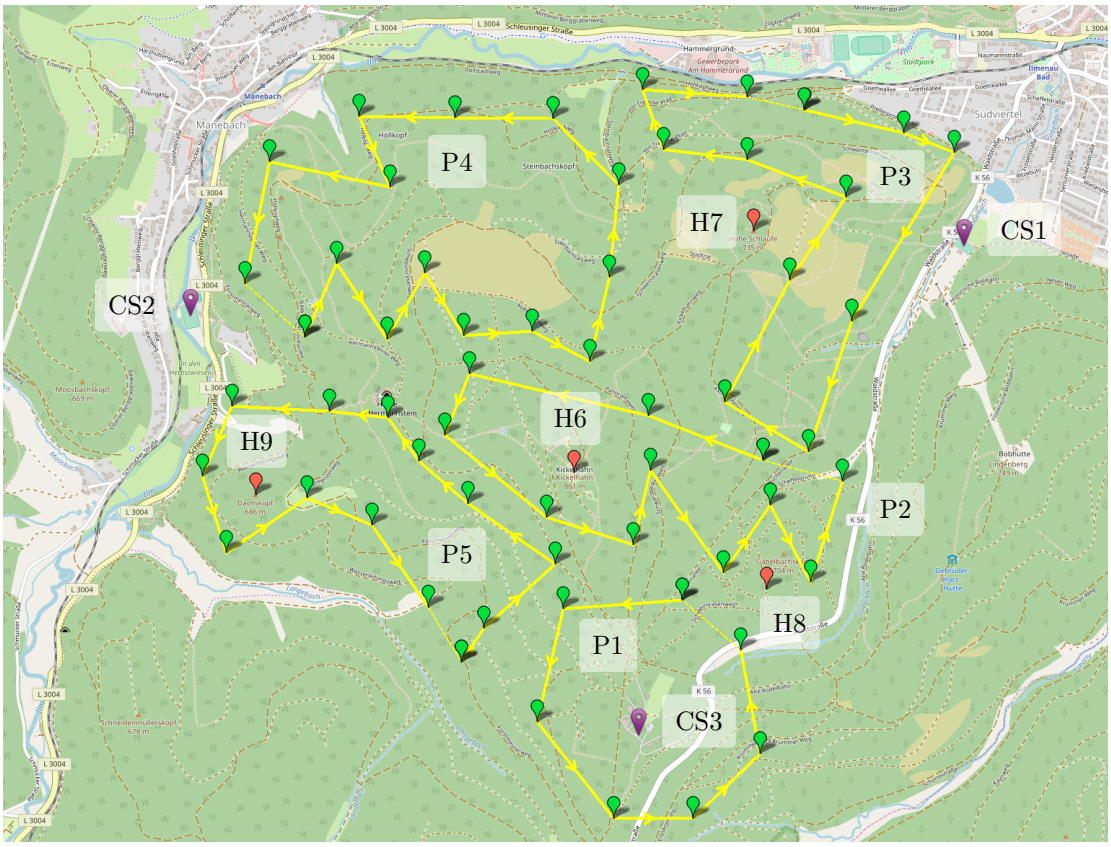

Figure 8.2 – Cartographic map of the application scenario region, showing planned point-to-point missions ('P', green/yellow), hovering missions ('H', red), and charging stations ('CS', purple).

for the listed response actions. Missions 1 to 5 cover different areas of the disaster region, namely the Hotel Gabelbach, the main Kickelhahn hiking trails, the forest parts close to Ilmenau and Manebach, and the southern part of the forest. Additionally, missions 6 to 9 were planned to provide a backbone for a heterogeneous decentralized multi-hop ad hoc network, as motivated in Section 3.1.1. Steady hovering nodes are therefor planned on top of the four highest elevations in the affected region: the Kickelhahn, the Hohe Schlaufe, the Gabelbachskopf, and the Dachskopf.

In Figure 8.2 the missions are presented in the scenario region. All missions consist of either hovering or point-to-point maneuvers and are to be executed indefinitely, until the coordinator terminates the disaster response actions. All maneuvers are planned at approximately 100 meters above ground to stay close to the field but in safe distance to the fire, resulting in climbing and descending flights along the forest's elevation profile.

Parts of the routes are planned along the major dirt roads and hiking trails, as trapped humans and rescue personnel are more likely to stay on these.

Three charging stations are positioned around the disaster area, in locations that are easy to reach for the response personnel and that offer the necessary open space. Number and locations were chosen, so that every mission is close to at least one charging station. Charging station 1 is located at the tennis court Ritzebühl in Ilmenau, charging station 2 operates from the sports field in Manebach, the third charging station is installed in the parking lot of Hotel Gabelbach. They are shown as 'CS' points in Figure 8.2.

The discussed details resemble a potential real-world application. Some decisions were also made for the sake of representative evaluation results. To that end, missions vary in length and altitude difference, and are near and far to close-by charging stations.

The goal of this chapter is to evaluate the presented resource management system in general, and the effects of different involved strategies in particular. The application scenario offers one specific example problem and is deemed a fitting candidate for further analysis and evaluation.

8.2. Scenario Setup Configuration for General Evaluation

The fictional disaster scenario was described from a non-technical disaster response viewpoint. The utilization of UAVs introduces additional technical aspects and questions that need to be discussed and decided prior to the utilization. These were already broadly discussed in Chapter 5 during the requirements analysis. While specific decisions will be subject to the following sections on strategy evaluation, in this section we want to shortly discuss and determine invariant aspects and parameters for all evaluation steps and for our model-based simulation environment.

- All utilized UAVs are assumed to be of the same build and to show the same movement behavior and energy consumption properties (cf. Requirement [REQ-D-303]).
- All UAVs follow the movement behavior and energy consumption profile as discussed and derived in Section 4.6.

- At the beginning of every simulation run, available fully charged UAVs are placed equally distributed at the charging stations.
- All charging stations have sufficient charging and waiting spots for all UAVs in the simulation available (cf. Requirement [REQ-F-125]).
- Hovering maneuvers have to have a certain time resolution to conform with the strategy to plan UAV replacement at maneuver transition points. We decided to configure every hover maneuver with a 20 seconds duration.
- Prediction of future maneuver energy consumption is estimated under consideration of a safety margin, as discussed in Section 4.4. If not otherwise stated, a 95 % quantile will be applied for all estimates.
- Communication link or communication network limitations, as defined by Requirement [REQ-D-308], are assumed to have no considerable effect on the simulation results. This is justifiable by the expectation of a heterogeneous decentralized multihop ad hoc network, providing constant communication means [Beg+13].
- The simulation does not simulate particular weather conditions, which notably means that no strong winds or extreme temperatures are considered. Potential implications by the forest fire on our UAVs in the field are assumed to be negligible, justifiable by the minimum flight altitude of 100 meters above ground.

8.3. General Results and Evaluation of Base Requirements

A first simulation experiment was executed, to analyze general system behavior, systematic dependencies, resource utilization trends, and system fitness under the previously defined base requirements. The experiment was carried out with the configuration listed in Table 8.1.

The simulation time was chosen as three days, to represent a long scenario duration and to ensure the development of stationary results for consolidated performance data. Enough simulation run repetitions were chosen to level out unique state trajectories in single simulation runs.

Table 8.1 – Mass simulation configuration for general evaluation.

	Setting	Rationale
Overall UAV count	100	(uncritical)
Overall CS count	3	(challenging)
Overall missions	9	(diverse)
Simulation time	72 hours	(realistic, stationary results)
Repetitions	24	(cf. Section 7.4)
Replacement Strategy	"Latest Opportunity"	(cf. Section 6.4.1)
Replacing Node Selection	"Shortest Provision"	(cf. Section 6.5.1)

The simulation framework produces performance data for all UAVs and all charging stations in all simulation runs. The extent of performance data produced was described in Section 7.4. The section also introduced our R script to post-process and analyze the data, resulting in values and diagrams presented throughout this chapter.

Before evaluating general results and the base requirements, we need to have a look at the independence of individual nodes and identify potential systematic correlation with aspects of the scenario.

8.3.1. Preliminary Analysis of Systematic Independence

We expect no systematic differences between different simulation runs, but suspect weak systematic relation between individual UAVs, CSs and other aspects of the scenario. Common causes for potential dependencies are discussed below.

Simulation run independence Different simulation runs start with the same initial conditions. The underlying UAV movement and energy consumption profile, and the resource management strategies are furthermore identical across simulation runs. However, every simulation run performs differently, due to the imposed simulation run randomness. Therefore, the simulation runs should result in varying decisions and performance results, but are comparable for a statistical evaluation.

UAV utilization equality The random influence on UAV behavior affects performance data, but also decisions with regard to resource management. In simulation, the selection of a replacement UAV for a mission is done by random among suited candidates.

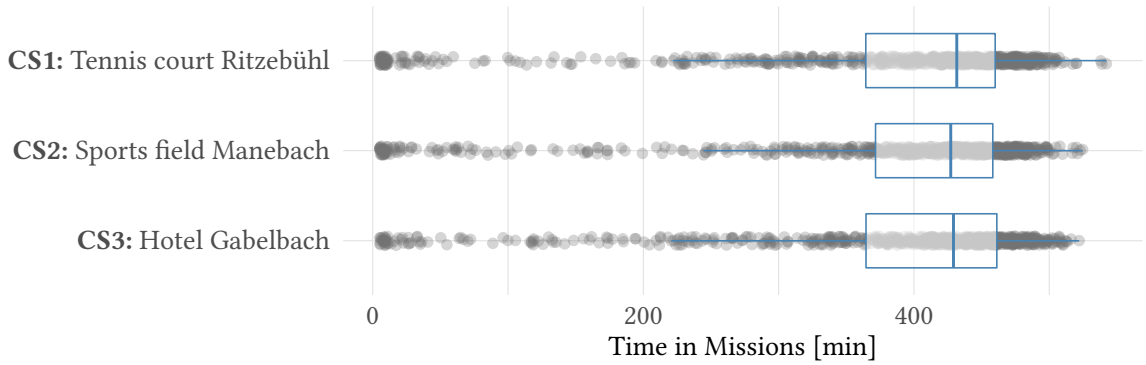

Figure 8.3 – Evaluation of the influence of the initial UAV location on the later simulation behavior. Every dot represents one UAV in simulation.

That should result in a uniform utilization of all UAVs available to the scenario. After a sufficient simulation time, the utilization of UAVs is hence expected to converge at a common quota.

Independence from initial UAV location A potential influencing factor is the initial location of individual UAVs. In the scenario, UAVs are preplanned to be equally distributed among the charging stations, irrespective of the simulation run randomness. This could lead to segmentation and the indicated weak systematic correlation between performance values and the UAV ID or initial UAV position, respectively, especially after only a short simulation time. Figure 8.3 shows the overall time in mission of all UAVs from all simulation runs, matched with their respective initial charging station. The diagram suggests that the initial location does not seem to have significant influence on the UAV utilization throughout the simulation. We will thus ignore the initial location in further analysis steps.

Separation due to CS popularity We expect different popularities of charging stations due to the extent of individual missions and their distance to nearby CSs. Resource management strategies, discussed in Chapter 6, generally aim to reduce the flight distance from and to missions, leading to a tendency of missions being served by a specific charging station. The scenario was designed to not intensify such effects, by preplanning missions to be near and far from charging stations and equally distributed between them. Nevertheless, Figure 8.4 shows a clear difference in overall served amount of UAVs by the available charging stations. The previously mentioned suspected segmentation does, however, not show as an issue, when Figure 8.3

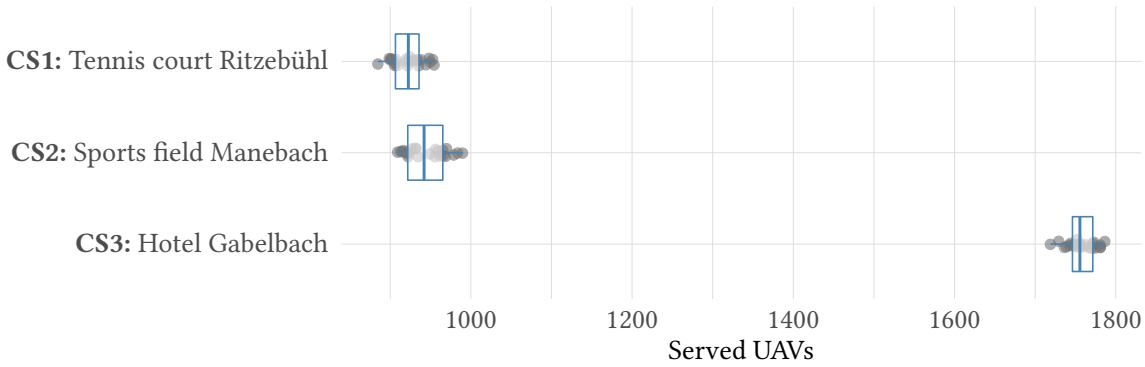

Figure 8.4 – Amount of served UAVs by the three charging stations. Every dot represents one simulation run.

is considered in combination with Figure 8.4. An explanations could be the transition between charging station realms in cases of temporary shortages, a constellation anticipated by the experiment. charging stations are seen as part of the scenario and their popularity for service provision is insignificant for further analysis and our focus on UAV utilization and resource management strategies.

We found all mentioned dependencies to be insignificant for further resource management focused evaluation. We will henceforth consider performance data from different UAVs from different simulation runs to be independent, comparable and fit to be consolidated for statistic evaluation.

8.3.2. Discussion of General Performance Data

The first experiment was performed with a moderate configuration without pushing for extremes or critical boundaries. Consolidated statistics shall set a base line for further evaluation steps. Figure 8.5 and Table 8.2 show noteworthy statistics about the experiment performance data.

We want to highlight the percentage of overall time spent in productive mission execution. With only 8.8 % it represents just a small portion of the UAV life cycle. The charging phase claims over one half of the whole life time, as was already expected due to the slow recharging process. It is also interesting to notice the half-half ratio between mission execution and maintenance flights, both in time and energy consumption. As

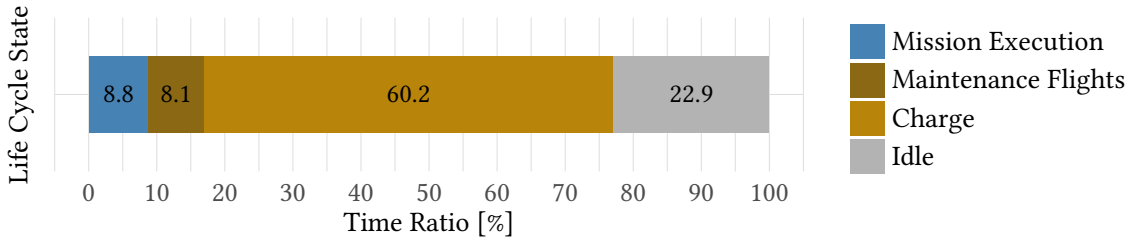

Figure 8.5 – Distribution of time ratio spent in the UAV life cycle phases.

discussed before, parts of the life cycle spent in maintenance flights and idle phases are subject to potential optimization.

The high average number of life cycle iterations is also worth noting. In combination, the aggregated life cycle data once again emphasizes the necessity and opportunity of a resource management system to automatically, reliably, and safely support continuous disaster scenario utilization of UAVs.

8.3.3. Analysis of Continuity and Recirculation Fulfillment

Base requirements towards a general resource management system were defined in Section 5.4. The system must be able to observe the scenario and must provide the necessary means and apply the necessary actions to fulfill continuity and recirculation. Verification of base requirement fulfillment by the simulation framework in the presented scenario is a precondition for further fine-grained evaluation steps.

Continuity is responsible for an unterminated or uninterrupted mission execution by the method of successive UAV utilization, exchange, and replacement. Recirculation on the other hand has to ensure the enabling of reutilization of UAVs by recharging at a charging station.

In order to verify the fulfillment of these requirements, three properties have to be shown in the simulation results:

- No termination of a mission
- No deterministic interruption of a mission
- No in-mission failure of UAVs (cf. Requirement [REQ-N-204])

Table 8.2 – General performance data analysis results. If not otherwise stated, they account for all UAVs over the full 72 hours as mean over all repetitions.

	Mean value	Remarks
Life Cycles per UAV	50.46	σ = 9.66
Replacements per hour	64.52	(across 9 missions)
Energy consumption per UAV		
• per life cycle [mA h]	4459.7	σ = 47.5
• in mission execution [%]	53.4	
• in maintenance flights [%]	46.8	
• per day [mA h]	69 392.1	
Energy demand per day [kWh]	101.47	(approx. 10x normal household)

All simulation runs and the generated performance data were analyzed accordingly. Termination, which is the unplanned break-off of continuous mission execution, is checked by dedicated program logic during and at the end of a simulation run. None of the simulation runs of the first experiment ended in terminated missions.

Interruption of a mission, in the limits of the previously discussed assumptions, abstractions and restrictions, is possible in the form of a delayed replacement and exchange process. Delay can have one of two reasons: Exchange communication duration and replacing UAV arrival time. Generally, we can assume the size of mission data to be rather compact and thus quickly communicated. Additional measures could be the communication of data over short distance, without interruption of the UAV movement. The latter reason of delay in UAV arrival time is linked to the absolute navigation speed control behavior discussed in Section 4.3.2. In real-world application, the potential short delays resulting from either of the described reasons, could easily be mitigated by according countermeasures. Due to the expected magnitude of potential influence in comparison to more central aspects, the aspect of interrupted mission execution will not be further considered during this evaluation.

Failure of the UAV system could happen due to one of two reasons: Spontaneous hardware/software failure or systematic failure due to a depleted battery. The former was excluded from the scope of this thesis in Section 5.3.2.

Failure of a UAV due to premature battery depletion is possible because of uncertain outside factors and resulting varying energy consumption by the UAV. The topic was discussed in-depth in Chapter 4. In Requirements [REQ-N-203] and [REQ-N-204] we formally specified probability thresholds for those events. Table 8.3 lists all events of premature battery depletions during the first experiment and compares them with the overall amount of mission executions performed by all UAVs across all simulation runs.

Table 8.3 – Events of premature battery depletion during the first experiment.

	Life cycles	Failure and loss due to battery depletion, during	
		maintenance flight	mission execution
Count	112 045	475	0
Ratio [%]		0.42	0

The case of depletion during mission execution was found to be improbable. The probability of depletion during maintenance flights is far lower than the formally defined threshold of 5 %.

In conclusion we can say, that the simulation framework and the chosen application scenario fulfill the base requirements. In the next sections, the potential of different resource management strategies on performance data computed above will be evaluated.

8.4. Impact of Safety Margin Quantile Selection

An important part of the energy consumption profile discussion in Chapter 4 was the consideration of uncertainty and the inclusion of safety margins in profile-based predictions. The prediction of a process behavior outcome based on a pessimistic value off its statistical mean decreases the chance of underestimation and therefore increases the safety of the system with regard to failure propagation resulting out of overestimation. In Section 4.4.1 we highlighted the importance of a good quantile value selection as the deciding factor for safety margins in predictions and their effect on the system operation. We expected a higher probability for insufficient predictions for smaller quantiles and a lower energy efficiency for bigger quantiles.

Experiments with the same simulation configuration as in the previous section (cf. Table 8.1) were carried out for five quantile settings. Table 8.4 shows comparable results to evaluate the quantile selection.

Table 8.4 – Premature battery depletion and mean life cycle consumption for different safety margin quantile settings.

	Premature terminations	Failures during maintenance flight [%]	Mean consumption per life cycle [mA h]
$p = 0.50$	24	—	—
$p = 0.75$	13	1.88	4843.9
$p = 0.95$	0	0.42	4453.9
$p = 0.975$	0	0.39	4352.2
$p = 0.99$	0	0.37	4240.3

The quantile setting $p = 0.50$ is an extreme example, as it represents the mean value of a normal distribution, resulting in mean values for predictions of energy consumption. This setting renders the idea of a quantile-based safety margin ineffective. The resulting simulation behavior was as expected not favorable. All 24 simulation run repetitions terminated prematurely, due to over-optimistic predictions, leading to errors in the replacement process, eventually violating the mission termination base requirement. Similar but alleviated simulation behavior was recorded for the quantile setting $p = 0.75$ with over half of the simulation run repetitions failing. Values in the latter two columns only account for successful simulation runs.

The performance metrics for UAV failure during maintenance flights and the mean energy consumption in single life cycles are interesting in comparison. The failure rate drops with a quantile increase, however so does the life cycle consumption. Our expectation of increased safety and reliability with the trade-off of decreased energy efficiency is thereby confirmed.

It is also worth mentioning, that the failure rates of all quantile settings stay below the 2 % defined as threshold in Requirement [REQ-N-203]. With a better understanding of general performance of the scenario given in Table 8.2, we have to reevaluate this threshold. An average of 64.52 replacements per hour results in the same amount of maintenance flights returning to a charging station. Over the course of 24 hours, and under the highest failure probability of 1.88 %, we have to expect 29 failing UAVs. This

number is not acceptable. Future work should look into different strategies to minimize the probability of battery depletion during maintenance flights, while decreasing the generally applied quantile setting. A trade-off between the minimization of the number of failing UAVs and the maximization of energy efficiency forms yet another optimization problem.

Further evaluation steps will be performed with the safe setting $p = 0.95$, which can also be recommended as a general setting for safe but efficient applications.

8.5. Evaluation of Replacement Optimization

In Section 6.4 and Section 6.5, strategies for the details of replacement scheduling and execution were discussed and defined. Their simulation and evaluation with attention to performance and energy efficiency improvement is the goal of this section.

8.5.1. Replacement Scheduling Strategies

We introduced three replacement scheduling strategies: the latest opportunity heuristic, the shortest return heuristic, and the bi-objective heuristic.

The major difference between the three strategies is the handling of multiple charging stations and the relative distances to them over the course of a mission. In order to evaluate the impact of replacement planning, two changes were done to the experiment configuration:

1. Missions ‘H6’ to ‘H9’ are left out. These missions consist of hovering maneuver and remain steady at a single location. They are therefore not affected by differences between the strategies.
2. So far, the coverage with CSs was sparse. For most missions, the distance to the nearest charging station for all maneuver transitions had only one minimum. In order to add local minima and to thereby support the potential improvement by the second and third heuristic, we planned additional charging stations in proximity to the application field.

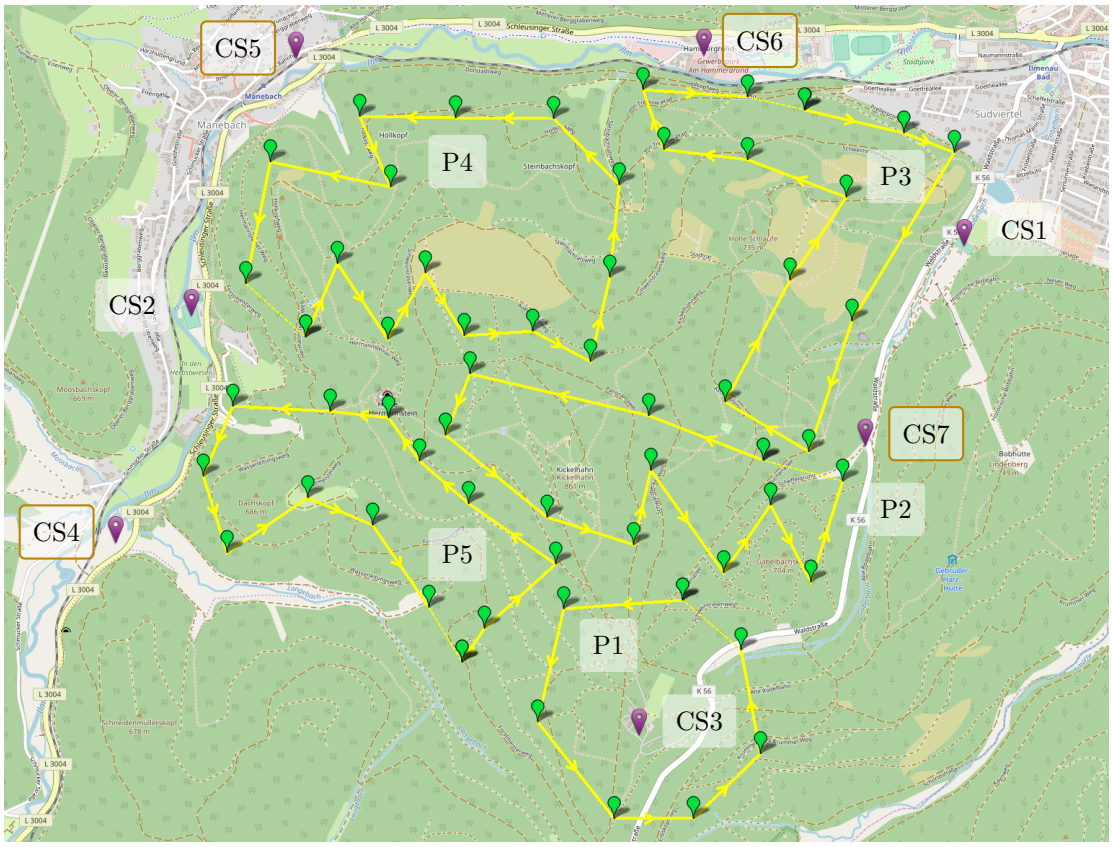

Figure 8.6 – Modified scenario response constellation for the evaluation of replacement scheduling (cf. Figure 8.2). Additional CS for replacement scheduling strategy evaluation are highlighted.

Figure 8.6 illustrates the modified response constellation of missions and charging stations in the application field.

Performance data was generated with the simulation configuration in Table 8.1 but with all three replacement strategies. Figure 8.7 shows the ratio of time spent in the UAV life cycle phases, as mean of all UAVs over all simulation runs, differentiated by the three strategies.

The shortest return heuristic, in comparison to the latest opportunity heuristic, resulted in a significantly worse ratio between mission execution and maintenance flights, while unwanted time in idling phases increased. As we already expected, the shortest return heuristic (cf. Section 6.4.2) has the tendency to favor an extreme behavior of unnecessarily short mission phases, resulting in worse overall system performance. This is also visible in the total amount of simulation run life cycles of 2312 under the shortest return

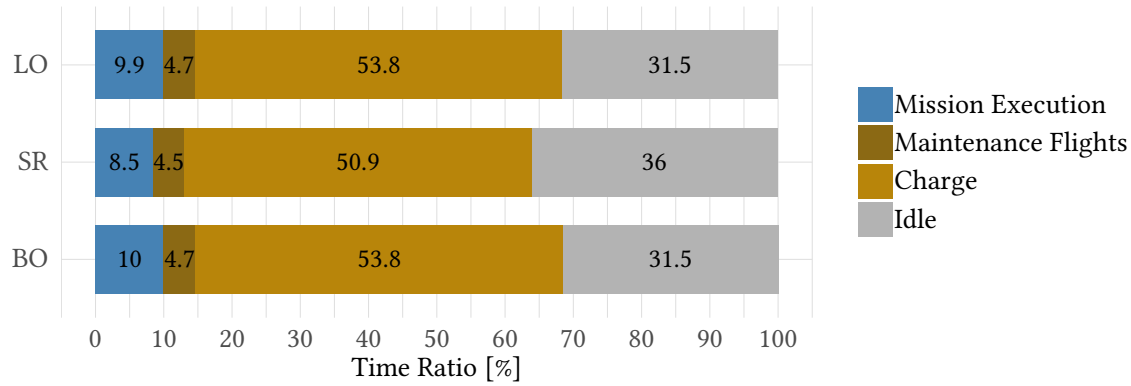

Figure 8.7 – Distribution of time spent in the UAV life cycle phases, compared for the three replacement strategies: Latest Opportunity, Shortest Return, and Bi-Objective (with $w = 0.5$). Be aware that individual numbers are rounded to one decimal place.

heuristic in comparison to 1801 under the latest opportunity heuristic – an increase of 28.4 percent.

Results under the bi-objective heuristic surprise by an almost identical time ratio distribution in comparison to the latest opportunity heuristic. With 1821 life cycles per UAV, the bi-objective heuristic also matches the latest opportunity heuristic by 1.1 percent difference.

The resemblance of values of the two different heuristics is unexpected but explainable. We know that the bi-objective heuristic covers the other heuristics with the extreme weight values $w = 0.0$ and $w = 1.0$. We anticipated a trade-off behavior at $w = 0.5$, however that does not seem to be the case. A subsequent experiment with multiple intermediate weight values should give a better understanding of the influence of the two involved objectives. Additionally we should be able to identify a near-optimal trade-off value.

Figure 8.8 shows aggregated results for simulation performance values averaged over 12 simulation runs per weight value. Energy efficiency represents the percentage of energy invested in mission execution in relation to the overall invested energy. Both diagrams show that there is in fact almost no difference caused by w values between 0.5 to 1.0. We see the reason for that in the proportions of the scalarized Equation 6.12 from page 115:

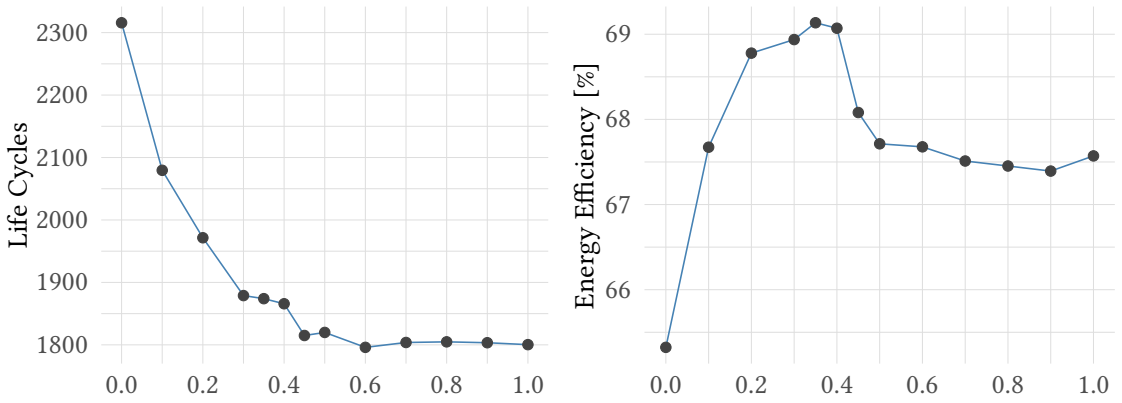

Figure 8.8 – Influence of bi-objective weight w on the average life cycles per simulation run and the energy efficiency.

$$f_{BO}(w) = \max_{k} \left(w \sum_{i=1}^{k} E_M(i) - (1\text{-}w) E_R(k) \right) \qquad \text{(6.12 revisited)}$$

The first part of the equation is a sum and hence multiple times bigger than the second part. This imbalance results in a shifted impact of w on the function value.

Furthermore interesting is the other side of the total range, $w = 0$, representing the shortest return heuristic. The energy efficiency for the heuristic marks the minimum of the whole range and therefore confirms the previously drawn assumption of being the least favorable solution.

Weight values between 0.3 to 0.4 seem to represent an interesting trade-off range, with the highest energy efficiency, yet low life cycle count. An incremental search for the optimal weight value would be possible, but not meaningful. We can expect different optimal values for different system configurations and application scenarios. However, as the general dimensions of maneuvers and mission constellations should be similar, we believe that a common trade-off value of $w = 0.35$ is a good setting for the bi-objective heuristic, making it the recommended of the three replacement scheduling strategies presented.

Ultimately, the difference between the trade-off solution and the latest opportunity heuristic is marginal. We anticipated a clear improvement of energy efficiency, and thus a reduced energy and UAV demand. The gained energy efficiency improvement

only amounts to 1.57 %. We identify the main reason for this outcome in the large spatial distance between missions and charging stations. Even with the additional charging stations added, the time spent on maintenance flights, illustrated in Figure 8.7, is around 50 percent of the time in mission execution. Missions are generally long-spanning and charging stations are only positioned at the borders of the application field, resulting in long provision and return flight distances. Mission and charging station specifics are however not in the decision space of the resource management system and can hence not be further improved.

In any case, the bi-objective heuristic has shown clear potential advantages over the others and could result in higher efficiency improvements in other constellations. We recommend the bi-objective heuristic as the general replacement scheduling strategy.

8.5.2. Replacing UAV Selection Strategies

Replacing UAV selection is another aspect of resource management, as discussed in Section 6.5. Two strategies were presented, one trivial and one leveraging the possibilities of our movement and energy consumption prediction profile. A good replacing UAV selection strategy should be able to provide more applicable energy for the actual mission execution after provisioning. This should increase the possible length of mission execution for a single UAV, and therefore the overall energy efficiency.

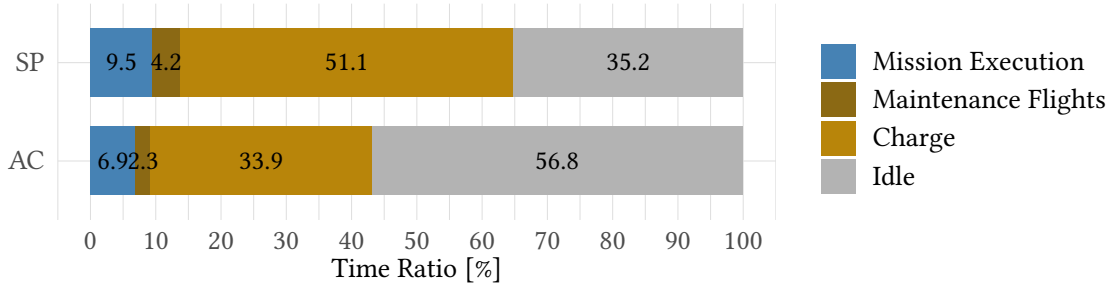

Figure 8.9 – Distribution of time spent in the UAV life cycle phases, compared for the two replacing UAV selection strategies Shortest Provision and Applicable Charge.

Yet another experiment was executed following the configuration in Table 8.1, for both replacing UAV selection strategies and with 16 repetitions per strategy. Time ratio distribution of both strategies is shown in Figure 8.9.

The first difference that meets the eye is the ratio of time spent in mission execution. While the drop in maintenance flight time ratio is enjoyable, the alleged superior strategy seems to cause a slightly shorter time spent in missions. What is counterintuitive at first can be explained by an interesting discovery, when consulting further analysis results denoted in Table 8.5.

Table 8.5 – Selected mean performance results in comparison for both replacing UAV selection strategies: Shortest Provision and Applicable Charge.

	Energy consumption per life cycle [mA h]	Life cycles per UAV	Replacements per hour	Energy efficiency [%]
SP	4461.1	50.4	64.5	53.3
AC	4605.5	37.3	47.8	66.2

The system performance seems to have generally improved under the applicable charge selection strategy. The average energy consumed in life cycles increased, while the average number of life cycles per UAV has dropped. The strategy seems to have caused an improvement of energy efficiency, which reduced the need for UAV replacements, resulting in an overall lower ratio of time spent in mission execution.

The shorter duration spent by a UAV in charging phases and the longer time of idling confirms the statement.

The location and charging state of UAVs selectable as replacing UAV turn out to be important factors for the overall efficiency and gross resource utilization of the application scenario.

8.6. Optimization Potential of Varied UAV Amounts

So far, all evaluation steps were performed with a simulation configuration of 100 available UAVs. In this section, we want to analyze the impact of decreased UAV availability. The financial costs of hardware acquisition, as well as the challenges of transportation to and preparation at the scenario site, motivate the interest in a minimal amount of necessary UAVs to still permit a UAV-aided application scenario response within the defined requirements.

Additionally, we are interested in the overall energy consumption of the whole system of UAVs. The metric is important, as global energy supply could be limited or has to be allocated ahead of time and general magnitude and minimal values might be of interest for the scenario applicability.

The experiment was carried out under a new simulation configuration, taking into account the findings from previous sections. The experiment uses the identified superior strategies. As both are aimed at energy efficiency improvement and UAV count reduction, we do not expect noteworthy results under the simpler strategies. Table 8.6 shows changes to the experiment configuration in comparison to Table 8.1.

Table 8.6 – Mass simulation configuration for the final evaluation with varied UAV count, cf. Table 8.1.

	Setting
Overall UAV count	20 to 400
Overall CS count	3
Repetitions	24
Replacement Strategy	"Bi-Objective Heuristic" with ($w = 0.35$)
Replacing Node Selection	"Applicable Charge Approach"

The overall amount of UAVs available was varied between 20 to 100 UAVs with a step size of 5, interesting ranges were simulated for in-between values. Further settings to analyze a potential saturation of the resource management system were chosen in the range from 100 to 400 with a step size of 50.

8.6.1. Minimal Amount of UAVs for Continuous Fulfillment

Simulations with 20 to 55 UAVs failed across all simulation run repetitions. In these simulations, the system was not able to continuously provide replacing UAVs past a certain amount of time. UAVs were charged slower than they were needed and the system eventually "dried out". Even when being able to support response actions for limited durations, we deem these configurations not fitting for an effective support of disaster response with likely non-foreseeable durations.

Figure 8.10 compares the UAV amount setting with the time, at which simulation runs terminated due to no selectable UAVs for replacement, or because the cutoff duration of 72 hours was reached.

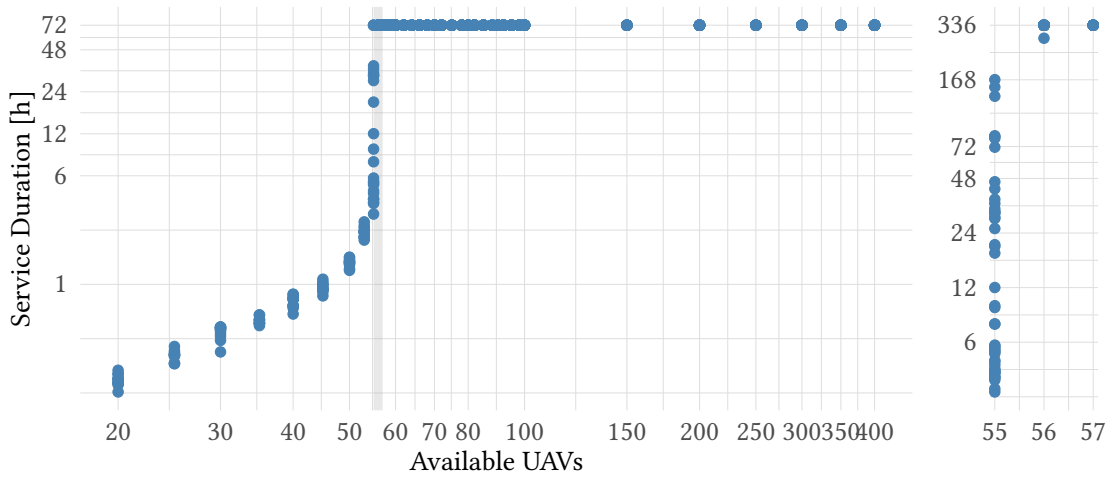

Figure 8.10 – Duration of failure-free scenario response fulfillment for different settings of available UAVs, capped at 72 h in the left diagram. The gray highlighted range of interesting corner cases is magnified in the right-hand diagram, capped at 336 h.

In our application scenario, with the described configuration, 57 UAVs turns out to be the minimum amount for continuous scenario support. The number was obtained in a separate experiment for 55 to 57 UAVs, with a excessively heightened cutoff duration of 336 hours (14 days) and with 48 simulation repetitions. Results for these simulations are shown in the right-hand diagram of Figure 8.10.

While all simulation runs terminated prematurely for experiment settings of 55 UAVs and below, only one out of 48 simulation runs failed for the setting of 56 UAVs. Further simulation repetitions would yield more failing cases. The results indicate that 55 UAVs is a critical edge case for our application scenario and chosen configuration, while experiments with 56 UAVs succeed with a high probability. Therefore, 57 UAVs represents the minimum amount of UAVs for continuous fulfillment of response tasks in the given application scenario configuration.

8.6.2. Minimal Overall Energy Demand for Continuous Fulfillment

The gross energy demand of the UAV fleet generally depends on the complexity of the application scenario at hand, and on the efficiency of UAV utilization.

Please take note that the given number represents energy charged into the batteries of UAVs. It does not consider the dissipation loss of the charger, or the energy consumption by other parts of the disaster response equipment, like the ground control station system.

In Table 8.2, initial experiment results yielded a daily energy demand of 101.47 kWh. Better replacement scheduling and replacing UAV selection strategies, as well as a varied total UAV amount, should have significant impact on the overall energy demand.

The new experiment configuration utilizes the better strategies identified in the previous sections. Figure 8.11 illustrates the daily energy demand of the various simulated UAV amounts, aggregated for individual repetitions. Values seem to differ between repetitions, but the actual variance relative to the mean is low.

Simulation results for 100 UAVs disclose an average daily energy demand of 82.55 kWh. That is an improvement of 18.6 % over the initial experiment result, based on the implemented more efficient replacement strategies.

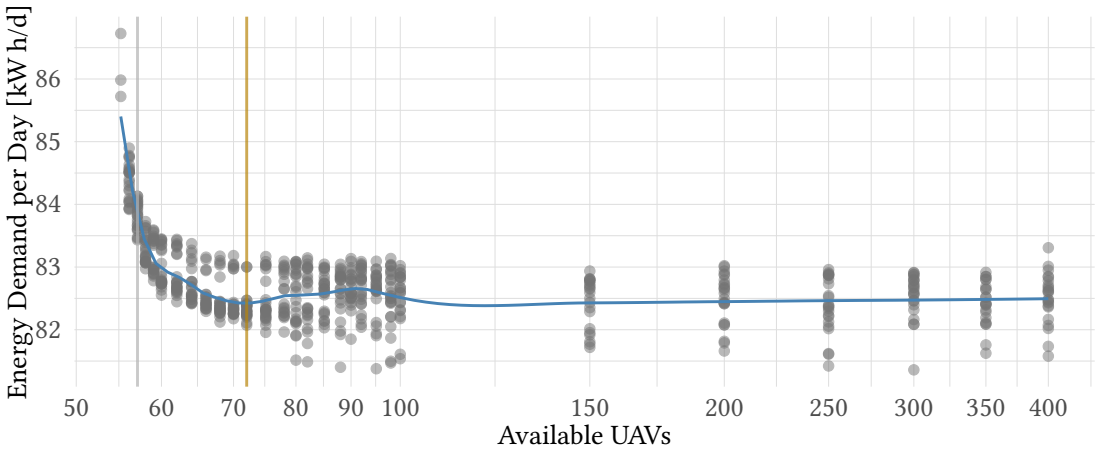

Figure 8.11 – Daily energy demand by all UAVs in the application scenario, given per absolute number of UAVs. Every dot represents a repetition.

For an increased amount of available UAVs, no significant difference compared to results with the initial 100 UAVs is visible. The depicted trend line suggests a local maximum in the range of approximately 75 to 100 UAVs, while the individual points do not indicate such a trend and their variance is considerably higher than the offset of the local maximum. We conclude that the daily energy demand is approximately equal among all experiments between 75 to 400 UAVs and explain deviation by the high potential differences between experiments due to the probabilistic elements of the simulation.

Approximately identical energy demand of simulations with more than a certain number of UAVs can be explained by the saturation of the scenario. When a sufficient amount of UAVs enables the fulfillment of all scenario missions without shortages, e.g., during replacing UAV selection, the addition of more idling UAVs does not contribute to the performance of the system of systems. Additional UAVs are effectively never used.

Identification of the smallest number of UAVs to still offer UAV saturation in the scenario, while generating the least energy demand compared to lower UAV amounts, is an interesting characteristic value for the utilization in an application scenario. Its meaning and special importance will be the subject of the following section. Judging by the illustrate trend line of averaged values, we identify 72 UAVs as the amount with the lowest energy demand between the monotonic increase to the left and the saturation to the right. 72 UAVs is therefore the minimal amount of UAVs for energy demand saturation.

8.6.3. Combined Resource Utilization Optimization

An interesting range for further discussion is the range of UAV amounts between the minimal amount for saturation and the minimal amount for continuous fulfillment. Figure 8.11 illustrates the anticipated development. A lower amount of UAVs increases the off chance of local shortages of fully-charged and nearby replacing UAVs. Replacement has to be performed by a less than optimal candidate, thus reducing the energy efficiency of individual UAVs and increasing the overall energy demand. This effect intensifies till the point of the minimal UAV amount, with the highest energy demand of the whole experiment.

The two extremes, and the range of intermediate solutions, create a Pareto optimal set. This set can be obtained by defining an optimization problem with prevailing constraints and by applying multi-objective optimization methods. Since a good trade-off between the two extremes is preferable, the weighted sum approach mentioned in Section 6.4.3 can also be applied here. With one fixed choice of weights, one of the Pareto optimal points will be computed. The trade-off is influenced by choosing suitable weights, resulting in different obtained points from the optimal set.

Potential prevailing constraints are for example short-term transportation limitations for UAVs beyond a certain amount, or a limited storage for electrical energy in case of no steady power grid connection.

One obvious optimization criterion is of financial nature. UAVs are expensive in initial purchase and require periodic maintenance and repair. Besides that, every device has a life time expectancy, resulting in costs per utilization. Transportation of certain amounts of UAVs to the application field could be linked to further costs. On the other side of the equation, total electrical energy costs and potential costs of energy storage allocation have to be considered. Following an according analysis, an optimization function can be derived and a solution from the Pareto optimal set selected. The discussion of financial costs is not in the scope of this thesis.

For the application goal of UAV-aided disaster response, the unbound effective utilization of a sufficient amount of UAVs is the primary focus. As long as none of the mentioned or related scenario constraints are present, our recommendation for the utilized amount of UAVs in the scenario is the minimal amount for energy demand saturation.

9. Conclusions and Perspectives

The work on this thesis results in three preliminary artifacts. During the environment analysis, we were able to understand and formalize the domain of UAV utilization in disaster response scenarios. We found UAVs to be applicable in existing and novel use cases of disaster scenarios, in order to advance disaster response and to prevent loss of human life and damage to nature. The result of this analysis is a conceptional UAV response model.

The second artifact is the developed simulation and prediction model on the flight behavior and energy consumption of UAVs. The model is general and transferable to all UAV types, but moreover measured and parameterized to reflect the behavior and consumption of our specific testbed UAV. Besides the capability of the model to mimic the real-world object, it furthermore offers the functionality to predict future development. The creation of an accurate and precise representation of the real-world UAV is an important task in light of the following step.

The third preliminary artifact is our presented discrete event simulation framework. It unites the conceptional scenario response model and the flight behavior and energy consumption model of UAVs in a flexible UAV fleet simulation environment for strategy evaluation in a resource management system. It therefore poses as the base for further research into the field.

Our preliminary work on realistic models and the simulation framework is motivated by the development approach of modeling and simulation-based systems engineering. Changes in details of complex intertwined systems have wide-reaching effects on other parts of the whole, making the evaluation of design changes on a theoretical level almost impossible. An accurate, flexible, and modular real-world representation in a simulated environment offers the necessary means for development and testing of new technologies and methods in the context of a complex system of systems.

The second half of the presented thesis addresses the central research question. With the simulation framework at hand, we are now able to easily implement and simulate aspects of a UAV resource management system, and evaluate the feasibility and efficiency of the system and therein applied strategies for replacement coordination.

Alongside a thorough discussion of the resource management system requirements, we present an extended conceptional UAV response model and discuss methods for our continuity and recirculation approach. The approach builds on the idea of a non-disruptive replacement process, which consists of multiple steps at disparate points in time. Various aspects of the replacement process have therefor been covered by developed strategies to improve these and the resulting energy efficiency of the system.

All of these aspects depend on the existence of a reliable UAV flight behavior and energy consumption prediction model. It is important to understand the distinction between the aforementioned simulation model and the prediction model. The former is part of our effort to create a representation of the real-world, following the M&SBSE approach, while the latter is part of the development solution for the resource management system. The prediction model and all relevant parts of the resource management system are modular components included in the simulation framework. They are designed to be detachable and included in a real-world system with little effort. This option is not only cost- and time-efficient, it also ensures the utilization of a well verified and evaluated system in a real-world application.

Three aspects are discussed and different solutions are evaluated through simulation on the example of a mock application scenario: the safety margin quantile selection, the replacement scheduling strategy, and the replacing UAV selection strategy.

First evaluation results show that our concept of a research management system is fully capable of providing a continuous service for all missions and therefore fulfills the base requirements of no interruption or termination of the disaster scenario response.

The importance of safety margin inclusion in the prediction of future UAV behavior was analyzed first. Experiments with simulation configurations, in which mean values without added safety margins are used during prediction, ended in terminated missions and therefore in violated disaster response fulfillment. Experiments with a safety margin setting did not portray such behavior. An added safety margin effectively eliminates the risk of mid-mission failure due to depletion. The experiment results also show that

higher quantile values make failure cases significantly less likely. The failure probability is traded for utilization efficiency and a compromise needs to be found.

Even the lowest simulated quantile setting results in relatively low failure rates. A failure rate of around 1 percent was found to be too high, as it results in a significant amount of failing UAVs in the mass-application of a disaster scenario. Future work should concentrate on safety margin planning in dependence on the remaining capacity, on a planned reserve, or a combination of both, to eliminate the chance of failure resulting out of battery depletion.

For the planning process of replacement scheduling, two simple strategies and a superior strategy are presented. The bi-objective heuristic shows the highest potential for optimization and the discussed weight setting for the heuristic should be acceptable for all potential application scenarios.

This heuristic should, in theory, improve the replacement location selection over the default strategy, resulting in shorter maintenance flights and better energy efficiency. However, simulation behavior seems less affected by the strategy and only an improvement of 1.57 percent can be observed in the experiment results. The reason for this outcome is seen in the far distance between charging stations and missions designated to UAVs, following the restriction of the operation field of the disaster scenarios. The proportion between maintenance flights and mission execution flights is therefore only marginally improved by a good replacement location planning. Nonetheless, other application scenarios could provide better located charging stations and yield a higher strategy improvement. Worsening of energy efficiency by the strategy is not possible. We deem the bi-objective heuristic as a meaningful addition to an improved resource management system.

The third analyzed aspect of the replacement process is the replacing UAV selection strategy. A simple approach, which decides based on the provisioning distance, is compared with the more sophisticated applicable charge approach, taking multiple factors into account. A comparison is meaningful, because the second strategy relies heavily on the highlighted flight behavior and energy consumption prediction model. The potential of such a model as part of the resource management solution becomes clear, when looking at the evaluation results. In the example of our application scenario, the strategy is

able to improve the energy efficiency of the overall system by 12.9 percent, while extending the single-UAV utilization time, thus reducing the total amount of maintenance processes.

The mentioned strategies for replacement process improvement are part of the bigger goal to improve the overall disaster response resource efficiency. The term of efficiency is evaluated in two directions. First, by the minimum total number of provided UAVs in the scenario, and secondly by a minimum total energy demand of all UAVs. Experiments resulted in two unequal numbers. The range between these numbers spans a Pareto optimal set for a multi-objective optimization problem. One of the potential optima is motivated for a finance-oriented optimization problem, however an in-depth discussion following the incentive is out of the focus of this thesis.

In conclusion, we present a working resource management system fulfilling all initially defined requirements towards a UAV-aided disaster response. The discussed improvements are able to increase the UAV energy efficiency, decrease the needed amount of provided UAVs, and reduce the overall energy demand by almost 20 percent.

As initially claimed does the resource management system work as a transparent layer between physical UAVs and logical mission execution entities, commanded by a simulated mission control. All simulation environment implementations specific to the resource management solution could be detached from the framework and included in the firmware of a real UAV and mission control system. The extensive verification and evaluation of the implemented components for resource management will stay valid in the process, reducing risk and cost.

The provided simulation framework offers a wide range of configurable components and is easy to extend. Future work could benefit from the existing M&SBSE environment to test and evaluate novel UAV fleet management research ideas, like further strategy improvements, so far disregarded restrictions, or decentralized control and management realizations.

A. Appendix

A.1. Open Source Contributions

The creation of this thesis was accompanied by the development of various software components. All efforts were provided or contributed to the open source software community. Below the noteworthy software projects are listed with short descriptions, URLs, contribution details, and source/comment lines of code (SLOC/CLOC).

A.1.1. ArduPilot Logfile Maneuver Analysis Script

URL:	https://github.com/ThomDietrich/ardupilot-energy-analysis
Contribution:	Novel development
License:	GNU General Public License Version 3 (GPLv3)
SLOC (CLOC):	898 (324)

ArduPilot/ArduCopter dataflash logfile analysis script developed in the statistical computing and graphics programming language R. The script was developed specifically for the benefit of this thesis and is oriented at spatial movement and energy consumption analysis. Refer to Section 4.1.2 for a detailed description of the intended use case and the performed analysis steps.

A.1.2. Multi-UAV Resource Management DES Framework

URL:	https://github.com/ThomDietrich/multiUAV-simulation
Contribution:	Novel development
License:	Academic Public License (OMNeT++)
SLOC (CLOC):	9411 (1817)

Discrete event simulation framework, developed in OMNeT++/C++, aimed at UAV movement, energy management, and signal propagation. The simulation framework is a novel development and offers potential in related research fields. Refer to Chapter 7 for a detailed description of the structure, functionality and extendibility of the framework.

Contributions to the simulation framework source code were made under our supervision and guidance in the following student works:

- Bachelor thesis by Ludwig Breitsprecher [Bre18]
  - Implementation of the intelligent charging station concept
  - Analysis and interpolation of a realistic CCCV charging processes
  - Addition of preemptive charging termination
  - Creation of a graphical representation of a charging station

- Research project by Michael Sommer [Som18]
  - Planning of scenarios for tests and productive simulation
  - Implementation of the shortest return heuristic
  - Improvement of visual representation of UAVs and flight paths
  - General testing, improvement, and bug fixing

A.1.3. Multi-UAV DES Framework Analysis Script

URL:	https://github.com/ThomDietrich/multiUAV-simulation-analysis
Contribution:	Novel development
License:	GNU General Public License Version 3 (GPLv3)
SLOC (CLOC):	394 (120)

Analysis script for performance data produced by the multi-UAV resource management simulation framework (cf. Appendix A.1.2) developed in the statistical computing and graphics programming language R. The script generates values and diagrams and is the basis for results in Chapter 8. The repository also contains all raw data used for the analysis results presented in the evaluation chapter.

Please refer to Section 7.4 for a detailed list of performance metrics recorded in simulation and analyzed by the script.

A.1.4. Mission Planner GCS Software

URL:	https://github.com/ArduPilot/MissionPlanner
Official Webpage:	http://ardupilot.org/planner
Contribution:	Addition of features
License:	GNU General Public License Version 3 (GPLv3)

Mission Planner Ground Control Station [Ard18b]. Compare Section 3.3.2 for details.

- Pull request #1473:
  https://github.com/ArduPilot/MissionPlanner/pull/1473
  - Add air distance to the Flight Plan view
- Pull request #1652:
  https://github.com/ArduPilot/MissionPlanner/pull/1652
  - Result of the associated bachelor thesis by Tobias Krüger [Krü18]
  - A summary of the work is given in the introduction of Chapter 4
  - Add the energy consumption profile feature as a core component

  - Add an energy consumption profile configuration panel view
  - Add energy consumption estimates to the Flight Plan view
  - Add a guided (re-)calibration of the energy consumption profile

A.1.5. ArduPilot Flight Controller Firmware

URL:	https://github.com/ArduPilot/ardupilot
Official Webpage:	http://ardupilot.org/ardupilot
Contribution:	Addition of features
License:	GNU General Public License Version 3 (GPLv3)

Flight controller firmware for copters, planes, rovers, submarines, antenna trackers, and other simple or sophisticated remote controlled mobile robotics. [Ard18a]

- Implementation of a marker-based precise UAV landing method
- Result of the associated bachelor thesis by Matthias Mark [Mar16]
- Basis for automated landing at a charging station, in accordance with Requirement [REQ-F-124]

A.1.6. MAVLink Communication Library

URL:	https://github.com/mavlink/mavlink
Official Webpage:	https://mavlink.io/en
Contribution:	Addition of swarm and maintenance functionality
License:	GNU Lesser General Public License Version 3 (LGPLv3)

Micro air vehicle link (MAVLink) message marshalling library for UAVs.

- Extension: https://github.com/ThomDietrich/mavlink/tree/multimav
  - Compare Section 3.3.3.1 for details
  - Based on the associated work by Kati Neudert [Neu14]
  - Published at *International Conference on Autonomous Robot Systems and Competitions 2016* (ICARSC'16) [Die+16]

A.2. 3DR Solo Prediction Model Data

In this section we present data for the parameterized energy consumption prediction model for our testbed 3DR Solo quadcopter. Compare Section 4.6 for related details and application instructions. Values were generated using the R script presented in Appendix A.1.1 from 12 selected benchmark flights with 79 individual maneuvers.

A.2.1. Average Speed Lookup Table

The speed of an ArduPilot based quadcopter is selected by the flight controller depending on the maneuver climb or descent angle. In Table A.1 values for speed selection by our 3DR Solo Quadcopter are given for distinct angles.

A.2.2. Point-to-Point Maneuver Power Draw

The average power draw during a point-to-point maneuver mainly depends on the climb or descent angle of the maneuver. Table A.1 contains values for average power draw at distinct angles, measured during our empirical analysis.

A.2.3. Maneuver Variance Partial Autocorrelation Lag Values

Numbers in the following tables are intermediate characteristic values for our 3DR Solo quadcopter. They were generated in the autocorrelation analysis and are applied during energy consumption prediction. As described in Section 4.4.2.2, values were cut off at the latest lag of an autocorrelation above a value defined by a confidence interval, chosen as 0.95. Lags beyond that point were nulled and are grayed out in the following tables.

The values are specifically needed for variance inference in order to simulate realistic model behavior, and to predict consumptions with added safety margins.

Table A.1 – Empirical analysis results for speed selection and power draw by our 3DR Solo during distinct climb and descent angles.

Angle [°]	Maneuver Flight Speed [m/s]		Mean Power Draw [W]
	Mean (μ)	Std. Deviation (σ)	
−90.0	1.84	0.031	248.7
−75.6	1.84	0.023	263.7
−57.9	2.01	0.055	251.7
−34.8	2.45	0.041	253.5
−15.6	3.58	0.127	235.1
0.0	8.05	0.409	241.1
15.6	6.02	0.099	274.7
34.8	3.34	0.055	295.6
57.9	2.81	0.171	307.2
75.6	2.72	0.006	313.7
90.0	2.72	0.030	307.0

Table A.2 – Hover flight by our 3DR Solo quadcopter: partial autocorrelations of the power draw time series, given by lag index.

	Index	*1*	*2*	*3*	*4*	*5*	*6*	*7*	*8*	*9*	*10*
Hover		0.682	−0.058	0.233	0.076	0.096	−0.028	−0.060	0.036	0.067	0.057
	10+	0.017	0.014	−0.009	0.085	0.000	0.000	0.000	0.000	0.000	0.000

Table A.3 – Climb and descent flight by our 3DR Solo quadcopter: partial autocorrelations of the power draw time series, given by lag index.

	Index	*1*	*2*	*3*	*4*	*5*	*6*	*7*	*8*	*9*	*10*
−90.0°		0.603	−0.099	0.327	0.043	0.116	0.029	0.031	0.031	0.035	−0.001
	10+	0.006	0.022	−0.009	0.025	0.021	0.034	0.016	0.038	0.019	0.000
	20+	0.049	0.001	−0.040	0.038	0.015	0.000	0.000	0.000	0.000	0.000
−75.6°		0.544	−0.194	0.425	0.020	0.083	0.034	0.051	0.013	0.058	0.032
	10+	−0.048	0.030	−0.005	−0.047	−0.015	0.031	−0.062	−0.016	0.009	0.023
	20+	0.076	0.088	0.023	−0.053	0.058	0.026	−0.047	−0.026	0.020	0.000
−57.9°		0.546	−0.136	0.283	0.049	0.047	−0.026	−0.015	0.008	0.025	−0.045
	10+	−0.021	0.021	0.014	−0.055	−0.035	0.005	−0.033	−0.007	0.009	−0.028
	20+	0.001	−0.024	−0.006	−0.029	0.023	0.015	0.000	0.000	0.000	0.000
−34.8°		0.635	−0.066	0.254	0.011	−0.035	−0.041	−0.022	0.005	−0.008	0.018
	10+	−0.060	0.015	0.054	−0.015	0.019	0.000	0.000	0.000	0.000	0.000
	20+	0.000	0.000	0.000	0.000	0.000	0.000	0.000	0.000	0.000	0.000
−15.6°		0.747	−0.023	0.143	−0.085	−0.141	−0.046	−0.066	−0.078	0.026	−0.077
	10+	0.011	0.014	0.032	0.033	−0.009	−0.013	0.023	−0.035	−0.037	−0.016
	20+	0.029	−0.074	−0.046	−0.019	−0.003	0.041	0.000	0.000	0.000	0.000
0.0°		0.624	−0.049	0.150	0.042	0.012	−0.053	0.035	0.000	0.000	0.000
	10+	0.000	0.000	0.000	0.000	0.000	0.000	0.000	0.000	0.000	0.000
	20+	0.000	0.000	0.000	0.000	0.000	0.000	0.000	0.000	0.000	0.000
15.6°		0.714	−0.090	−0.008	−0.149	−0.101	−0.036	−0.102	−0.077	0.105	0.000
	10+	0.000	0.000	0.000	0.000	0.000	0.000	0.000	0.000	0.000	0.000
	20+	0.000	0.000	0.000	0.000	0.000	0.000	0.000	0.000	0.000	0.000
34.8°		0.847	0.002	0.173	−0.055	−0.002	−0.058	−0.001	0.025	−0.088	−0.068
	10+	−0.041	−0.047	−0.035	−0.072	−0.122	0.024	−0.035	−0.066	0.001	0.044
	20+	0.000	0.006	0.014	−0.012	0.000	−0.062	−0.039	−0.066	0.006	0.045
57.9°		0.701	0.004	0.422	0.077	0.048	0.007	−0.029	−0.015	0.045	−0.019
	10+	−0.053	0.033	0.031	−0.072	−0.077	−0.005	0.017	−0.039	−0.012	−0.017
	20+	−0.003	−0.030	−0.022	−0.001	0.045	−0.001	0.018	−0.032	0.052	0.000
75.6°		0.649	−0.083	0.353	0.086	0.012	0.049	0.099	−0.035	−0.006	−0.094
	10+	0.044	−0.039	0.023	−0.067	−0.103	0.076	0.037	−0.118	−0.059	−0.005
	20+	0.023	−0.070	−0.054	−0.126	−0.001	0.056	0.004	−0.014	0.069	0.000
90.0°		0.599	−0.083	0.369	0.106	0.092	0.002	−0.012	0.029	0.074	−0.030
	10+	−0.033	0.038	0.072	−0.034	−0.066	0.011	0.034	0.018	−0.002	−0.031
	20+	−0.017	0.000	−0.050	−0.021	−0.032	0.019	0.013	−0.006	0.046	0.000

List of Nomenclature

Charge charging. The process of recharging a depleted or partly depleted battery of a UAV, taking place at a charging station (cf. Section 6.2.2). (pp. 94, 103, 116, 117, 119, 146, 156, X)

Continuity continuity. The uninterrupted and unterminated support of all scenario missions and hence the enabling of the UAV-aided scenario operation (cf. Section 5.4.2. (pp. 96, 147)

Idle idling. A phase of the UAV life cycle in which it does not perform a task nor consume or receive electric energy (cf. Section 6.2.2). (pp. 103, 104, 106, 107, 116–119, 152, 156, 160, X)

Maintenance maintenance. Processes and phases in the UAV life cycle planned by the resource management system, responsible for enabling the support of a mission/scenario. Comprises all but the Mission Execution phase of the UAV life cycle (cf. Sections 5.4 and 6.2.3). (pp. 88, 91, 93, 94, 96, 101, 104)

Maneuver maneuver. A maneuver is an atomic action by a UAV. See Section 3.2.3 for a differentiation of maneuver classes.

Mission mission. The concept of a mission in the scope of UAV-aided disaster response shall be defined as the combination of multiple maneuvers. A mission can be of arbitrary size in both the spatial and temporal dimension. See Section 3.2.2 for a more detailed description.

Node node. A general term for a component of the disaster response system of systems. In the context of this work, a node is either a UAV, a CS, or a GCS. (pp. 2, 30, 31, 46, 95, 121, 140, 144)

Provision provisioning. The process of selecting a UAV as the replacing or fulfilling UAV for mission execution, and the coordination of its timely arrival by planning according flight maneuvers (cf. Section 6.2.1). (pp. 94, 103, 117–119, 155)

Recirculate recirculation. The process of re-enabling a depleted or partly depleted UAV for scenario utilization, through the navigation to and recharging at a charging station (cf. Section 5.4.3. (pp. 96, 103, 147)

Replace replacement. The process of replacing one UAV by another to sustain mission execution (cf. Section 6.2.3). (pp. 94, 148)

Return returning. The process of returning a replaced UAV after mission execution to a charging station for recharging (cf. Section 6.2.1). (p. 94)

Safety Margin safety margin. During process planning and value estimation, an additionally imposed amount to account for uncertainty and safety violations due to resulting overshoot. In energy consumption prediction, a safety margin is added to protect against premature battery depletion and therefore against catastrophic hardware failure (cf. Section 4.4.1. (pp. 3, 36, 49, 71, 72, 81, 85, 110, 112, 134, 143, 164, V)

Utilization utilization. Comprises all phases or actions of active UAV use in the context of a scenario/mission. This includes flights during, from, or to a mission, but also hovering maneuvers or potential other forms of mission support. Utilization does not include Charging or Idling (cf. Section 6.2.1). (p. 102)

List of Abbreviations

CCCV constant current constant voltage. A multistage battery charging method consisting of a first stage of constant charging current and a second stage of maintained constant battery voltage. A multistage method is needed to protect the battery from physical and chemical impairment.

CS charging station. A ground-based device to enable landing and charging of UAVs, offering one or more landing and charging spots. (pp. 5, 39, 40, 61, 71, 90, 94–97, 101, 103, 105–111, 113, 116, 117, 124, 134, 135, 142–146, 145, 147, 150, 151, 154, 157, 165, IV, IX–XI, XXI)

CSV A comma-separated values file contains values in a table as a series of ASCII text lines organized so that each column value is separated by a comma from the next column's value and each row starts a new line. (pp. 53, 54)

ESC The electronic speed controller is a device connecting a flight controller and motors to provide power and control speed. (p. 19)

GCS ground control station. A central ground-based system that provides the facilities for rule-based coordination, observation, and human control of UAVs. In a disaster response scenario, the ground control station is part of the mission control (MC) system. (pp. 10, 29, 40, 43, 44, 46, 50, 95–97, 117, 126, 159, IX, XII)

GPLv3 GNU General Public License Version 3. A free copyleft license for software in the open source context and other kinds of works. Compare for details: `https://www.gnu.org/licenses/gpl-3.0.en.html`

HDOP horizontal dilution of precision. A 2D precision quality indicator for horizontal GPS location data, accounting for the effects of imperfect satellite positions, atmospheric refraction and unwanted multipath propagation. (p. 56)

ICS intelligent charging station. A charging station for UAVs, with the additional functionality of self-organization of waiting and charging spots, arriving and departing UAVs, and local resources. (pp. 40, 46, 47, 101, 102, 122, 124)

IMU inertial measurement unit. An integrated multi-axis sensor combining precision gyroscopes, accelerometers, magnetometers, and pressure sensors. Readings are combined and pre-processed to provide reliable position and motion data for stabilization and navigation tasks. (pp. 18, 19)

LGPLv3 GNU Lesser General Public License Version 3. A free copyleft license for software in the open source context and other kinds of works. The LGPLv3 extends the GPLv3 by additional permissions to link or use LGPLv3 licensed software as part of non-LGPL software. Compare for details: `https://www.gnu.org/licenses/lgpl-3.0.en.html` (pp. 45, IV)

LiPo lithium-ion polymer. A rechargeable lithium-ion battery featuring a polymer electrolyte. This lithium-ion battery type provides higher specific energy (capacity per weight ratio), making it the ideal choice for weight-critical applications such as UAVs. (pp. 22, 23, 26–28, XVII, XIX)

LUT lookup table. An array or matrix used in computer programming to hold values rather than calculating or deriving them. LUTs are helpful in situations where computation is expensive or the underlying value function is unknown. (pp. 81–85, 133)

MAV micro aerial vehicle. A small unmanned aircraft with automated flight capabilities. The abbreviation is putting special focus on the form factor. (p. 10)

MAVLink micro air vehicle link. MAVLink is a community-driven message library project for coordination of micro air vehicles. It is a very lightweight, header-only message marshalling library and follows a modern hybrid publish-subscribe and point-to-point design pattern [Mei+18]. (pp. 45–47)

MBSE model-based systems engineering. The formalized application of modeling to support system requirements, design, analysis, verification, and validation activities. The approach begins in the conceptual design phase and continues throughout development and later life cycles. (pp. 4, 7, XIII)

MC mission control. A central ground-based system that coordinates the scenario-oriented mission assignment to UAVs. The mission control is also responsible for resource management decisions and actions. The ground personnel interacts with the mission control for effective information transfer and UAV utilization. The mission control includes a ground control station (GCS). (pp. 43, 89, 116, 166, XI)

M&SBSE modeling and simulation-based systems engineering. A form of the MBSE approach, extended by the emphasis on simulation-based verification, evaluation, and optimization of a system. (pp. 4, 6, 163, 164, 166)

SoC state-of-charge. The currently available charge inside a rechargeable battery in percentage points to its maximum possible charge under consideration of decreasing state-of-health [Pop+08]. (pp. 23–28, 40–42, 85, 95, 104, 107, 110, 117–119, XIX)

SoH state-of-health. The general condition of a battery and its ability to deliver the specified performance in comparison with its factory conditions or with a fresh battery of the same model [Pop+08]. (pp. 22–26, 28, 42, 53, XIII)

sUAS small unmanned aircraft system. A small UAS. A small unmanned aircraft and its associated elements (including communication links and the components that control the small UA) that are required for the safe and efficient operation without the possibility of direct human intervention from within or on the aircraft [FAA16a]. (p. 10)

SoS system of systems. A collection of systems that combine their resources and capabilities to form a more complex new system. The system of systems offers more functionality and performance than the sum of individual systems. (pp. , 1, 3, 6, 34, 35, 39, 95, 160, 163, IX)

UAS unmanned aircraft system. The combination of an unmanned aircraft and its associated radio communication link and ground control station. (pp. 10, XIII)

UAV unmanned aerial vehicle. An aircraft without a pilot onboard. The abbreviation implies automated flight capabilities. (pp. , , 1–20, 22, 25, 29, 32–47, 49–53, 57–62, 64–68, 70–72, 77, 79–81, 85, 87–111, 113, 114, 116–124, 126–128, 130–135, 137, 139, 140, 142–145, 144–147, 146, 148, 150, 152–161, 163–166, IV, IX–XII, XV–XVII, XIX–XXII)

VTOL vertical take-off and landing. A plane capable of taking off and landing vertically, having forward speeds comparable to those of conventional aircraft. (p. 13)

List of Symbols

Q_{max} maximum battery capacity. The rated capacity of a (new and unutilized) battery pack, given in mA h. (p. 22)

$Q(t)$ available charge in a battery. The currently available amount of electrical charge in a battery at a certain point in time, given in mA h.

I current flowing into or out of a battery. The electric charge provided to the battery during charging or by the battery during utilization.

Z battery impedance. A combination of internal resistance and reactance of a battery. The impedance of a battery is an indicator for its health and can be measured by injecting a small current high frequency AC charge into the battery.

τ battery voltage relaxation time. A measure for the electromotive force (EMF), a batteries internal force to provide energy to an outside load. Pop et al. [Pop+08, p. 47]

T_{bat} actual battery temperature. The temperature of a battery at a certain point in time. The battery temperature is influenced by the consumer behavior and the surrounding weather condition. Temperature is given in ℃.

U_{bat} battery terminal voltage. The nominal voltage of a battery cell or combined battery pack, given in V. (p. 22)

α climb or descent angle. The angle of the straight line described by a point-to-point maneuver on a vertical slope against the x-y-plane. (pp. 38, 56, 65, 67, 68, 70, 80, 81, 83, 84, XVI)

d point-to-point distance. The length of the straight line described by a point-to-point maneuver.

$M_h(t_c)$ hovering maneuver. A flight maneuver type characterized by a fixed position in air and a duration. The maneuver duration is given by the specific command to be executed by the UAV. (pp. 37, 44, 56, 59, 60, 75, 84, 110, 130, 151, X)

$M_m(\vec{s_c})$ point-to-point maneuver. A flight maneuver type characterized by a straight trajectory between two coordinates. Movement between those two points is expected to happen at constant speed. The maneuver direction and speed are given by the specific command to be executed by the UAV. (pp. 37, 44, 56, 59–63, 65, 67, 68, 70, 84, 110, 130, 141)

v flight speed. The movement speed of the UAV along a point-to-point maneuver trajectory. Speed is chosen by the on-board flight control based on the maneuver climb or descent angle.

$\vec{s}$ point-to-point maneuver trajectory. A straight line described by a point-to-point maneuver given as a three-dimensional vector. (pp. 38, 70, XVI)

List of Tables

List of Figures

List of Source Code Excerpts

Bibliography

Primary Sources

[3DR18] 3D Robotics, Inc. *Solo Development Guide*. 3D Robotics - Drone & UAV technology. 2018. URL: https://dev.3dr.com (visited on 2018-04-01). Licensed under: CC BY 4.0 (cit. on p. 40).

[ANS09] Mikael Asplund, Simin Nadjm-Tehrani, and Johan Sigholm. "Emerging Information Infrastructures: Cooperation in Disasters". In: *Critical Information Infrastructure Security: Third International Workshop, CRITIS 2008, Rome, Italy, October13-15, 2008. Revised Papers*. Ed. by Roberto Setola and Stefan Geretshuber. Springer Berlin Heidelberg, 2009, pp. 258–270. DOI: 10.1007/978-3-642-03552-4_23 (cit. on p. 30).

[ARB15] A. Abdilla, A. Richards, and S. Burrow. "Power and endurance modelling of battery-powered rotorcraft". In: *Intelligent Robots and Systems (IROS), 2015 IEEE/RSJ International Conference on*. 2015-09, pp. 675–680. DOI: 10.1109/IROS.2015.7353445 (cit. on p. 3).

[Arc+15] J. C. del Arco, D. Alejo, B. C. Arrue, J. A. Cobano, G. Heredia, and A. Ollero. "Multi-UAV ground control station for gliding aircraft". In: *2015 23rd Mediterranean Conference on Control and Automation (MED)*. IEEE. IEEE, 2015-06-16, pp. 36–43. DOI: 10.1109/med.2015.7158726 (cit. on p. 46).

[Ard18a] ArduPilot Dev Team. *ArduPilot User and Developer Documentation. Open Source Autopilot*. jDrones. 2018. URL: http://ardupilot.org/ardupilot/ (visited on 2018-04-01). Licensed under: CC BY-SA 3.0 (cit. on pp. 43, 67, IV).

[Ard18b] ArduPilot Dev Team. *Mission Planner User and Developer Documentation. Ground Control Station for ArduPilot.* jDrones. 2018. URL: http://ardupilot.org/planner/ (visited on 2018-04-01). Licensed under: CC BY-SA 3.0 (cit. on pp. 43, III).

[BD91] Peter J. Brockwell and Richard A. Davis. *Time Series: Theory and Methods.* Springer Series in Statistics. Springer New York, 1991. 580 pp. DOI: 10.1007/978-1-4419-0320-4 (cit. on pp. 75 sq.).

[Beg+13] Peggy Begerow, Sebastian Schellenberg, Jochen Seitz, Thomas Finke, and Jürgen Schröder. "Reliable Multicast in Heterogeneous Mobile Ad-hoc Networks". In: *Combined Workshop on Self-Organizing, Adaptive, and Context-Sensitive Distributed Systems and Self-organized Communication in Disaster Scenarios* (2013-03-15). DOI: 10.14279/tuj.eceasst.56.811.806 (cit. on p. 143).

[BH06] Russell Bent and Pascal Van Hentenryck. *Online Stochastic Combinatorial Optimization.* The MIT Press, 2006. 247 pp. DOI: 10.7551/mitpress/5140.001.0001 (cit. on p. 6).

[BHR15] Paul Bupe, Rami Haddad, and Fernando Rios-Gutierrez. "Relief and emergency communication network based on an autonomous decentralized UAV clustering network". In: *SoutheastCon 2015.* IEEE, 2015-04-12, pp. 1–8. DOI: 10.1109/SECON.2015.7133027 (cit. on p. 4).

[BSK10] Axel Bürkle, Florian Segor, and Matthias Kollmann. "Towards Autonomous Micro UAV Swarms". In: *Journal of Itelligent & Robotic Systems* 61.1-4 (2010-10-27), pp. 339–353. DOI: 10.1007/s10846-010-9492-x (cit. on p. 34).

[Coo+12] Matthew Coombes, Owen McAree, Wen-Hua Chen, and Peter Render. "Development of an autopilot system for rapid prototyping of high level control algorithms". In: *Proceedings of 2012 UKACC International Conference on Control.* IEEE. IEEE, 2012-09-05, pp. 292–297. DOI: 10.1109/control.2012.6334645 (cit. on p. 46).

[CS16] Aoxia Chen and Pankaj K. Sen. "Advancement in battery technology: A state-of-the-art review". In: *2016 IEEE Industry Applications Society Annual*

Meeting. IEEE, 2016-10-06, pp. 1–10. DOI: 10.1109/IAS.2016.7731812 (cit. on p. 22).

[Das08] Prithviraj Dasgupta. "A Multiagent Swarming System for Distributed Automatic Target Recognition Using Unmanned Aerial Vehicles". In: *IEEE Transactions on Systems, Man, and Cybernetics - Part A: Systems and Humans* 38.3 (2008-03), pp. 549–563. DOI: 10.1109/TSMCA.2008.918619 (cit. on p. 5).

[Dem10] Martin Edward Dempsey. *Roadmap for Unmanned Aircraft Systems 2010-2035. Eyes of the Army*. Roadmap ADA518437. U. S. Army UAS Center of Excellence (ATZQ-CDI-C), 2010. 126 pp. (cit. on p. 11).

[Eur16] European Commission. *The EU Drone Policy. MEMO/16/4123*. Fact Sheet Memo MEMO/16/4123. European Commission, 2016-11-29 (cit. on p. 15).

[FAA16a] Federal Aviation Administration. *107-2 - Small Unmanned Aircraft Systems (sUAS)*. Tech. rep. Federal Aviation Administration, 2016-06-21 (cit. on p. XIII).

[FAA16b] Federal Aviation Administration. *Part 107: Operation and Certification of Small Unmanned Aircraft Systems*. Tech. rep. Federal Aviation Administration, 2016-06-21 (cit. on p. 15).

[For+10] Catherine Forbes, Merran Evans, Nicholas Hastings, and Brian Peacock. *Statistical Distributions*. 4th ed. John Wiley & Sons, Inc., 2010. 230 pp. DOI: 10.1002/9780470627242 (cit. on pp. 71, 81).

[GDT14] Daniele Gianni, Andrea D'Ambrogio, and Andreas Tolk. *Modeling and Simulation-Based Systems Engineering Handbook*. Ed. by Timothy George Kotnour and Waldemar Karwowski. Engineering Management. CRC Press, 2014-11-27. 513 pp. (cit. on pp. 4, 121).

[Gu+17] Haowei Gu, Ximin Lyu, Zexiang Li, Shaojie Shen, and Fu Zhang. "Development and experimental verification of a hybrid vertical take-off and landing (VTOL) unmanned aerial vehicle (UAV)". In: *2017 International Conference on Unmanned Aircraft Systems (ICUAS)*. IEEE, 2017-06-16. DOI: 10.1109/icuas.2017.7991420 (cit. on p. 15).

[Haf+15] A. T. Hafez, S. N. Givigi, Howard M. Schwartz, S. Yousefi, and M. Iskandarani. "Real time tactic switching for multiple cooperative UAVs via Model Predictive Control". In: *2015 Annual IEEE Systems Conference (SysCon) Proceedings*. IEEE, 2015, pp. 432–438. DOI: 10.1109/SYSCON.2015.7116789 (cit. on p. 4).

[HH94] Heinrich Hertz and Hermann von Helmholtz. *Gesammelte Werke von Heinrich Hertz*. Vol. 3: *Die Prinzipien der Mechanik in neuem Zusammenhange dargestellt*. German. 1894 (cit. on p. 14).

[Hiv18] HiveUAV. *The Hive Unmanned Aerial Vehicle Charger*. product webpage. HiveUAV. 2018. URL: http://hiveuav.com/product (visited on 2018-05-01) (cit. on p. 39).

[Hor13] John Horgan. *Unmanned Flight: The Drones Come Home*. Ed. by National Geographic Magazine. 2013-03-01. URL: http://ngm.nationalgeographic.com/2013/03/unmanned-flight/horgan-text (visited on 2018-01-05) (cit. on p. 11).

[ICA11] International Civil Aviation Organization. *Unmanned Aircraft Systems (UAS). CIR328*. CIR328. Tech. rep. CIR328. International Civil Aviation Organization, 2011 (cit. on p. 10).

[Kap61] David H. Kaplan. "Control System for Four Power Units and the Combination". Issue 3,008,524 (United States Patent). Convertawings Inc. 1961-11-14 (cit. on p. 11).

[Kha+16] Abdul Basit Khan, Van-Long Pham, Thanh-Tung Nguyen, and Woojin Choi. "Multistage constant-current charging method for Li-Ion batteries". In: *2016 IEEE Transportation Electrification Conference and Expo, Asia-Pacific (ITEC Asia-Pacific)*. IEEE, 2016-06-04, pp. 381–385. DOI: 10.1109/itec-ap.2016.7512982 (cit. on p. 26).

[LA11] Jonas Lundberg and Mikael Asplund. "Communication Problems in Crisis Response". In: *Proceedings of the 8th International ISCRAM Conference, Lisbon, Portugal, May 2011*. Information Systems for Crisis Response and Management, ISCRAM, 2011-05-23 (cit. on pp. 1, 30).

[LST12] Jeremie Leonard, Al Savvaris, and Antonios Tsourdos. "Towards a fully autonomous swarm of unmanned aerial vehicles". In: *Proceedings of 2012 UKACC International Conference on Control*. IEEE, 2012-09-05, pp. 286–291. DOI: 10.1109/control.2012.6334644 (cit. on p. 5).

[LST13] Jeremie Leonard, Al Savvaris, and Antonios Tsourdos. "Energy Management in Swarm of Unmanned Aerial Vehicles". In: *2013 International Conference on Unmanned Aircraft Systems (ICUAS)*. IEEE, 2013-05, pp. 124–133. DOI: 10.1109/ICUAS.2013.6564681 (cit. on pp. 5, 39).

[Lu13] Xin Lu. "Online Optimization Problems". Ph.D. Thesis. Massachusetts Institute of Technology, Sloan School of Management, Operations Research Center, 2013-03-17. 153 pp. HDL: 1721.1/82724 (cit. on p. 6).

[LY15] Chih-Chung Lo and Shih-Wei Yu. "A two-phased evolutionary approach for intelligent task assignment & scheduling". In: *2015 11th International Conference on Natural Computation (ICNC)*. IEEE, 2015-08-17, pp. 1092–1097. DOI: 10.1109/ICNC.2015.7378144 (cit. on p. 34).

[MCL16] Fabio Morbidi, Roel Cano, and David Lara. "Minimum-Energy Path Generation for a Quadrotor UAV". In: *2016 IEEE International Conference on Robotics and Automation (ICRA)*. IEEE, 2016-05, pp. 1492–1498. DOI: 10.1109/icra.2016.7487285 (cit. on p. 3).

[MD14] Mark W. Mueller and Raffaello D'Andrea. "Stability and control of a quadrocopter despite the complete loss of one, two, or three propellers". In: *2014 IEEE International Conference on Robotics and Automation (ICRA)*. IEEE, 2014-06-07. DOI: 10.1109/icra.2014.6906588 (cit. on p. 14).

[Meg08] Nicole Megow. "Coping with Incomplete Information in Scheduling – Stochastic and Online Models". In: *Operations Research Proceedings 2007*. Ed. by Jörg Kalcsics and Stefan Nickel. Springer Berlin Heidelberg, 2008, pp. 17–22. DOI: 10.1007/978-3-540-77903-2_3 (cit. on p. 6).

[Mei+11] Lorenz Meier, Petri Tanskanen, Friedrich Fraundorfer, and Marc Pollefeys. "PIXHAWK: A system for autonomous flight using onboard computer vision". In: *2011 IEEE International Conference on Robotics and Automation*.

IEEE. IEEE, 2011, pp. 2992–2997. DOI: 10.1109/ICRA.2011.5980229 (cit. on p. 46).

[Mei+18] Lorenz Meier et al. *MAVLink Developer Guide. MAVLink Micro Air Vehicle Message Marshalling Library*. GitBook. 2018. URL: https://mavlink.io/en (visited on 2018-04-01). Licensed under: CC BY 4.0 (cit. on pp. 46, XII).

[MGK12] Emi Mathews, Tobias Graf, and K.S.S.B Kulathunga. "Biologically Inspired Swarm Robotic Network Ensuring Coverage and Connectivity". In: *2012 IEEE International Conference on Systems, Man, and Cybernetics (SMC)*. IEEE. IEEE, 2012-10-17, pp. 84–90. DOI: 10.1109/icsmc.2012.6377681 (cit. on p. 30).

[MHO14] Øyvind Magnussen, Geir Hovland, and Morten Ottestad. "Multicopter UAV Design Optimization". In: *2014 IEEE/ASME 10th International Conference on Mechatronic and Embedded Systems and Applications (MESA)*. 2014-09-12, pp. 1–6. DOI: 10.1109/MESA.2014.6935598 (cit. on p. 15).

[Mic+11] Bernard Michini, Tuna Toksoz, Joshua Redding, Matthew Michini, Jonathan How, Matthew Vavrina, and John Vian. "Automated Battery Swap and Recharge to Enable Persistent UAV Missions". In: *Infotech@Aerospace*. 2011-03-31, p. 10. DOI: 10.2514/6.2011-1405 (cit. on p. 39).

[Mie98] Kaisa Miettinen. *Nonlinear Multiobjective Optimization*. Vol. 12. International Series in Operations Research & Management Science. Springer US, 1998. 298 pp. DOI: 10.1007/978-1-4615-5563-6 (cit. on p. 114).

[Mil06] Robert Miller. *Hurricane Katrina: Communications & Infrastructure Impacts. ADA575202*. book chapter. National Defense University, 2006-01 (cit. on p. 1).

[Mit11] Andreas Mitschele-Thiel. "GRK 1487: Self-organized Mobile Communication Systems for Disaster Scenarios (MOBICOM)". In: *Joint Workshop of the German Research Training Groups in Computer Science*. Ed. by Johannes Hölzl. Gito Verlag, 2011-06-24, pp. 213–232 (cit. on p. 2).

[MO07] Ivan Maza and Anibal Ollero. "Multiple UAV cooperative searching operation using polygon area decomposition and efficient coverage algorithms".

In: *Distributed Autonomous Robotic Systems 6*. Springer Japan, 2007, pp. 221–230. DOI: 10.1007/978-4-431-35873-2_22 (cit. on pp. 4, 30).

[Moo18] Mark Moore. "Vehicle Collaboration Strategy and Common Reference Models". In: *Recordings and Content from the 2nd Annual Uber Elevate Summit*. Los Angeles: Uber Technologies Inc., 2018-05-09 (cit. on p. 15).

[OL10] R. Lyman Ott and Michael Longnecker. *An Introduction to Statistical Methods and Data Analysis*. 6th ed. Cengage Learning Inc., 2010. 1296 pp. (cit. on p. 74).

[Ort+13] H. J. Ortiz-Peña, M. Sudit, M. Hirsch, M. Karwan, and R. Nagi. "A multi-perspective optimization approach to UAV resource management for littoral surveillance". In: *Proceedings of the 16th International Conference on Information Fusion*. 2013-07-12, pp. 492–498. IEEE Xplore: 6641320 (cit. on p. 5).

[Pop+08] Valer Pop, Henk Jan Bergveld, Dmitry Danilov, Paul P.L. Regtien, and Peter H.L. Notten. *Battery Management Systems. Accurate State-of-Charge Indication for Battery-Powered Applications*. Philips Research Book Series. Springer Netherlands, 2008. 226 pp. DOI: 10.1007/978-1-4020-6945-1 (cit. on pp. 20 sq., 23 sqq., XIII, XV).

[Qua17] Quan Quan. *Introduction to Multicopter Design and Control*. 1st ed. Springer Singapore, 2017. 384 pp. DOI: 10.1007/978-981-10-3382-7 (cit. on p. 12).

[Rae14] James DeShaw Rae. *Analyzing the Drone Debates: Targeted Killing, Remote Warfare, and Military Technology*. Palgrave pivot. Palgrave Macmillan US, 2014-03-16. 147 pp. DOI: 10.1057/9781137381576 (cit. on p. 11).

[RD08] Piotr Rudol and Patrick Doherty. "Human Body Detection and Geolocalization for UAV Search and Rescue Missions Using Color and Thermal Imagery". In: *2008 IEEE Aerospace Conference*. 2008-03-08, pp. 1–8. DOI: 10.1109/AERO.2008.4526559 (cit. on p. 4).

[Rei+15] D. G. Reina, M. Askalani, S. L. Toral, F. Barrero, E. Asimakopoulou, and N. Bessis. "A Survey on Multihop Ad Hoc Networks for Disaster Response

Scenarios". In: *International Journal of Distributed Sensor Networks* 11.10 (2015). DOI: 10.1155/2015/647037 (cit. on pp. 1, 4, 30 sq.).

[Sas+14] Martin Saska, Jan Chudoba, Libor Precil, Justin Thomas, Giuseppe Loianno, Adam Tresnak, Vojtech Vonasek, and Vijay Kumar. "Autonomous deployment of swarms of micro-aerial vehicles in cooperative surveillance". In: *Unmanned Aircraft Systems (ICUAS), 2014 International Conference on*. IEEE, 2014-05, pp. 584–595. DOI: 10.1109/ICUAS.2014.6842301 (cit. on pp. 30, 34).

[Sas15] M. Saska. "MAV-swarms: Unmanned aerial vehicles stabilized along a given path using onboard relative localization". In: *Unmanned Aircraft Systems (ICUAS), 2015 International Conference on*. 2015-06, pp. 894–903. DOI: 10.1109/ICUAS.2015.7152376 (cit. on p. 34).

[SBS98] SBS Implementers Forum. *System Management Bus Specification. Revision 1.1*. Smart Battery System Specifications. Tech. rep. SBS Implementers Forum, 1998-12-11. 39 pp. (cit. on p. 42).

[Seg+11] Florian Segor, Axel Bürkle, Matthias Kollmann, and Rainer Schönbein. "Instantaneous autonomous aerial reconnaissance for civil applications: A UAV based approach to support security and rescue forces". In: *Proceedings of the Sixth International Conference on Systems (ICONS)*. 2011-01-28, pp. 72–76. NBN: urn:nbn:de:0011-n-1736847 (cit. on p. 4).

[Sky18] Skysense, Inc. *Skysense Outdoor Charging Pad*. product webpage. Skysense, Inc. 2018. URL: http://www.skysense.co/charging-pad-outdoor (visited on 2018-05-01) (cit. on p. 39).

[SM13] Tobias Simon and Andreas Mitschele-Thiel. "A Self-Organized Message Ferrying Algorithm". In: *2013 IEEE 14th International Symposium on "A World of Wireless, Mobile and Multimedia Networks" (WoWMoM)*. IEEE, 2013-06-07, pp. 1–6. DOI: 10.1109/WoWMoM.2013.6583439 (cit. on p. 33).

[SNS11] Roland Siegwart, Illah Reza Nourbakhsh, and Davide Scaramuzza. *Introduction to Autonomous Mobile Robots (Intelligent Robotics and Autonomous Agents series)*. 2nd ed. Intelligent Robotics and Autonomous Agents. MIT Press, 2011-02-01. 472 pp. (cit. on p. 9).

[Sta07] Ned Stafford. "Spy in the sky". In: *Nature* 445.7130 (2007-02-22), pp. 808–809. DOI: 10.1038/445808A (cit. on p. 11).

[Tow06] Frances Fragos Towsend. *The Federal Response to Hurricane Katrina: Lessons Learned*. Review. Assistant to the President for Homeland Security and Counterterrorism, The White House, USA, 2006-02-23 (cit. on p. 1).

[Tra16] Lance Traub. "Calculation of Constant Power Lithium Battery Discharge Curves". In: *Batteries* 2 (2016-06-11). Ed. by Andreas Jossen, p. 17. DOI: 10.3390/batteries2020017 (cit. on p. 27).

[UAV04] UAV Task Force. *A-NPA 16-2005. Policy for Unmanned Aerial Vehicle (UAV) certification*. Ed. by European Aviation Safety Agency. EASA. 2004-05-11. URL: https://www.easa.europa.eu/document-library/notices-of-proposed-amendments/npa-16-2005 (cit. on p. 10).

[Ure+15] N. Kemal Ure, Girish Chowdhary, Tuna Toksoz, Jonathan P. How, Matthew A. Vavrina, and John Vian. "An Automated Battery Management System to Enable Persistent Missions With Multiple Aerial Vehicles". In: *IEEE/ASME Transactions on Mechatronics* 20.1 (2015-02-01), pp. 275–286. DOI: 10.1109/TMECH.2013.2294805 (cit. on pp. 5, 39).

[Var99] A. Varga. "Using the OMNeT++ discrete event simulation system in education". In: *IEEE Transactions on Education* 42.4 (1999-11), pp. 372–383. DOI: 10.1109/13.804564 (cit. on p. 127).

[VH+18] András Varga, Rudolf Hornig, et al. *OMNeT++ Documentation. Network Simulation Framework*. OpenSim Ltd. 2018. URL: https://www.omnetpp.org/documentation (visited on 2018-04-01) (cit. on pp. 127, 135).

[Vre11] Tjark Vredeveld. "Stochastic online scheduling". In: *Computer Science - Research and Development* 27.3 (2011-04-06), pp. 181–187. DOI: 10.1007/s00450-011-0153-5 (cit. on p. 6).

[Wan+16] Xiaoyan Wang, Hao Zhou, Lei Zhong, Yusheng Ji, Kiyoshi Takano, Shigeki Yamada, and Guoliang Xue. "Capacity-Aware Cost-Efficient Network Reconstruction for Post-Disaster Scenario". In: *2016 IEEE 27th Annual Inter-*

national Symposium on Personal, Indoor, and Mobile Radio Communications (PIMRC). Valencia, Spain: IEEE, 2016-09-08. DOI: 10.1109/pimrc.2016.7794910 (cit. on pp. 4, 30).

[Yan+10] Jingyu Yan, Guoqing Xu, Huihuan Qian, and Yangsheng Xu. "Battery Fast Charging Strategy Based on Model Predictive Control". In: *2010 IEEE 72nd Vehicular Technology Conference - Fall*. IEEE, 2010-09-09, pp. 1–8. DOI: 10.1109/VETECF.2010.5594382 (cit. on p. 26).

[Zim08] Armin Zimmermann. *Stochastic Discrete Event Systems. Modeling, Evaluation, Applications*. Springer-Verlag Berlin Heidelberg, 2008. 392 pp. DOI: 10.1007/978-3-540-74173-2 (cit. on p. 127).

[ZZ15] Zhengcheng Zhang and Sheng Shui Zhang. *Rechargeable Batteries*. Ed. by Zhengcheng Zhang and Sheng Shui Zhang. Materials, Technologies and New Trends. Springer International Publishing, 2015. 712 pp. DOI: 10.1007/978-3-319-15458-9 (cit. on p. 22).

Publications

The following publications were published at international conferences in relation to the work on this thesis. They are sorted in descending chronological order.

[Die+17] Thomas Dietrich, Silvia Krug, Thomas Hotz, and Armin Zimmermann. "Towards Energy Consumption Prediction with Safety Margins for Multicopter Systems". In: *11th EAI International Conference on Performance Evaluation Methodologies and Tools (VALUETOOLS 2017)*. Venice, Italy: ACM Press, 2017-12-07. DOI: 10.1145/3150928.3150964 (cit. on p. 50).

[DKZ17a] Thomas Dietrich, Silvia Krug, and Armin Zimmermann. "A Discrete Event Simulation and Evaluation Framework for Multi UAV System Maintenance Processes". In: *2017 IEEE International Systems Engineering Symposium (ISSE)*. IEEE, 2017-10-13, pp. 1–6. DOI: 10.1109/syseng.2017.8088280 (cit. on p. 122).

[DKZ17b] Thomas Dietrich, Silvia Krug, and Armin Zimmermann. "An Empirical Study on Generic Multicopter Energy Consumption Profiles". In: *2017 Annual IEEE International Systems Conference (SysCon)*. Montreal, Canada: IEEE, 2017-04-27, pp. 1–6. DOI: 10.1109/SYSCON.2017.7934762 (cit. on p. 50).

[Die+16] Thomas Dietrich, Oleksandr Andryeyev, Armin Zimmermann, and Andreas Mitschele-Thiel. "Towards a Unified Decentralized Swarm Management and Maintenance Coordination Based on MAVLink". In: *2016 International Conference on Autonomous Robot Systems and Competitions (ICARSC)*. IEEE, 2016-05-06. DOI: 10.1109/ICARSC.2016.64 (cit. on pp. 40, 46 sq., 130, IV).

[BDZ15] Christoph Bodenstein, Thomas Dietrich, and Armin Zimmermann. "Computationally Efficient Multiphase Heuristics for Simulation-based Optimization". In: *Proceedings of the 5th International Conference on Simulation and Modeling Methodologies, Technologies and Applications (SIMULTECH 2015)*. Science and Technology Publications, Lda, 2015-07-23, pp. 95–100. DOI: 10.5220/0005518000950100 (cit. on p. 136).

[DMZ13] Thomas Dietrich, Ralph Maschotta, and Armin Zimmermann. "Multi-UAV Node Placement Strategies for Meshed Field Coverage". In: *ISWCS 2013 The Tenth International Symposium on Wireless Communication Systems*. VDE, 2013-08-30, pp. 1–3. IEEE Xplore: 6629856 (cit. on p. 33).

Student Works and Theses

Literature in this list was created by students as mandatory seminar, project, or final thesis of their respective courses of studies. All assignments were offered and supervised in the context of this thesis. The respective documents are written in the German language and not necessarily publicly available. Please query the author of this thesis for a copy if desired. The list is sorted in descending chronological order.

[Bre18] Ludwig Breitsprecher. *Konzeption und Implementierung einer intelligenten Ladestation in einer diskreten eventbasierten Simulationsumgebung*. German. Bachelorarbeit. Ilmenau: Technische Universität Ilmenau, 2018-01-05. 60 pp. (cit. on pp. 41 sq., 122, II).

[Krü18] Tobias Krüger. *Erfassung und Auswertung empirischer Daten von Multicoptern zur Erzeugung individueller Energieprofile in "Mission Planner"*. German. Bachelorarbeit. Ilmenau: Technische Universität Ilmenau, 2018-01-04. 40 pp. (cit. on pp. 50, 127, III).

[Som18] Michael Sommer. *Development and Verification of an MBSE Framework for UAV Fleet Management*. English. Research Project. Ilmenau: Technische Universität Ilmenau, 2018-08-15. submission pending (cit. on pp. 122, 138, II).

[Gri16] Vanessa Gries. *Battery Management and Monitoring in Autonomous Robotics*. German. Hauptseminar. Ilmenau: Technische Universität Ilmenau, 2016-02-10. 23 pp. (cit. on p. 20).

[Mar16] Matthias Mark. *Optical-Flow-Sensor gestützte Marker-bezogene Landung eines Multicopters auf ArduCopter-Basis*. German. Bachelorarbeit. Ilmenau: Technische Universität Ilmenau, 2016-07-01. 49 pp. (cit. on p. IV).

[PLB16] Anna-Lena Peh, Daniel Löber, and Uwe Brackenhoff. *Batteriemessung und -simulation eines Multicopters*. German. Projektseminar. Ilmenau: Technische Universität Ilmenau, 2016-08-08. 32 pp. (cit. on p. 49).

[Wil16] Jonathan Will. *Intelligente Multicopter-Ladestation auf MAVLink/Ardupilot Basis*. German. Hauptseminar. Ilmenau: Technische Universität Ilmenau, 2016-03-01. 19 pp. (cit. on p. 127).

[Har15] Paul Harig. *Entwicklung eines Hard- und Softwaresystems zur autonomen Landung von Multicoptern mit optischem Flusssensor*. German. Masterarbeit. Ilmenau: Technische Universität Ilmenau, 2015-04-27. 66 pp. (cit. on p. 127).

[Büd14] Niclas Büdenbender. *Entwicklung eines realitätsnahen Energiemodells zur Vorwärts-Simulation von Quadcopter-Systemen*. German. Bachelorarbeit. Il-

menau: Technische Universität Ilmenau, 2014-07-28. 63 pp. (cit. on pp. 3, 49).

[Mou14] Hakim Moussaoui. *GPS und andere Techniken zur Positionsbestimmung*. German. Hauptseminar. Ilmenau: Technische Universität Ilmenau, 2014-01-09. 23 pp. (cit. on p. 18).

[Neu14] Kati Neudert. *Befehlssatz für autonome Multi-UAV Systeme*. German. Hauptseminar. Ilmenau: Technische Universität Ilmenau, 2014-03-24. 19 pp. (cit. on pp. 47, IV).

[Sch13] Thomas Schmalz. *Akkumulatortechnologien im Modellbau*. German. Hauptseminar. Ilmenau: Technische Universität Ilmenau, 2013-10-11. 23 pp. (cit. on p. 20).

Eidesstattliche Erklärung

Ich versichere, dass ich die vorliegende Arbeit ohne unzulässige Hilfe Dritter und ohne Benutzung anderer als der angegebenen Hilfsmittel angefertigt habe. Die aus anderen Quellen direkt oder indirekt übernommenen Daten und Konzepte sind unter Angabe der Quelle gekennzeichnet.

Weitere Personen waren an der inhaltlich-materiellen Erstellung der vorliegenden Arbeit nicht beteiligt. Insbesondere habe ich hierfür nicht die entgeltliche Hilfe von Vermittlungs- bzw. Beratungsdiensten (Promotionsberater oder anderer Personen) in Anspruch genommen. Niemand hat von mir unmittelbar oder mittelbar geldwerte Leistungen für Arbeiten erhalten, die im Zusammenhang mit dem Inhalt der vorgelegten Dissertation stehen.

Die Arbeit wurde bisher weder im In- noch im Ausland in gleicher oder ähnlicher Form einer Prüfungsbehörde vorgelegt.

Ich bin darauf hingewiesen worden, dass die Unrichtigkeit der vorstehenden Erklärung als Täuschungsversuch bewertet wird und gemäß § 7 Abs. 10 der Promotionsordnung den Abbruch des Promotionsverfahrens zur Folge hat.

Thomas Dietrich
Ilmenau, 2018-08-09